Electronic Supplementary Information

Synthesis of [60]fullerene-fused dihydrobenzooxazepines *via* the palladium-catalyzed oxime-directed C–H bond activation and subsequent electrochemical functionalization

Chen Wang,[a] Zhan Liu,[a] Zheng-Chun Yin[a] and Guan-Wu Wang*[a,b]

[a]*CAS Key Laboratory of Soft Matter Chemistry, Hefei National Laboratory for Physical Sciences at Microscale, and Department of Chemistry, University of Science and Technology of China, Hefei, Anhui 230026, P. R. China*
E-mail: gwang@ustc.edu.cn; Fax: +86 0551 63607864; Tel: +86 0551 63607864
[b]*State Key Laboratory of Applied Organic Chemistry, Lanzhou University, Lanzhou, Gansu 730000, P. R. China*

Table of Contents

1. General information

NMR spectra were recorded on a 400 or 500 MHz NMR spectrometer. ^{1}H NMR chemical shifts were determined relative to TMS or residual $CDCl_2CDCl_2$ (δ 5.92 ppm). ^{13}C NMR chemical shifts were determined relative to TMS or residual $CDCl_2CDCl_2$ (δ 72.86 ppm) or residual DMSO (δ 39.52 ppm). Data for ^{1}H NMR and ^{13}C NMR are reported as follows: chemical shift (δ, ppm), multiplicity (s = singlet, d = doublet, t = triplet, m = multiplet). High-resolution mass spectra (HRMS) were measured with MALDI-TOF in a negative mode.

2. General procedure for the reaction of C_{60} and oximes 1a–p

A dry 25-mL tube equipped with a magnetic stirrer was charged with C_{60} (36.0 mg, 0.05 mmol), **1** (0.10 or 0.15 mmol), $Pd(TFA)_2$ (0.005 mmol or 0.01 mmol), $Na_2S_2O_8$ (0.10 mmol) or $K_2S_2O_8$ (0.10 mmol). After dissolving the solids in anhydrous *ortho*-dichlorobenzene (ODCB) (5 mL) by sonication, trifluoroacetic acid (TFA) (0.25 mL or 0.5 mL) was added in the reaction system. Then, the tube was stirred in an oil bath at the pre-determined reaction temperature for the desired time. The reaction mixture was filtered through a silica gel plug to remove insoluble material. After the solvent had been evaporated in *vacuo*, the residue was separated on a silica gel column with carbon disulfide (CS_2) as the eluent to recover unreacted C_{60}, and then the eluent was switched to CS_2/ dichloromethane (DCM) to give product **2**.

3. Synthesis and spectral data of compounds 2a–p and 3a–c

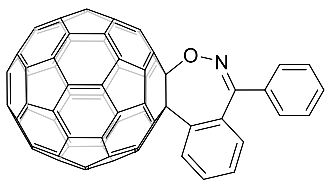

2a

By following the general procedure, a mixture of C_{60} (36.0 mg, 0.05 mmol), **1a** (20.2 mg, 0.10 mmol), $Pd(TFA)_2$ (1.8 mg, 0.005 mmol), $Na_2S_2O_8$ (24.1 mg, 0.10 mmol) and TFA (0.25 mL) in ODCB (5 mL) at 100 °C for 13 h afforded recovered C_{60} (18.4 mg, 51%) and **2a** (14.0 mg, 31%), amorphous brown solid; ^{1}H NMR (400 MHz, $CDCl_2CDCl_2/CS_2$) δ 8.04 (d, J = 7.4 Hz, 1H), δ 7.82 (d, J = 7.2 Hz, 2H), δ 7.62 (t, J = 7.4 Hz, 1H), δ 7.54 (t, J = 7.3 Hz, 2H), δ 7.24 (t, J = 7.4 Hz, 1H), δ 7.15 (t, J = 7.3 Hz, 1H), δ 6.46 (d, J = 8.2 Hz, 1H); ^{13}C NMR (101 MHz, $CDCl_2CDCl_2/CS_2$) δ 168.88 (*C*=N), 151.32, 146.76, 146.62, 146.25, 145.35, 145.34, 145.15, 145.07, 144.84, 144.72, 144.27, 144.20, 144.15, 144.02, 143.95, 143.43, 143.38, 141.89, 141.71, 141.68, 141.63, 141.15, 141.08, 140.96, 140.78, 140.61, 139.98, 139.87, 136.92, 135.63, 135.19, 134.03, 130.85, 129.46, 128.18, 128.10, 127.26, 125.04, 123.45, 116.30, 86.09 (sp^3-*C* of C_{60}), 70.84 (sp^3-*C* of C_{60});

FT-IR ν/cm^{-1} (KBr) 1656, 1592, 1514, 1479, 1341, 1316, 1259, 1185, 797, 746, 708, 696, 644, 575, 526; UV-Vis ($CHCl_3$) λ_{max}/nm (log ε) 257 (5.20), 314 (4.75), 428 (4.52), 687 (3.58); MALDI-TOF MS *m/z* calcd for $C_{73}H_9NO$ [M]$^-$ 915.0690, found 915.0687.

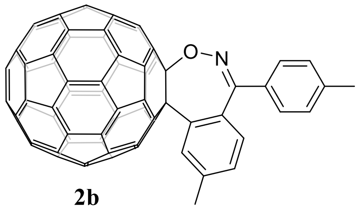

2b

By following the general procedure, a mixture of C_{60} (36.1 mg, 0.05 mmol), **1b** (33.8 mg, 0.15 mmol), Pd(TFA)$_2$ (1.8 mg, 0.005 mmol), $Na_2S_2O_8$ (24.2 mg, 0.10 mmol) and TFA (0.25 mL) in ODCB (5 mL) at 110 °C for 15 h afforded recovered C_{60} (21.4 mg, 59%) and **2b** (8.0 mg, 17%), amorphous brown solid; ^{1}H NMR (400 MHz, $CDCl_2CDCl_2/CS_2$) δ 7.82 (s, 1H), 7.70 (d, *J* = 7.9 Hz, 2H), 7.32 (d, *J* = 7.9 Hz, 2H), 6.96 (d, *J* = 8.4 Hz, 1H), 6.38 (d, *J* = 8.4 Hz, 1H), 2.47 (s, 3H), 2.38 (s, 3H); ^{13}C NMR (101 MHz, $CDCl_2CDCl_2/CS_2$) δ 168.74 (*C*=N), 151.45, 146.74, 146.70, 146.24, 145.33, 145.31, 145.12, 145.03, 144.82, 144.73, 144.58, 144.18, 144.12, 144.04, 144.00, 143.42, 143.39, 141.87, 141.68, 141.66, 141.63, 141.31, 141.16, 141.06, 140.95, 140.78, 140.64, 139.94, 137.66, 136.89, 135.55, 134.00, 133.16, 132.40, 129.34, 128.85, 128.70, 127.40, 125.26, 116.16, 86.19 (sp^3-*C* of C_{60}), 70.84 (sp^3-*C* of C_{60}), 20.84, 20.04; FT-IR ν/cm^{-1} (KBr) 1652, 1608, 1514, 1492, 1428, 1335, 1269, 1177, 1133, 1089, 827, 807, 766, 572, 526; UV-Vis ($CHCl_3$) λ_{max}/nm (log ε) 257 (5.20), 314 (4.76), 428 (4.59), 687 (3.75); MALDI-TOF MS *m/z* calcd for $C_{75}H_{13}NO$ [M]$^-$ 943.1003, found 943.1008.

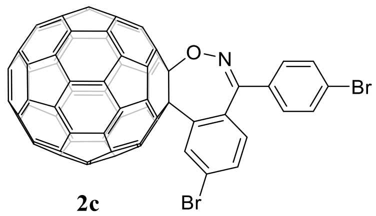

2c

By following the general procedure, a mixture of C_{60} (36.1 mg, 0.05 mmol), **1c** (52.6 mg, 0.15 mmol), Pd(TFA)$_2$ (3.4 mg, 0.01 mmol), $Na_2S_2O_8$ (24.0 mg, 0.10 mmol) and TFA (0.5 mL) in ODCB (5 mL) at 100 °C for 13 h afforded recovered C_{60} (18.0 mg, 50%) and **2c** (10.5 mg, 20%), amorphous brown solid; ^{1}H NMR (500 MHz, $CDCl_2CDCl_2$) δ 8.14 (d, *J* = 2.0 Hz, 1H), 7.70 (s, 4H), 7.35 (dd, *J* = 8.9, 2.0 Hz, 1H), 6.39 (d, *J* = 8.9 Hz, 1H); ^{13}C NMR (126 MHz, $CDCl_2CDCl_2$) δ 167.87 (*C*=N), 150.42, 146.79, 146.26, 146.22, 145.35, 145.14, 145.06, 144.86, 144.62, 144.23, 144.20, 144.04, 143.61, 143.48, 143.38, 143.30, 141.86, 141.70, 141.67, 141.56, 141.07, 140.97, 140.96, 140.74, 140.49, 140.03, 138.76, 136.99, 135.63, 134.14, 133.44, 131.84, 131.60, 131.21, 128.95, 128.00, 125.83, 117.48, 116.00, 86.38 (sp^3-*C* of C_{60}), 70.20 (sp^3-*C* of C_{60}); FT-IR ν/cm^{-1} (KBr) 1661, 1586, 1514, 1477, 1389, 1333, 1311, 1279, 1248, 1130, 1068, 1011, 937, 840, 808, 785, 750, 575, 504, 527; UV-Vis ($CHCl_3$)

λ_{max}/nm (log ε) 255 (5.15), 315 (4.73), 428 (4.19), 686 (3.17); MALDI-TOF MS *m/z* calcd for $C_{73}H_7{}^{79}Br_2NO$ [M]‾ 1070.8900, found 1070.8903.

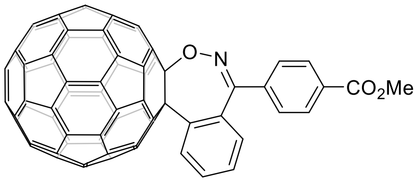

2d

By following the general procedure, a mixture of C_{60} (36.2 mg, 0.05 mmol), **1d** (25.5 mg, 0.10 mmol), Pd(TFA)$_2$ (1.8 mg, 0.005 mmol), $Na_2S_2O_8$ (23.9 mg, 0.10 mmol) and TFA (0.25 mL) in ODCB (5 mL) at 100 °C for 7 h afforded recovered C_{60} (15.4 mg, 43%) and **2d** (12.2 mg, 25%), amorphous brown solid; ^{1}H NMR (400 MHz, $CDCl_2CDCl_2$) δ 8.20 (d, *J* = 8.1 Hz, 2H), 8.08 (d, *J* = 7.4 Hz, 1H), 7.90 (d, *J* = 8.1 Hz, 2H), 7.27 (dd, *J* = 8.3, 7.4 Hz, 1H), 7.17 (t, *J* = 8.3 Hz, 1H), 6.40 (d, *J* = 8.3 Hz, 1H), 3.94 (s, 3H); ^{13}C NMR (101 MHz, $CDCl_2CDCl_2$) δ 168.07 (*C*=N), 165.29 (*C*=O), 151.36, 146.86, 146.58, 146.32, 145.42, 145.22, 145.16, 144.93, 144.78, 144.29, 144.23, 144.09, 143.98, 143.97, 143.51, 143.41, 141.95, 141.78, 141.73, 141.68, 141.16, 141.03, 140.82, 140.62, 140.07, 139.32, 139.29, 136.97, 135.89, 134.08, 131.80, 129.92, 129.50, 128.31, 127.29, 125.34, 123.99, 116.21, 86.25 (sp^3-*C* of C_{60}), 70.82 (sp^3-*C* of C_{60}), 51.81; FT-IR ν/cm^{-1} (KBr) 1725, 1655, 1514, 1480, 1430, 1343, 1278, 1190, 1143, 1105, 1005, 950, 866, 791, 774, 743, 630, 577, 527; UV-Vis ($CHCl_3$) λ_{max}/nm (log ε) 254 (5.03), 315 (4.58), 428 (4.35), 682 (3.29); MALDI-TOF MS *m/z* calcd for $C_{75}H_{11}NO_3$ [M]‾ 973.0744, found 973.0738.

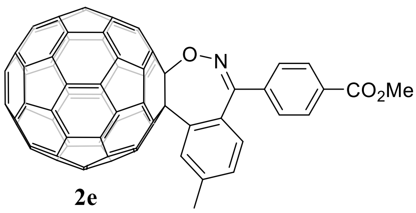

2e

By following the general procedure, a mixture of C_{60} (36.1 mg, 0.05 mmol), **1e** (27.3 mg, 0.10 mmol), Pd(TFA)$_2$ (1.8 mg, 0.005 mmol), $Na_2S_2O_8$ (24.4 mg, 0.10 mmol) and TFA (0.25 mL) in ODCB (5 mL) at 100 °C for 10 h afforded recovered C_{60} (16.8 mg, 47%) and **2e** (15.4 mg, 31%), amorphous brown solid; ^{1}H NMR (500 MHz, $CDCl_2CDCl_2$) δ 8.19 (d, *J* = 8.1 Hz, 2H), 7.88 (d, *J* = 8.1 Hz, 2H), 7.85 (s, 1H), 6.97 (d, *J* = 8.5 Hz, 1H), 6.26 (d, *J* = 8.5 Hz, 1H), 3.94 (s, 3H), 2.37 (s, 3H); ^{13}C NMR (126 MHz, $CDCl_2CDCl_2$) δ 167.74 (*C*=N), 165.24 (*C*=O), 151.42, 146.78, 146.56, 146.24, 145.34, 145.14, 145.07, 144.84, 144.72, 144.21, 144.13, 144.10, 144.01, 143.97, 143.45, 143.35, 141.87, 141.69, 141.65, 141.61, 141.10, 141.08, 140.95, 140.75, 140.56, 139.99, 139.42, 136.86, 136.80, 135.78, 134.00, 133.97, 131.58, 129.88, 129.37, 129.04, 127.15, 125.46, 115.90, 86.29 (sp^3-*C* of C_{60}), 70.74 (sp^3-*C* of C_{60}), 51.70, 20.01; FT-IR ν/cm^{-1} (KBr) 1725, 1655, 1517, 1493, 1430, 1342, 1269, 1102, 1016, 871, 805, 791, 771, 728, 709, 571, 526; UV-Vis ($CHCl_3$) λ_{max}/nm (log ε) 254 (5.03), 314 (4.58), 427 (4.36), 682 (3.26); MALDI-TOF MS *m/z* calcd for $C_{76}H_{13}NO_3$

[M]‾ 987.0901, found 987.0908.

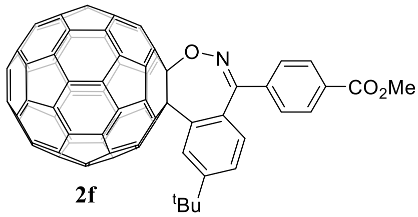

2f

By following the general procedure, a mixture of C_{60} (36.3 mg, 0.05 mmol), **1f** (31.5 mg, 0.10 mmol), $Pd(TFA)_2$ (1.8 mg, 0.005 mmol), $Na_2S_2O_8$ (24.0 mg, 0.10 mmol) and TFA (0.25 mL) in ODCB (5 mL) at 100 ^oC for 11 h afforded recovered C_{60} (14.1 mg, 39%) and **2f** (15.0 mg, 29%), amorphous brown solid; ^1H NMR (500 MHz, $CDCl_2CDCl_2$) δ 8.20 (d, J = 8.3 Hz, 2H), 8.0 (d, J = 2.1 Hz, 1H), 7.89 (d, J = 8.3 Hz, 2H), 7.18 (dd, J = 8.8, 2.1 Hz, 1H), 6.29 (d, J = 8.8 Hz, 1H), 3.94 (s, 3H), 1.30 (s, 9H); ^{13}C NMR (126 MHz, $CDCl_2CDCl_2$) δ 167.76 (*C*=N), 165.31 (*C*=O), 151.58, 147.48, 146.78, 146.61, 146.23, 145.34, 145.13, 145.07, 144.85, 144.74, 144.22, 144.12, 144.01, 143.97, 143.45, 143.36, 141.89, 141.70, 141.65, 141.62, 141.10, 141.09, 140.95, 140.75, 140.56, 140.07, 139.56, 136.82, 136.62, 135.85, 134.00, 131.52, 129.40, 127.11, 125.66, 121.60, 115.62, 86.39 (sp^3-*C* of C_{60}), 70.98 (sp^3-*C* of C_{60}), 51.71, 33.69, 30.41; FT-IR ν/cm^{-1} (KBr) 2957, 1731, 1655, 1492, 1432, 1364, 1341, 1274, 1188, 1102, 1020, 791, 774, 705, 574, 527; UV-Vis ($CHCl_3$) λ_{max}/nm (log ε) 254 (5.11), 314 (4.66), 427 (4.45), 681 (3.24); MALDI-TOF MS *m/z* calcd for $C_{79}H_{19}NO_3$ [M]‾ 1029.1370, found 1029.1362.

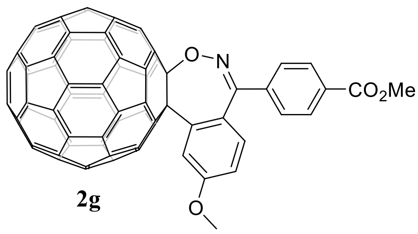

2g

By following the general procedure, a mixture of C_{60} (35.9 mg, 0.05 mmol), **1g** (43.5 mg, 0.15 mmol), $Pd(TFA)_2$ (1.8 mg, 0.005 mmol), $Na_2S_2O_8$ (24.0 mg, 0.10 mmol) and TFA (0.25 mL) in ODCB (5 mL) at 100 ^oC for 13 h afforded recovered C_{60} (21.5 mg, 60%) and **2g** (15.4 mg, 31%), amorphous brown solid; ^1H NMR (500 MHz, $CDCl_2CDCl_2$) δ 8.19 (d, J = 8.3 Hz, 2H), 7.88 (d, J = 8.3 Hz, 2H), 7.56 (d, J = 2.7 Hz, 1H), 6.71 (dd, J = 9.1, 2.7 Hz, 1H), 6.31 (d, J = 9.1 Hz, 1H), 3.94 (s, 3H), 3.79 (s, 3H); ^{13}C NMR (126 MHz, $CDCl_2CDCl_2$) δ 167.36 (*C*=N), 165.26 (*C*=O), 155.99, 151.13, 146.78, 146.52, 146.24, 145.36, 145.33, 145.13, 145.08, 144.84, 144.68, 144.20, 144.17, 144.14, 144.02, 143.84, 143.42, 143.35, 141.87, 141.69, 141.64, 141.60, 141.06, 141.05, 140.93, 140.75, 140.55, 139.99, 139.40, 136.83, 135.75, 134.04, 132.24, 131.51, 131.25, 129.39, 127.16, 116.96, 113.67, 110.58, 86.31 (sp^3-*C* of C_{60}), 70.68 (sp^3-*C* of C_{60}), 55.03, 51.74; FT-IR ν/cm^{-1} (KBr) 1722, 1655, 1513, 1492, 1428, 1351, 1271, 1185, 1105, 1018, 866, 801, 789, 773, 726, 709, 597, 574, 526; UV-Vis ($CHCl_3$) λ_{max}/nm (log ε) 255 (5.12), 315 (4.69), 428 (4.11), 685 (3.07); MALDI-TOF

MS *m/z* calcd for $C_{76}H_{13}NO_4$ [M]¯ 1003.0850, found 1003.0857.

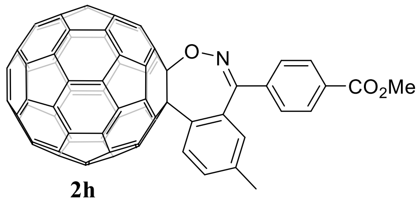

2h

By following the general procedure, a mixture of C_{60} (36.2 mg, 0.05 mmol), **1h** (27.5 mg, 0.10 mmol), Pd(TFA)$_2$ (1.8 mg, 0.005 mmol), $Na_2S_2O_8$ (24.3 mg, 0.10 mmol) and TFA (0.25 mL) in ODCB (5 mL) at 100 °C for 13 h afforded recovered C_{60} (17.5 mg, 48%) and **2h** (14.4 mg, 29%), amorphous brown solid; ^{1}H NMR (400 MHz, $CDCl_2CDCl_2$) δ 8.20 (d, J = 7.5 Hz, 2H), 7.97–7.88 (m, 3H), 7.09 (d, J = 7.4 Hz, 1H), 6.21 (s, 1H), 3.94 (s, 3H), 2.18 (s, 3H); ^{13}C NMR (101 MHz, $CDCl_2CDCl_2$) δ 167.96 (*C*=N), 165.21 (*C*=O), 151.44, 146.76, 146.48, 146.21, 145.32, 145.30, 145.11, 145.04, 144.82, 144.70, 144.19, 144.09, 144.02, 143.97, 143.88, 143.43, 143.30, 141.84, 141.67, 141.63, 141.57, 141.11, 141.05, 140.93, 140.71, 140.52, 139.95, 139.35, 139.31, 138.50, 136.81, 135.82, 133.88, 131.54, 129.28, 127.21, 124.79, 116.77, 86.46 (sp^3-*C* of C_{60}), 70.51 (sp^3-*C* of C_{60}), 51.71, 21.00; FT-IR ν/cm^{-1} (KBr) 1729, 1651, 1498, 1436, 1346, 1275, 1182, 1103, 1019, 866, 789, 771, 724, 712, 596, 574, 527; UV-Vis ($CHCl_3$) λ_{max}/nm (log ε) 256 (5.15), 315 (4.69), 428 (4.47), 688 (3.54); MALDI-TOF MS *m/z* calcd for $C_{76}H_{13}NO_3$ [M]¯ 987.0901, found 987.0902.

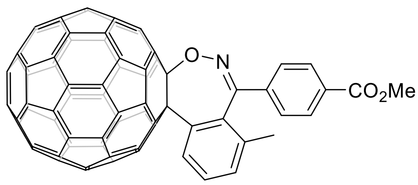

2i

By following the general procedure, a mixture of C_{60} (36.2 mg, 0.05 mmol), **1i** (26.9 mg, 0.10 mmol), Pd(TFA)$_2$ (1.8 mg, 0.005 mmol), $Na_2S_2O_8$ (24.4 mg, 0.10 mmol) and TFA (0.25 mL) in ODCB (5 mL) at 100 °C for 13 h afforded recovered C_{60} (20.3 mg, 56%) and **2i** (9.0 mg, 18%), amorphous brown solid; ^{1}H NMR (400 MHz, $CDCl_2CDCl_2$) δ 8.01 (d, J = 8.2 Hz, 2H), 7.97–7.92 (m, 3H), 7.34 (t, J = 7.5 Hz, 1H), 7.23 (d, J = 7.5 Hz, 1H), 3.86 (s, 3H), 2.04 (s, 3H); ^{13}C NMR (101 MHz, $CDCl_2CDCl_2$) δ 170.81 (*C*=N), 165.06 (*C*=O), 151.30, 146.83, 146.21, 145.30, 145.20, 145.09, 144.94, 144.83, 144.64, 144.36, 144.19, 144.04, 143.97, 143.81, 143.46, 143.15, 141.84, 141.70, 141.62, 141.35, 141.13, 140.93, 140.71, 140.44, 139.96, 139.92, 139.71, 136.87, 135.90, 133.90, 132.15, 131.46, 130.52, 128.86, 128.79, 126.91, 124.81, 122.52, 86.33 (sp^3-*C* of C_{60}), 72.25 (sp^3-*C* of C_{60}), 51.69, 19.79; FT-IR ν/cm^{-1} (KBr) 1727, 1655, 1463, 1431, 1276, 1245, 1188, 1105, 1018, 865, 818, 791, 766, 743, 720, 596, 563, 527; UV-Vis ($CHCl_3$) λ_{max}/nm (log ε) 256 (5.14), 316 (4.66), 427 (4.09); MALDI-TOF MS *m/z* calcd for $C_{76}H_{13}NO_3$ [M]¯ 987.0901, found 987.0903.

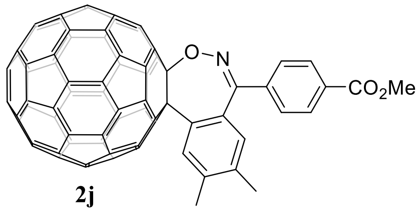

2j

By following the general procedure, a mixture of C_{60} (36.1 mg, 0.05 mmol), **1j** (28.7 mg, 0.10 mmol), $Pd(TFA)_2$ (1.8 mg, 0.005 mmol), $Na_2S_2O_8$ (24.3 mg, 0.10 mmol) and TFA (0.25 mL) in ODCB (5 mL) at 100 °C for 13 h afforded recovered C_{60} (21.4 mg, 59%) and **2j** (12.8 mg, 26%), amorphous brown solid; ^{1}H NMR (400 MHz, $CDCl_2CDCl_2$) δ 8.20 (d, J = 8.3 Hz, 2H), 7.89 (d, J = 8.3 Hz, 2H), 7.78 (s, 1H), 6.17 (s, 1H), 3.95 (s, 3H), 2.28 (s, 3H), 2.06 (s, 3H); ^{13}C NMR (101 MHz, $CDCl_2CDCl_2$) δ 167.69 (*C*=N), 165.25 (*C*=O), 151.55, 146.75, 146.57, 146.21, 145.32, 145.11, 145.04, 144.82, 144.72, 144.21, 144.19, 144.09, 143.97, 143.44, 143.32, 141.84, 141.67, 141.62, 141.59, 141.13, 141.06, 140.94, 140.72, 140.54, 139.96, 139.56, 137.11, 137.09, 136.78, 135.82, 133.88, 132.82, 131.40, 129.27, 127.35, 127.17, 125.62, 117.19, 86.38 (sp^3-*C* of C_{60}), 70.65 (sp^3-*C* of C_{60}), 51.70, 19.72, 18.69; FT-IR ν/cm^{-1} (KBr) 1730, 1650, 1497, 1430, 1349, 1272, 1190, 1102, 1019, 867, 791, 779, 726, 709, 575, 553, 526; UV-Vis ($CHCl_3$) λ_{max}/nm (log ε) 254 (5.15), 314 (4.70), 427 (4.46), 683 (3.41); MALDI-TOF MS *m/z* calcd for $C_{77}H_{15}NO_3$ [M]$^-$ 1001.1057, found 1001.1051.

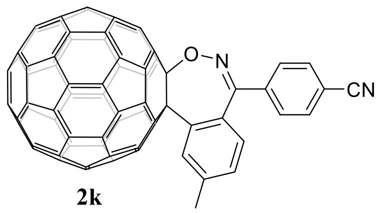

2k

By following the general procedure, a mixture of C_{60} (36.2 mg, 0.05 mmol), **1k** (23.7 mg, 0.10 mmol), $Pd(TFA)_2$ (1.8 mg, 0.005 mmol), $Na_2S_2O_8$ (24.3 mg, 0.10 mmol) and TFA (0.25 mL) in ODCB (5 mL) at 100 °C for 13 h afforded recovered C_{60} (18.1 mg, 50%) and **2k** (11.0 mg, 23%), amorphous brown solid; ^{1}H NMR (400 MHz, $CDCl_2CDCl_2$) δ 7.93 (d, J = 8.4 Hz, 2H), 7.86 (s, 1H), 7.84 (d, J = 8.4 Hz, 2H), 7.01 (d, J = 8.4 Hz, 1H), 6.26 (d, J = 8.4 Hz, 1H), 2.39 (s, 3H); the ^{13}C NMR spectrum of **2k** could not be obtained because of its poor solubility; FT-IR ν/cm^{-1} (KBr) 2221, 1651, 1493, 1428, 1346, 1261, 1110, 1012, 875, 848, 797, 752, 700, 575, 565, 526; UV-Vis ($CHCl_3$) λ_{max}/nm (log ε) 256 (5.19), 315 (4.73), 428 (4.21), 686 (3.16); MALDI-TOF MS *m/z* calcd for $C_{75}H_{10}N_2O$ [M]$^-$ 954.0798, found 954.0792.

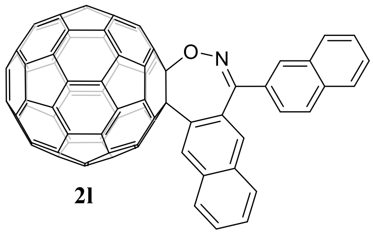

2l

By following the general procedure, a mixture of C_{60} (35.9 mg, 0.05 mmol), **1l** (44.3 mg, 0.15 mmol), $Pd(TFA)_2$ (1.8 mg, 0.005 mmol), $Na_2S_2O_8$ (24.3 mg, 0.10 mmol) and TFA (0.25 mL) in ODCB (5 mL) at 100 ^{o}C for 20 h afforded recovered C_{60} (24.0 mg, 67%) and **2l** (9.4 mg, 19%), amorphous brown solid; ^{1}H NMR (500 MHz, $CDCl_2CDCl_2$) δ 8.53 (s, 1H), 8.49 (s, 1H), 7.99–7.89 (m, 4H), 7.83 (d, J = 8.1 Hz, 1H), 7.63 (t, J = 7.6 Hz, 1H), 7.57 (t, J = 7.6 Hz, 1H), 7.40–7.29 (m, 3H), 6.85 (s, 1H); ^{13}C NMR (126 MHz, $CDCl_2CDCl_2$) δ 169.44 (*C*=N), 151.89, 146.78, 146.53, 146.26, 145.32, 145.14, 145.05, 144.83, 144.67, 144.19, 144.12, 144.00, 143.96, 143.45, 143.37, 141.85, 141.69, 141.64, 141.58, 141.14, 141.10, 140.98, 140.78, 140.59, 140.07, 137.46, 136.92, 135.81, 133.92, 133.76, 132.68, 132.25, 131.89, 130.85, 129.64, 128.65, 128.12, 127.86, 127.29, 127.10, 126.83, 126.69, 126.25, 126.18, 124.70, 123.67, 113.03, 86.30 (sp^3-*C* of C_{60}), 70.03 (sp^3-*C* of C_{60}); FT-IR ν/cm^{-1} (KBr) 1657, 1503, 1462, 1428, 1310, 1274, 1227, 1188, 1133, 864, 820, 773, 742, 577, 554, 528; UV-Vis ($CHCl_3$) λ_{max}/nm (log ε) 256 (5.24), 316 (4.77), 428 (4.63), 687 (3.70); MALDI-TOF MS *m/z* calcd for $C_{81}H_{13}NO$ $[M]^-$ 1015.1003, found 1015.1006.

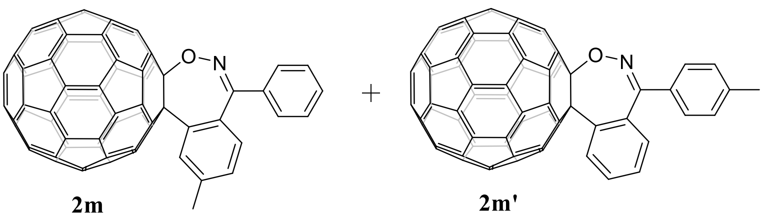

2m **2m'**

By following the general procedure, a mixture of C_{60} (35.9 mg, 0.05 mmol), **1m** (21.5 mg, 0.10 mmol), $Pd(TFA)_2$ (1.8 mg, 0.005 mmol), $Na_2S_2O_8$ (24.0 mg, 0.10 mmol) and TFA (0.25 mL) in ODCB (5 mL) at 100 ^{o}C for 20 h afforded recovered C_{60} (19.5 mg, 54%) and an isomeric mixture of **2m** and **2m'** (10.5 mg, 23%). Then, the mixture was separated twice by preparative thin-layer chromatography with CS_2 as the eluent to provide **2m** (6.1 mg, 13%) and **2m'** (4.4 mg, 10%), amorphous brown solid; **2m**: ^{1}H NMR (500 MHz, $CDCl_2CDCl_2$) δ 7.84–7.80 (m, 3H), 7.60 (t, J = 7.5 Hz, 1H), 7.53 (t, J = 7.4 Hz, 2H), 6.97 (dd, J = 8.6, 1.8 Hz, 1H), 6.33 (d, J = 8.6 Hz, 1H), 2.37 (s, 3H); ^{13}C NMR (126 MHz, $CDCl_2CDCl_2$) δ 168.93 (*C*=N), 151.47, 146.76, 146.62, 146.23, 145.313, 145.305, 145.11, 145.02, 144.82, 144.74, 144.44, 144.18, 144.10, 144.02, 143.99, 143.43, 143.36, 141.85, 141.66, 141.63, 141.59, 141.11, 141.07, 140.93, 140.74, 140.60, 139.95, 137.37, 136.86, 135.65, 135.25, 133.99, 133.50, 130.81, 129.55, 128.93, 128.14, 127.23, 125.25, 116.12, 86.23 (sp^3-*C* of C_{60}), 70.86 (sp^3-*C* of C_{60}), 20.01; FT-IR ν/cm^{-1} (KBr) 1652, 1509, 1492, 1423, 1342, 1262, 1164, 1099, 1020, 875, 805, 771, 704, 665, 656, 594, 573, 564, 526; UV-Vis ($CHCl_3$) λ_{max}/nm (log ε) 256

(5.14), 314 (4.68), 428 (4.46), 691 (3.30); MALDI-TOF MS *m/z* calcd for $C_{74}H_{11}NO$ $[M]^-$ 929.0846, found 929.0841; **2m'**: ^{1}H NMR (500 MHz, $CDCl_2CDCl_2/CS_2$) δ 8.05 (d, *J* = 7.4 Hz, 1H), 7.74 (d, *J* = 7.7 Hz, 2H), 7.33 (d, *J* = 7.7 Hz, 2H), 7.24 (t, *J* = 7.4 Hz, 1H), 7.19 (t, *J* = 7.7 Hz, 1H), 6.54 (d, *J* = 8.2 Hz, 1H), 2.45 (s, 3H); ^{13}C NMR (126 MHz, $CDCl_2CDCl_2/CS_2$) δ 169.11 (*C*=N), 151.35, 146.77, 146.63, 146.26, 145.34, 145.33, 145.14, 145.04, 144.84, 144.74, 144.42, 144.20, 144.14, 144.02, 143.98, 143.43, 143.38, 141.88, 141.70, 141.67, 141.62, 141.15, 141.08, 140.96, 140.78, 140.64, 140.07, 139.97, 136.95, 135.60, 134.05, 132.21, 129.50, 129.34, 128.78, 128.06, 127.48, 124.98, 123.29, 116.38, 86.11 (sp^3-*C* of C_{60}), 70.90 (sp^3-*C* of C_{60}), 20.85; FT-IR ν/cm^{-1} (KBr) 1651, 1595, 1510, 1478, 1341, 1316, 1260, 1180, 1099, 1019, 803, 768, 742, 597, 571, 545, 526; UV-Vis ($CHCl_3$) λ_{max}/nm (log ε) 256 (5.12), 314 (4.70), 427 (4.43), 690 (3.22); MALDI-TOF MS *m/z* calcd for $C_{74}H_{11}NO$ $[M]^-$ 929.0846, found 929.0839.

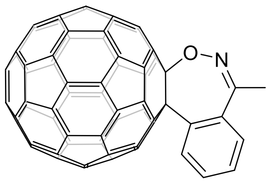

2n

By following the general procedure, a mixture of C_{60} (36.1 mg, 0.05 mmol), **1n** (20.5 mg, 0.15 mmol), $Pd(TFA)_2$ (3.4 mg, 0.01 mmol), $K_2S_2O_8$ (27.2 mg, 0.10 mmol) and TFA (0.25 mL) in ODCB (5 mL) at 100 ^{o}C for 20 h afforded recovered C_{60} (22.3 mg, 62%) and **2n** (5.9 mg, 14%), amorphous brown solid; ^{1}H NMR (500 MHz, $CDCl_2CDCl_2/CS_2$) δ 8.13 (d, *J* = 7.4 Hz, 1H), 7.74 (d, *J* = 8.4 Hz, 1H), 7.58 (dd, *J* = 8.4, 7.4 Hz, 1H), 7.38 (t, *J* = 7.4 Hz, 1H), 2.88 (s, 3H); ^{13}C NMR (101 MHz, $CDCl_2CDCl_2/CS_2$) δ 168.31 (*C*=N), 151.90, 146.97, 146.72, 146.21, 145.38, 145.34, 145.14, 145.03, 144.81, 144.70, 144.20, 144.10, 143.99, 143.86, 143.80, 143.43, 143.39, 141.88, 141.72, 141.70, 141.12, 141.05, 140.97, 140.65, 140.55, 139.97, 139.75, 136.41, 135.57, 133.94, 130.11, 128.92, 125.62, 123.68, 115.03, 85.91 (sp^3-*C* of C_{60}), 70.30 (sp^3-*C* of C_{60}), 26.99; FT-IR ν/cm^{-1} (KBr) 1670, 1600, 1483, 1437, 1365, 1340, 1313, 1247, 1185, 1157, 1038, 948, 898, 812, 743, 619, 598, 573, 563, 527; UV-Vis ($CHCl_3$) λ_{max}/nm (log ε) 255 (4.99), 314 (4.50), 428 (4.39), 685 (3.52); MALDI-TOF MS *m/z* calcd for $C_{68}H_7NO$ $[M]^-$ 853.0533, found 853.0535.

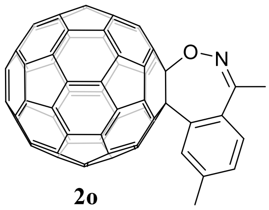

2o

By following the general procedure, a mixture of C_{60} (35.8 mg, 0.05 mmol), **1o** (22.8 mg, 0.15 mmol), $Pd(TFA)_2$ (3.5 mg, 0.01 mmol), $K_2S_2O_8$ (27.5 mg, 0.10 mmol) and TFA (0.25 mL) in ODCB (5 mL) at 100 ^{o}C for 16 h afforded recovered C_{60} (25.2

mg, 70%) and **2o** (5.5 mg, 13%), amorphous brown solid; ^{1}H NMR (500 MHz, $CDCl_2CDCl_2$) δ 7.91 (s, 1H), 7.62 (d, J = 8.3 Hz, 1H), 7.37 (d, J = 8.3 Hz, 1H), 2.84 (s, 3H), 2.46 (s, 3H); ^{13}C NMR (126 MHz, $CDCl_2CDCl_2$) δ 168.82 (*C*=N), 152.11, 146.93, 146.74, 146.19, 145.35, 145.32, 145.12, 144.98, 144.80, 144.76, 144.18, 144.06, 144.03, 143.98, 143.97, 143.45, 143.36, 141.84, 141.68, 141.66, 141.63, 141.06, 140.94, 140.60, 140.54, 139.93, 137.24, 136.38, 135.66, 133.93, 133.73, 130.31, 129.59, 125.91, 114.90, 86.08 (sp^{3}-*C* of C_{60}), 70.36 (sp^{3}-*C* of C_{60}), 27.07, 19.97; FT-IR ν/cm^{-1} (KBr) 1672, 1495, 1425, 1364, 1336, 1311, 1263, 1219, 1188, 1091, 1034, 877, 800, 705, 684, 637, 575, 564, 527; UV-Vis ($CHCl_3$) λ_{max}/nm (log ε) 255 (5.06), 313 (4.60), 428 (4.48), 684 (3.55); MALDI-TOF MS *m/z* calcd for $C_{69}H_9NO$ $[M]^-$ 867.0690, found 867.0681.

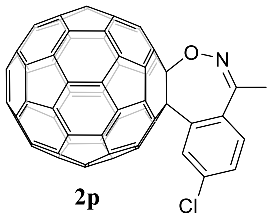

2p

By following the general procedure, a mixture of C_{60} (36.2 mg, 0.05 mmol), **1p** (25.8 mg, 0.15 mmol), $Pd(TFA)_2$ (3.3 mg, 0.01 mmol), $K_2S_2O_8$ (26.9 mg, 0.10 mmol) and TFA (0.25 mL) in ODCB (5 mL) at 100 ^{o}C for 10 h afforded recovered C_{60} (21.2 mg, 59%) and **2p** (4.1 mg, 9%), amorphous brown solid; ^{1}H NMR (400 MHz, $CDCl_2CDCl_2$) δ 8.07 (d, J = 2.2 Hz, 1H), 7.69 (d, J = 8.9 Hz, 1H), 7.54 (dd, J = 8.9, 2.2 Hz, 1H), 2.85 (s, 3H); ^{13}C NMR (101 MHz, $CDCl_2CDCl_2$) δ 168.81 (*C*=N), 151.23, 146.77, 146.64, 146.22, 145.38, 145.34, 145.14, 145.02, 144.83, 144.68, 144.20, 144.17, 144.03, 143.60, 143.41, 143.33, 143.30, 141.85, 141.69, 141.66, 141.06, 140.96, 140.94, 140.60, 140.47, 140.00, 138.31, 136.46, 135.63, 134.10, 132.20, 128.90, 128.70, 125.44, 116.07, 86.28 (sp^{3}-*C* of C_{60}), 69.85 (sp^{3}-*C* of C_{60}), 27.10; FT-IR ν/cm^{-1} (KBr) 1678, 1482, 1436, 1364, 1335, 1305, 1238, 1190, 1099, 979, 875, 803, 770, 624, 577, 564, 527; UV-Vis ($CHCl_3$) λ_{max}/nm (log ε) 256 (5.07), 313 (4.60), 428 (4.46), 682 (3.34); MALDI-TOF MS *m/z* calcd for $C_{68}H_6{}^{35}ClNO$ $[M]^-$ 887.0143, found 887.0132.

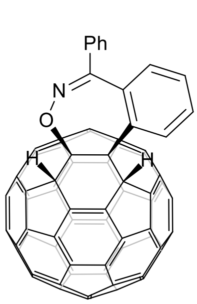

3a

18.4 mg (0.02 mmol) of **2a** was electroreduced by controlled potential electrolysis (CPE) at –1.18 V vs saturated calomel electrode (SCE) in 25 mL of ODCB containing 0.1 M *n*-butylammonium perchlorate (TBAP) under an argon atmosphere at room temperature. The electrolysis was terminated when the theoretical number of coulombs required for a full conversion of **2a** to **2a**$^{2-}$ was reached. Then, the dianion **2a**$^{2-}$ was allowed to react with TFA (2.5 μL, 0.03 mmol) at 25 °C for 10 min. The reaction mixture was filtered through a silica gel (200–300 mesh) plug with CS_2/CH_2Cl_2 (1:1, v/v) to remove TBAP. After evaporation in *vacuo*, the residue was separated on a silica gel (300–400 mesh) column with CS_2 to afford **3a** (7.7 mg, 42%) as an amorphous brown solid; ^{1}H NMR (500 MHz, $CDCl_2CDCl_2/CS_2$) δ 8.02 (d, J = 7.6 Hz, 1H), 7.64–7.50 (m, 5H), 7.32 (t, J = 7.5 Hz, 1H), 7.11 (t, J = 7.9 Hz, 1H), 6.51 (d, J = 1.8 Hz, 1H), 6.43 (d, J = 1.8 Hz, 1H), 6.26 (d, J = 8.5 Hz, 1H); ^{13}C NMR (126 MHz, $CDCl_2CDCl_2/CS_2$) δ 168.32 (*C*=N), 151.46, 148.21, 148.20, 147.73, 147.58, 147.32, 147.24, 146.88, 146.05, 145.93, 145.91, 145.83, 145.81, 145.58, 145.34, 145.33, 145.22, 144.92, 144.53, 144.31, 144.03, 143.98, 143.77, 143.63, 143.60, 143.38, 143.33, 143.28, 143.19, 143.18, 143.12, 143.07, 143.06, 142.72, 142.61, 142.57, 142.47, 142.07, 141.98, 141.94, 141.67, 141.44, 141.42, 141.36, 140.88, 140.78, 140.67, 140.48, 140.05, 139.94, 138.89, 137.74, 136.75, 136.41, 135.53, 134.94, 132.49, 130.54, 128.23, 127.88, 126.62, 124.53, 124.09, 115.14, 79.73 (sp^3-*C* of C_{60}), 63.00 (sp^3-*C* of C_{60}), 58.21 (sp^3-*C* of C_{60}), 56.25 (sp^3-*C* of C_{60}); FT-IR ν/cm^{-1} (KBr) 1658, 1592, 1515, 1479, 1441, 1342, 1315, 1261, 1188, 1141, 1098, 1022, 800, 743, 703, 696, 646, 638, 590, 565, 528, 520; UV-Vis ($CHCl_3$) λ_{max}/nm (log ε) 256 (4.36), 332 (4.43), 430 (3.71), 698 (3.11); MALDI-TOF MS *m/z* calcd for $C_{73}H_{11}NO$ [M]$^-$ 917.0846, found 917.0839.

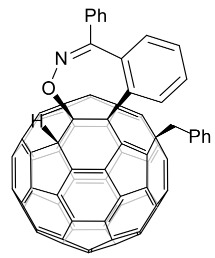

3b

9.2 mg (0.01 mmol) of **2a** was electroreduced by controlled potential electrolysis (CPE) at –1.18 V vs saturated calomel electrode (SCE) in 25 mL of ODCB containing 0.1 M TBAP under an argon atmosphere at room temperature. The electrolysis was terminated when the theoretical number of coulombs required for a full conversion of **2a** to **2a**$^{2-}$ was reached. Then, the dianion **2a**$^{2-}$ was allowed to react with benzyl bromide (5 μL, 0.04 mmol) at 25 °C for 30 min. The reaction mixture was filtered through a silica gel (200–300 mesh) plug with CS_2/CH_2Cl_2 (1:1, v/v) to remove TBAP. The same procedure was carried out for two times. After evaporation in *vacuo*, the residue was separated on a silica gel (300–400 mesh) column with CS_2 to afford **3b** (6.1 mg, 30%) as an amorphous brown solid; ^{1}H NMR (400 MHz, CS_2 with DMSO-d_6 as the external deuterium lock and containing TMS as the reference) δ 8.10 (d, J = 7.1 Hz, 1H), 7.69–7.46 (m, 5H), 7.36 (d, J = 6.8 Hz, 2H), 7.29 (t, J = 7.4 Hz, 1H), 7.27–7.20 (m, 2H), 7.16–7.07 (m, 2H), 6.34 (d, J = 8.2 Hz, 1H), 6.21 (s, 1H), 4.38 (d, J = 13.1 Hz, 1H), 4.17 (d, J = 13.1 Hz, 1H); ^{13}C NMR (126 MHz, CS_2 with DMSO-d_6 as the external deuterium lock and the reference) δ 166.48 (*C*=N), 155.87, 154.39, 151.16, 149.11, 148.53, 148.27, 148.20, 147.68, 147.65, 147.42, 147.36, 147.12, 146.84, 146.72, 146.55, 146.36, 146.21, 145.78, 145.72, 145.68, 145.58, 145.48, 145.36, 145.21, 144.81, 144.77, 144.66, 144.20, 144.15, 144.07, 143.97, 143.79, 143.78, 143.70, 143.66, 143.27, 143.00, 142.75, 142.70, 142.43, 142.32, 141.93, 141.89, 141.72, 141.43, 141.27, 140.92, 140.80, 140.76, 140.59, 140.09, 139.41, 139.06, 138.09, 136.82, 136.35, 135.27, 134.75, 133.27, 131.41, 130.72, 130.45, 129.96, 128.49, 127.77, 126.85, 125.21, 123.48, 115.92, 83.58 (sp^3-*C* of C_{60}), 62.72 (sp^3-*C* of C_{60}), 58.27 (sp^3-*C* of C_{60}), 55.63 (sp^3-*C* of C_{60}), 48.80; FT-IR ν/cm^{-1} (KBr) 1655, 1596, 1541, 1480, 1458, 1446, 1346, 1320, 1260, 1177, 1100, 1027, 799, 747, 699, 641, 590, 565, 526; UV-Vis ($CHCl_3$) λ_{max}/nm (log ε) 252 (4.97), 324 (4.51), 433 (3.71), 687 (3.40); MALDI-TOF MS *m/z* calcd for $C_{80}H_{17}NO$ $[M]^-$ 1007.1316, found 1007.1306.

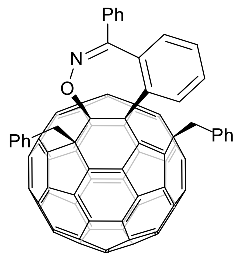

3c

18.4 mg (0.02 mmol) of **2a** was electroreduced by CPE at –1.18 V vs SCE in 50 mL of ODCB containing 0.1 M TBAP under an argon atmosphere at room temperature. The electrolysis was terminated when the theoretical number of coulombs required for a full conversion of **2a** to **2a**$^{2-}$ was reached. Then, the dianion **2a**$^{2-}$ was allowed to react with benzyl bromide (120 μL, 1.0 mmol) at 25 °C for 6 h. The reaction mixture was filtered through a silica gel (200–300 mesh) plug with CS_2 (1:1, v/v) to remove TBAP. After evaporation in *vacuo*, the residue was separated on a silica gel (300–400 mesh) column with CS_2 to afford **3c** (6.8 mg, 31%) as an amorphous brown solid; ^{1}H NMR (500 MHz, CS_2 with DMSO-d_6 as the external deuterium lock and containing TMS as the reference) δ 8.10 (d, *J* = 7.6 Hz, 1H), 7.63–7.49 (m, 4H), 7.44–7.31 (m, 5H), 7.27–7.20 (m, 3H), 7.12 (t, *J* = 7.8 Hz, 1H), 7.09–7.01 (m, 4H), 6.40 (d, *J* = 8.2 Hz, 1H), 4.81 (d, *J* = 12.1 Hz, 1H), 4.36 (d, *J* = 13.0 Hz, 1H), 4.15 (d, *J* = 13.0 Hz, 1H), 3.81 (d, *J* = 12.1 Hz, 1H); ^{13}C NMR (126 MHz, CS_2 with DMSO-d_6 as the external deuterium lock and the reference) δ 166.95 (*C*=N), 155.18, 154.93, 151.89, 150.83, 149.18, 148.94, 148.19, 147.77, 147.49, 147.46, 147.37, 147.14, 146.72, 146.20, 146.14, 145.95, 145.89, 145.77, 145.53, 145.48, 145.44, 145.34, 145.29, 145.00, 144.98, 144.72, 144.51, 144.24, 144.18, 144.02, 143.92, 143.85, 143.76, 143.70, 143.55, 143.42, 143.20, 142.91, 142.35, 142.18, 142.13, 141.97, 141.38, 141.30, 140.97, 140.73, 140.67, 140.56, 139.99, 139.42, 138.85, 138.69, 137.87, 137.81, 136.49, 136.27, 135.75, 134.82, 134.63, 132.98, 131.30, 131.12, 130.70, 129.93, 128.44, 128.14, 128.01, 127.74, 127.30, 126.81, 126.29, 124.96, 123.88, 117.36, 88.80 (sp^3-*C* of C_{60}), 64.22 (sp^3-*C* of C_{60}), 62.08 (sp^3-*C* of C_{60}), 58.31 (sp^3-*C* of C_{60}), 48.56, 44.76; FT-IR ν/cm^{-1} (KBr) 1656, 1597, 1494, 1480, 1454, 1446, 1345, 1319, 1259, 1175, 1143, 1099, 1023, 800, 793, 747, 698, 676, 642, 577, 535, 526; UV-Vis ($CHCl_3$) λ_{max}/nm (log ε) 250 (5.04), 323 (4.62), 449 (3.77), 698 (3.48); MALDI-TOF MS *m/z* calcd for $C_{87}H_{23}NO$ $[M]^-$ 1097.1785, found 1097.1778.

4. Kinetic isotope effect study for the formation of 2d

By following the general procedure, a mixture of C_{60} (36.0 mg, 0.05 mmol) with **1d** (12.8 mg, 0.05 mmol), **1d**-d_5 (12.9 mg, 0.05 mmol), $Pd(TFA)_2$ (1.8 mg, 0.005 mmol), $Na_2S_2O_8$ (24.1 mg, 0.10 mmol) and TFA (0.25 mL) in ODCB (5 mL) at 100 ^{o}C for 3 h. The same procedure had been carried out twice. The reaction mixtures from the two runs were combined and filtered through a silica gel plug to remove insoluble material. After the solvent had been evaporated in *vacuo*, the residue was separated on a silica gel column with CS_2 to afford recovered C_{60} (56.4 mg, 78%), and then with CS_2/DCM (4:1) to provide products **2d** and **2d**-d_4 (6.5 mg, 7%). The KIE was determined as 3.12 by analyzing the integrals in the ^{1}H NMR spectrum.

5. NMR spectra of compounds 2a–p and 3a–c

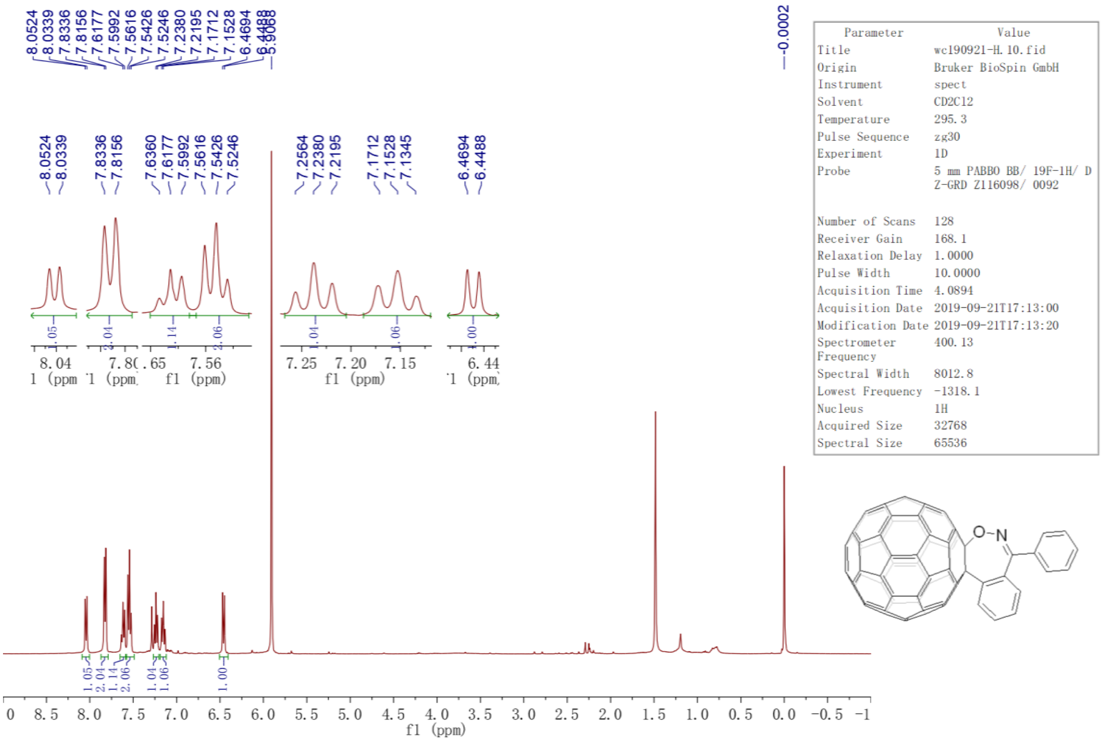

Figure S1 ^{1}H NMR (400 MHz, $CDCl_2CDCl_2/CS_2$) of compound 2a

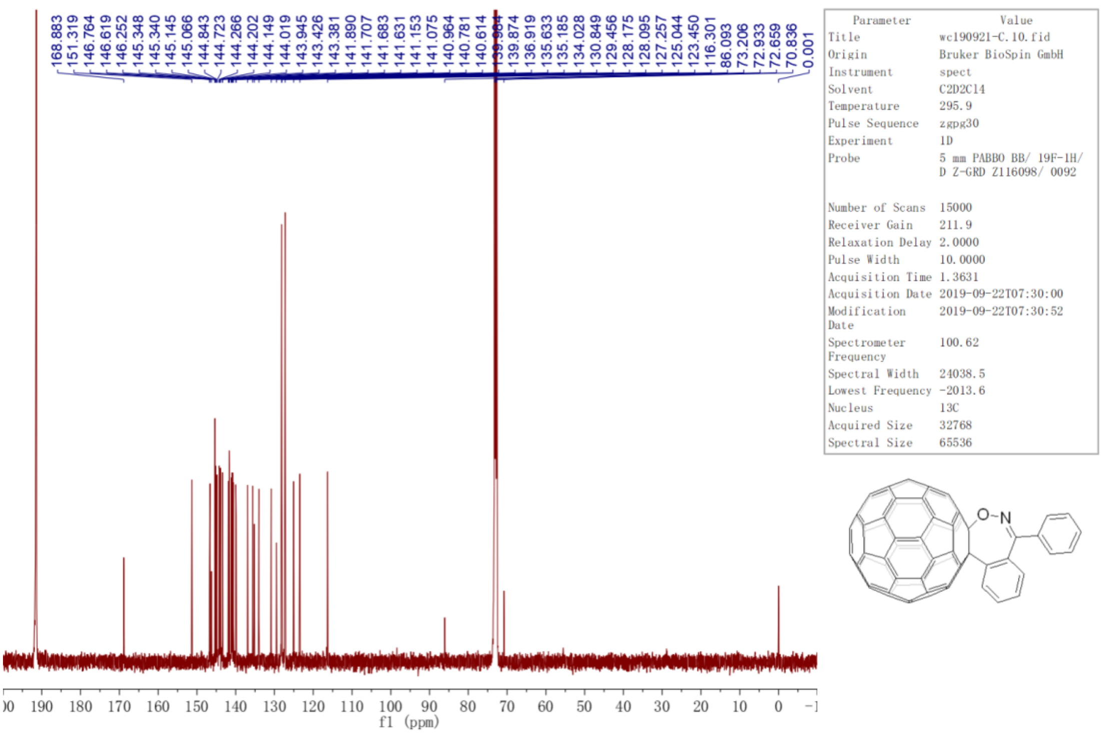

Figure S2 ^{13}C NMR (101 MHz, $CDCl_2CDCl_2/CS_2$) of compound 2a

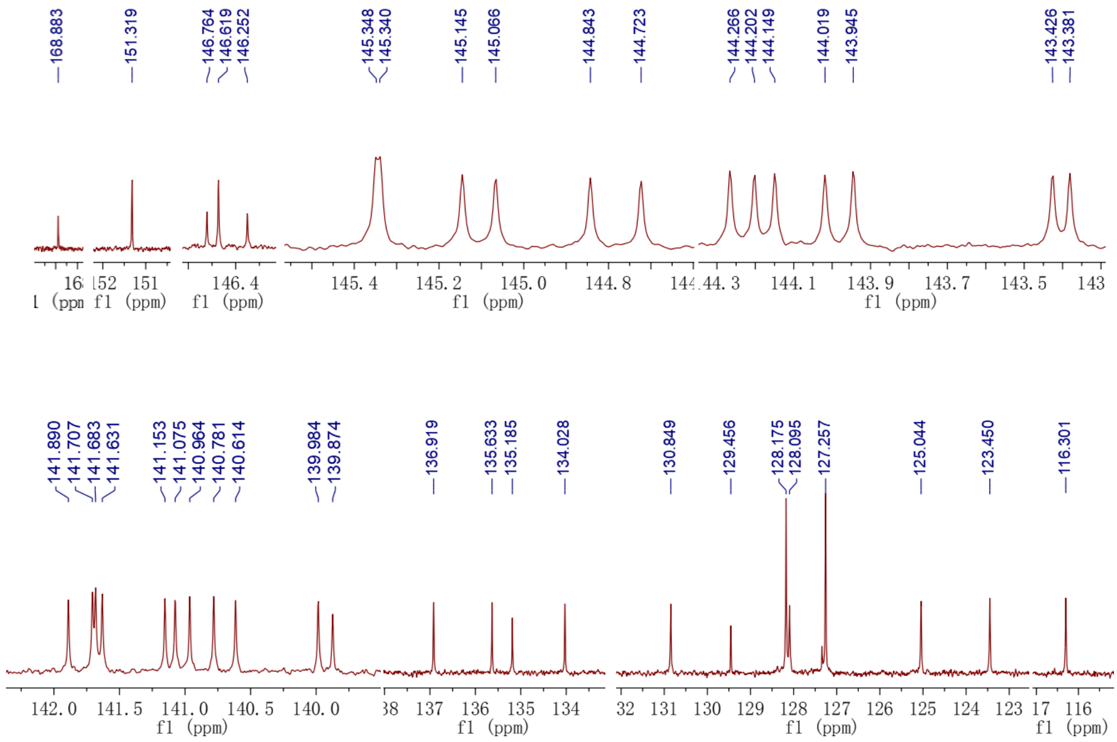

Figure S3 Expanded ^{13}C NMR (101 MHz, $CDCl_2CDCl_2/CS_2$) of compound 2a

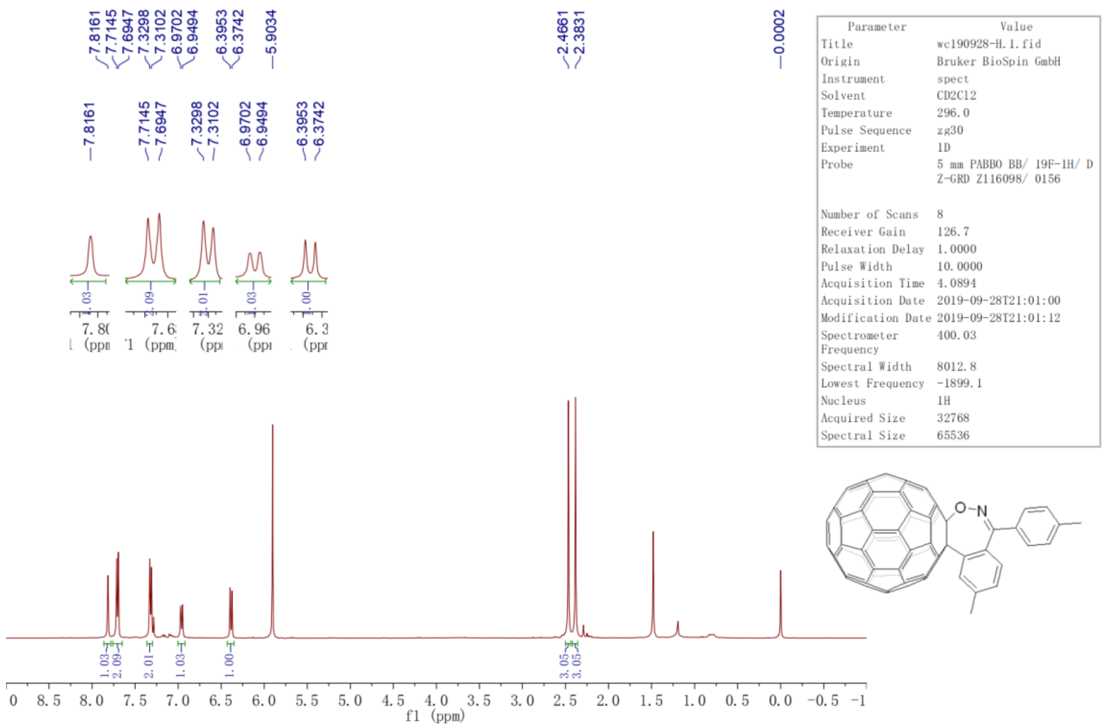

Figure S4 ^{1}H NMR (400 MHz, $CDCl_2CDCl_2/CS_2$) of compound 2b

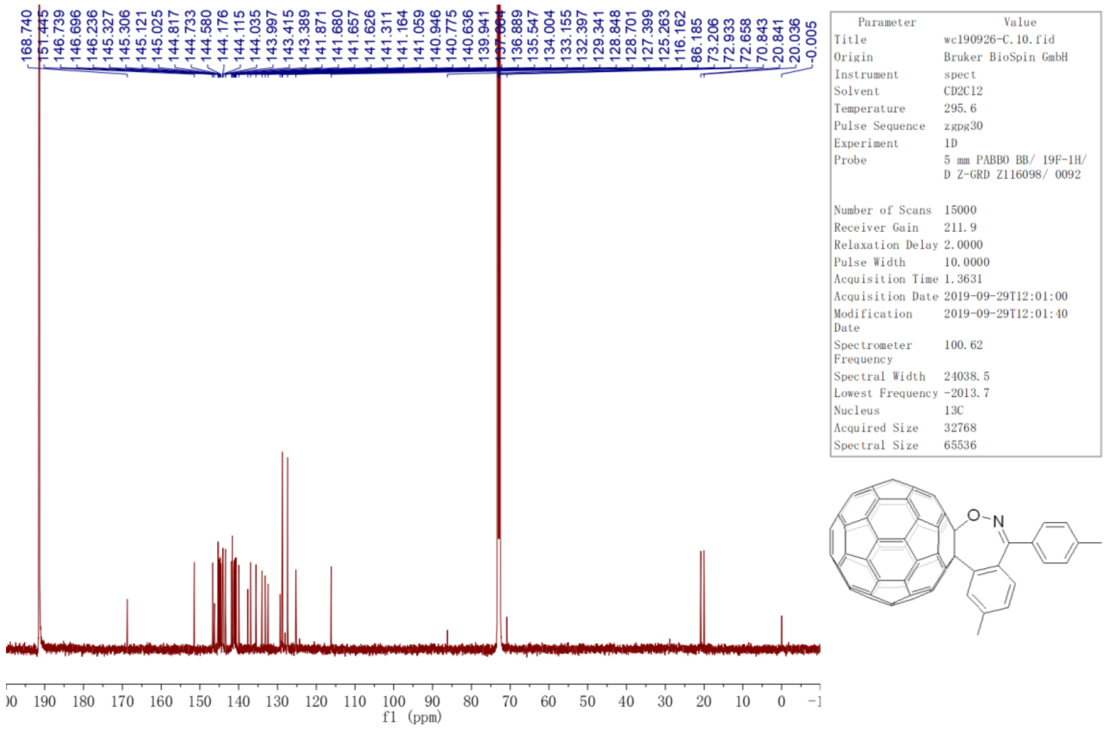

Figure S5 ^{13}C NMR (101 MHz, $CDCl_2CDCl_2/CS_2$) of compound 2b

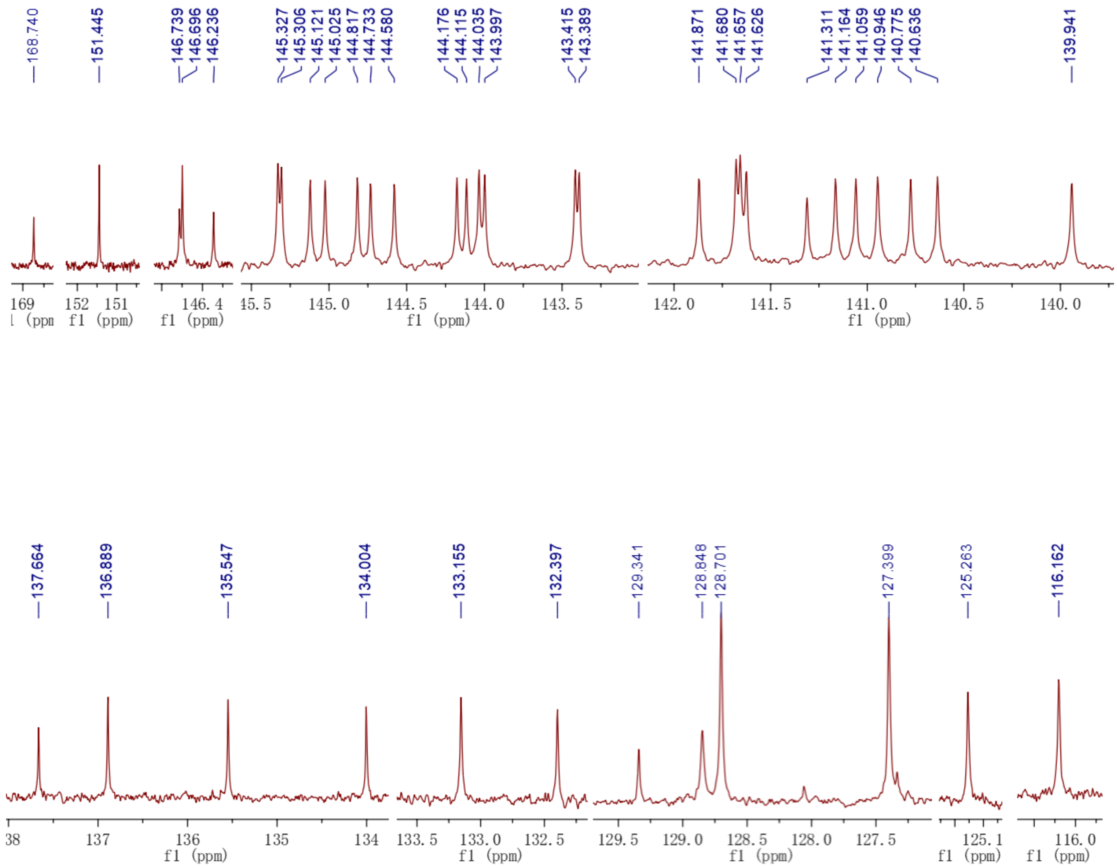

Figure S6 Expanded ^{13}C NMR (101 MHz, $CDCl_2CDCl_2/CS_2$) of compound 2b

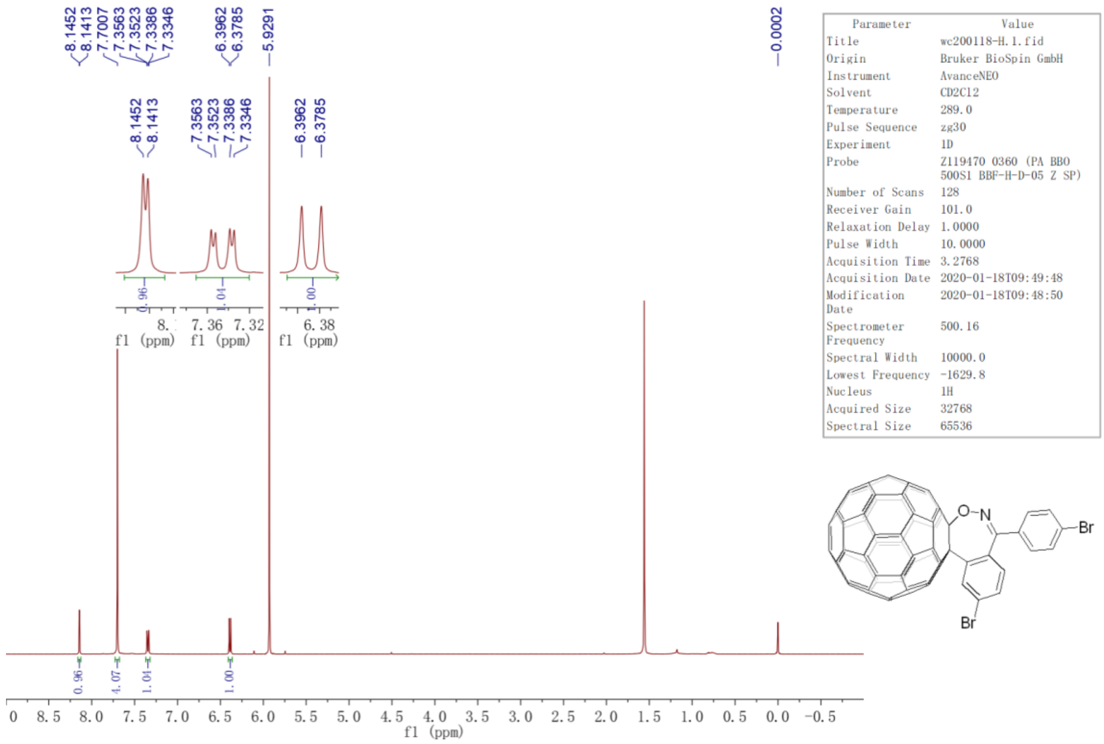

Figure S7 ^{1}H NMR (500 MHz, $CDCl_2CDCl_2$) of compound 2c

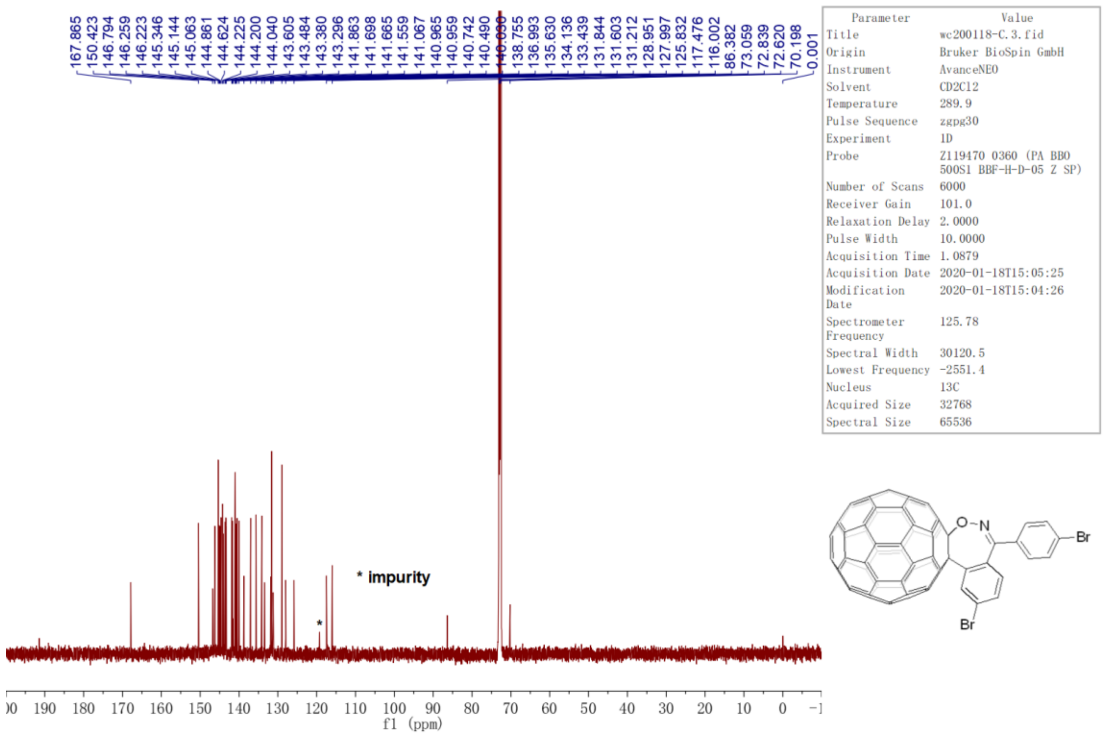

Figure S8 ^{13}C NMR (126 MHz, $CDCl_2CDCl_2$) of compound 2c

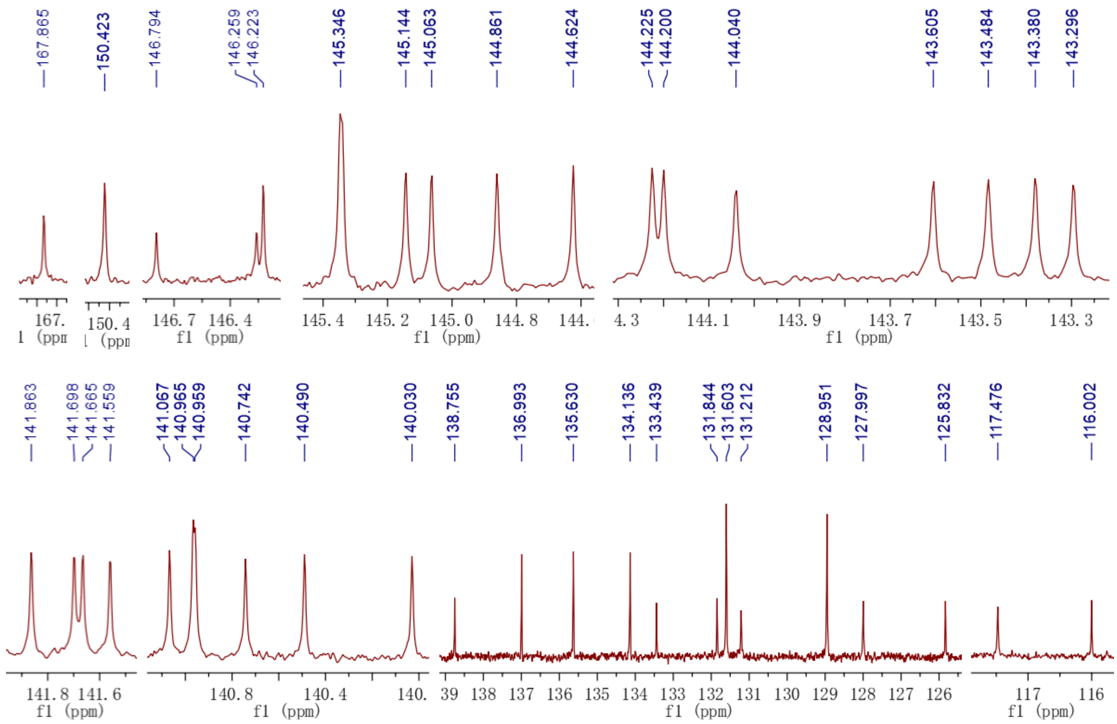

Figure S9 Expanded ^{13}C NMR (126 MHz, $CDCl_2CDCl_2$) of compound 2c

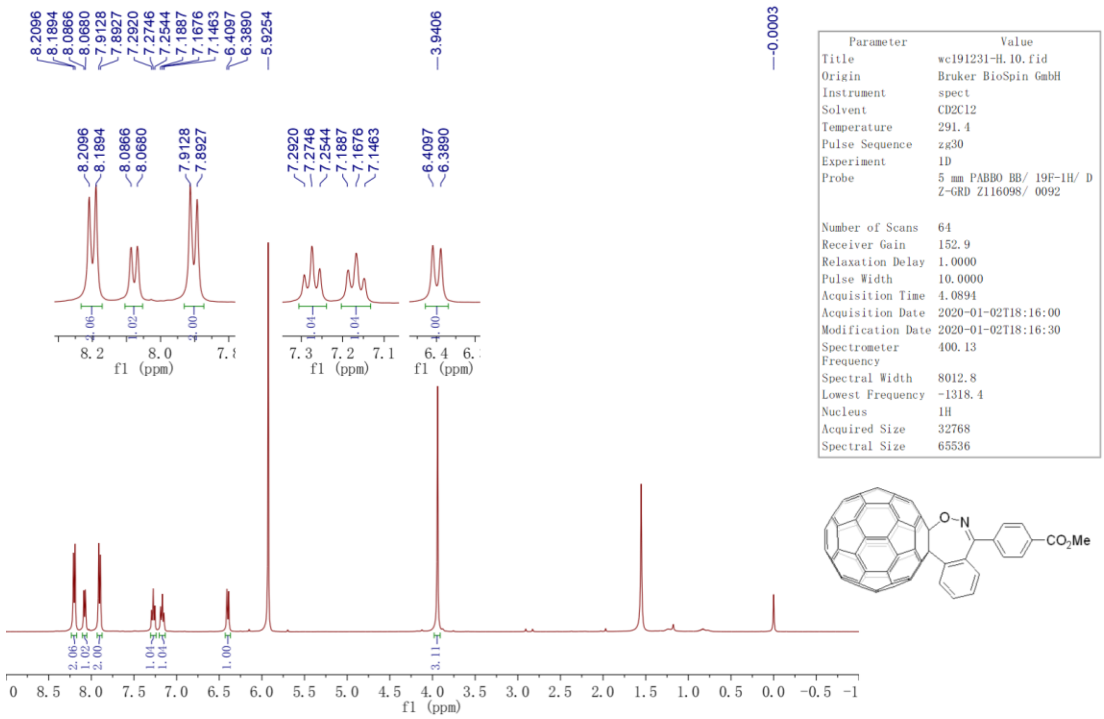

Figure S10 ^{1}H NMR (400 MHz, $CDCl_2CDCl_2$) of compound 2d

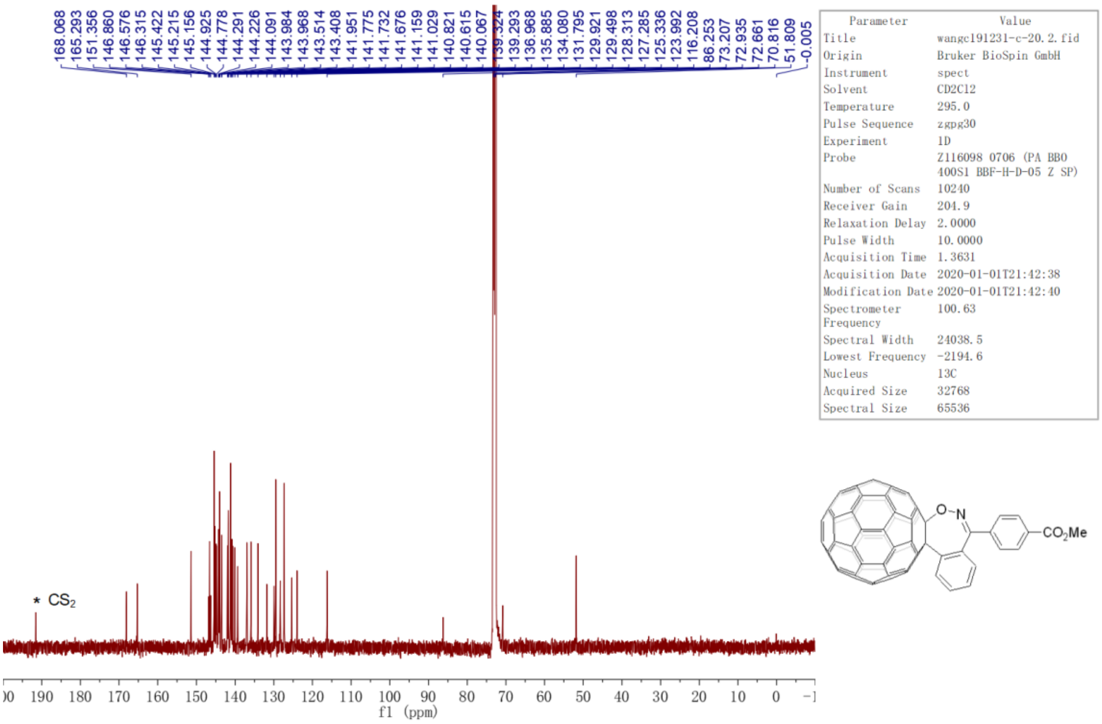

Figure S11 ^{13}C NMR (101 MHz, $CDCl_2CDCl_2$) of compound 2d

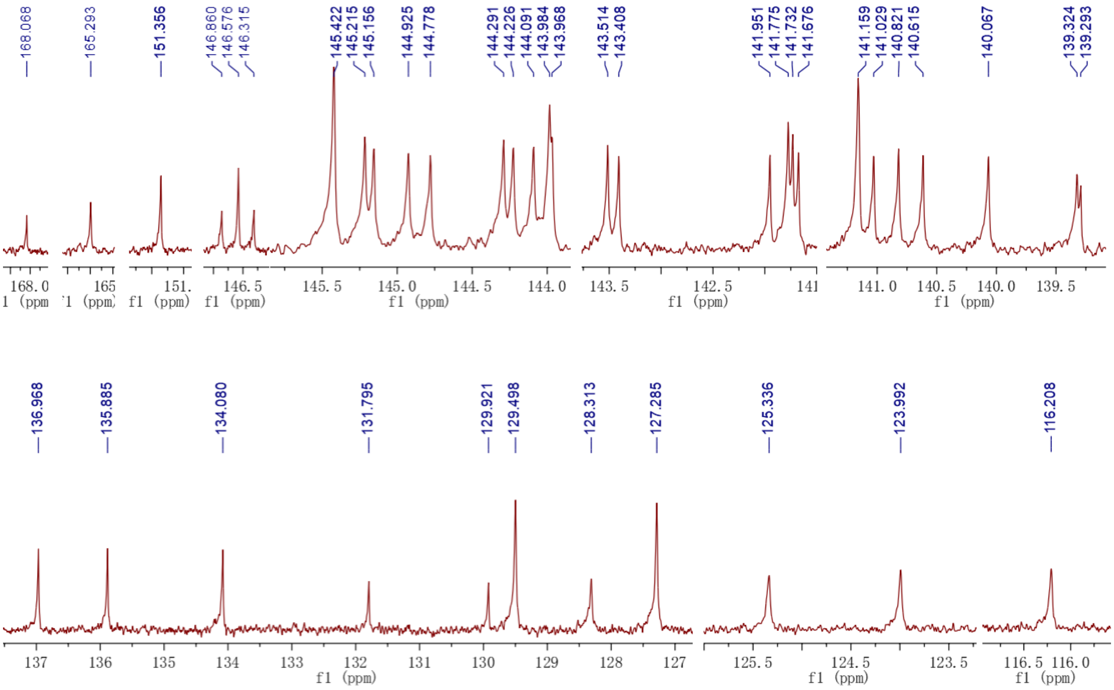

Figure S12 Expanded ^{13}C NMR (101 MHz, $CDCl_2CDCl_2$) of compound 2d

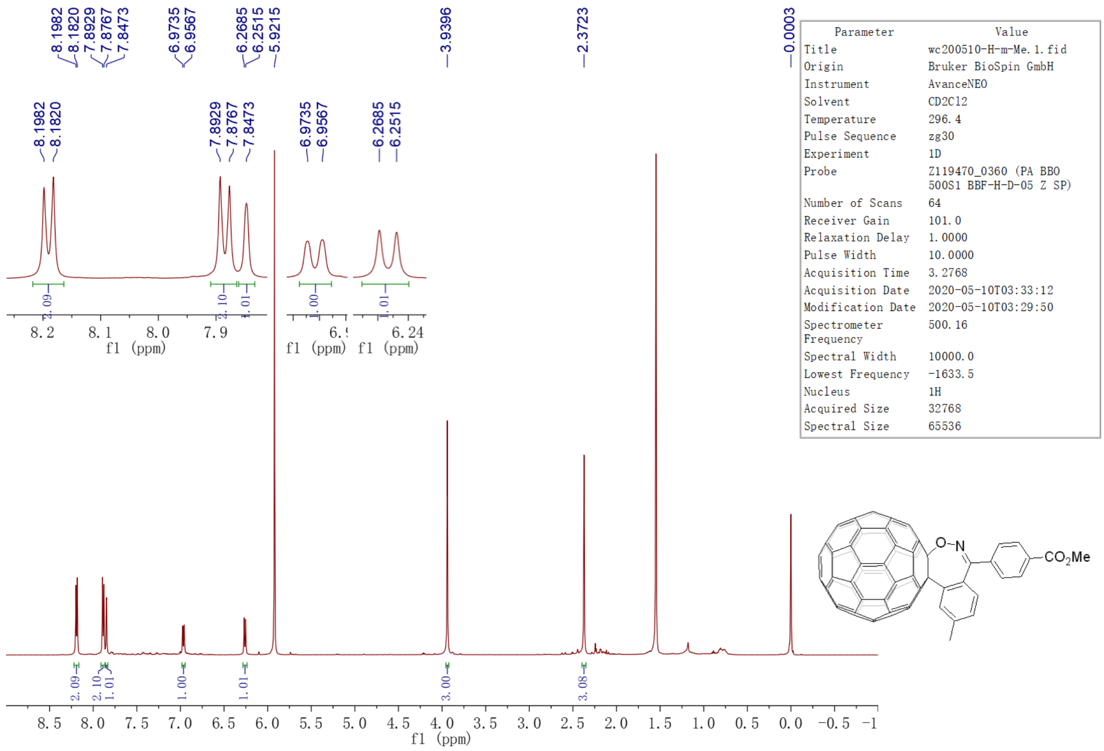

Figure S13 ^{1}H NMR (500 MHz, $CDCl_2CDCl_2$) of compound 2e

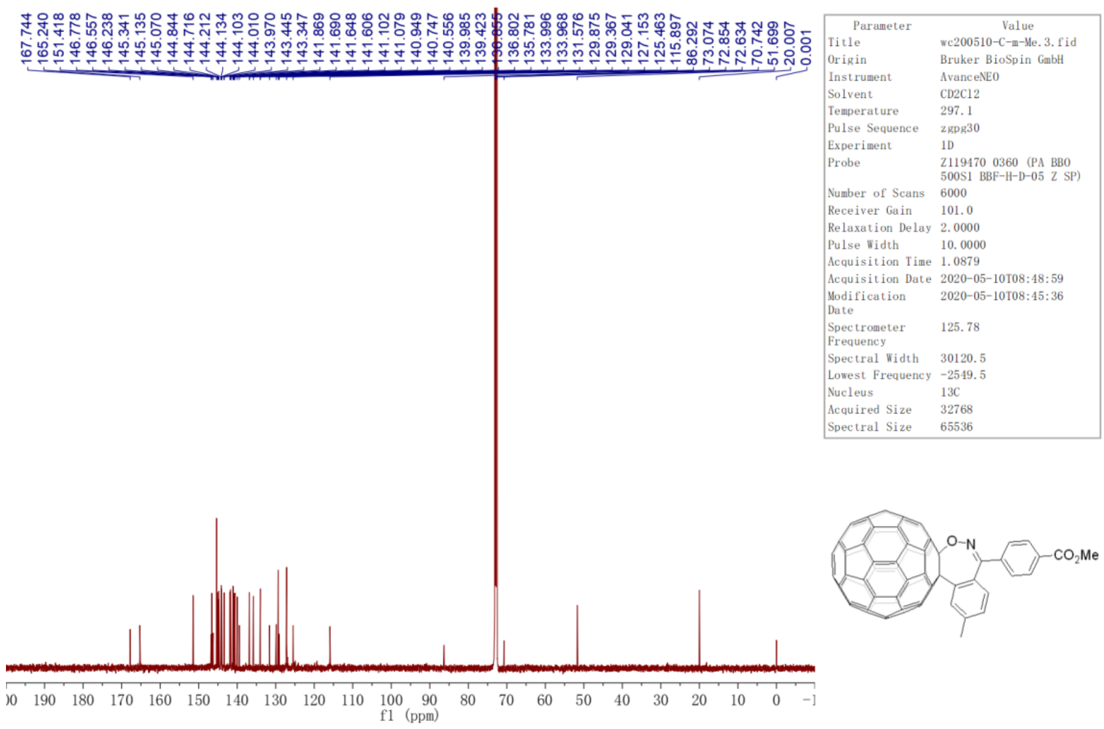

Figure S14 ^{13}C NMR (126 MHz, $CDCl_2CDCl_2$) of compound 2e

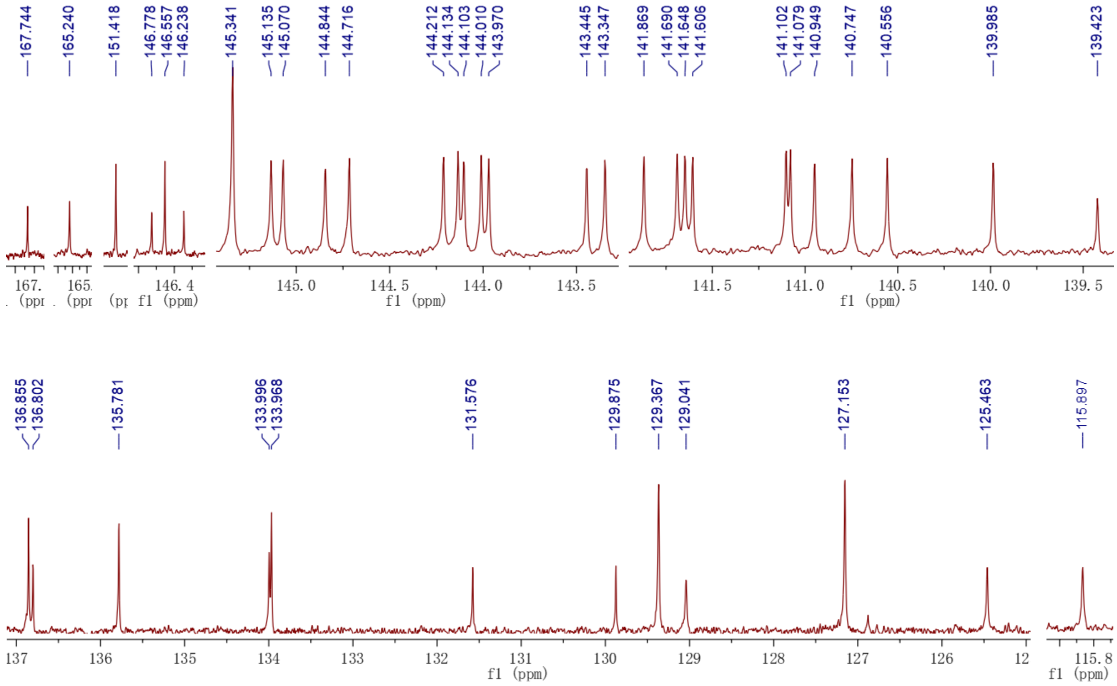

Figure S15 Expanded ^{13}C NMR (126 MHz, $CDCl_2CDCl_2$) of compound 2e

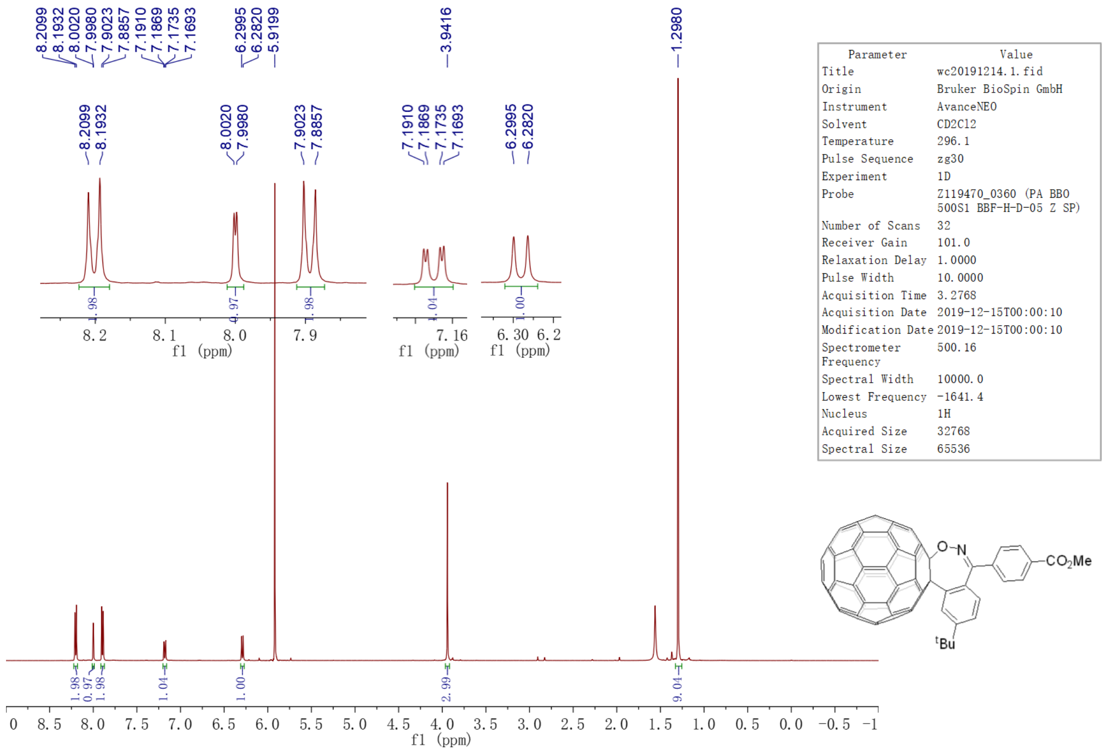

Figure S16 ^{1}H NMR (500 MHz, $CDCl_2CDCl_2$) of compound 2f

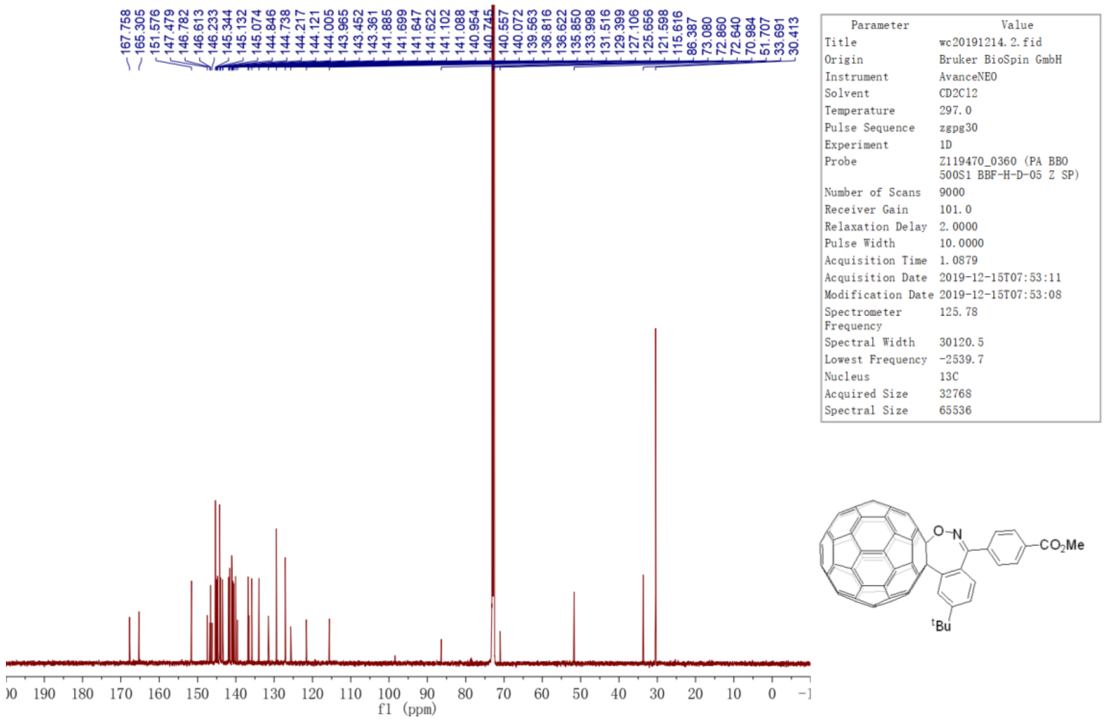

Figure S17 ^{13}C NMR (126 MHz, CDCl$_2$CDCl$_2$) of compound 2f

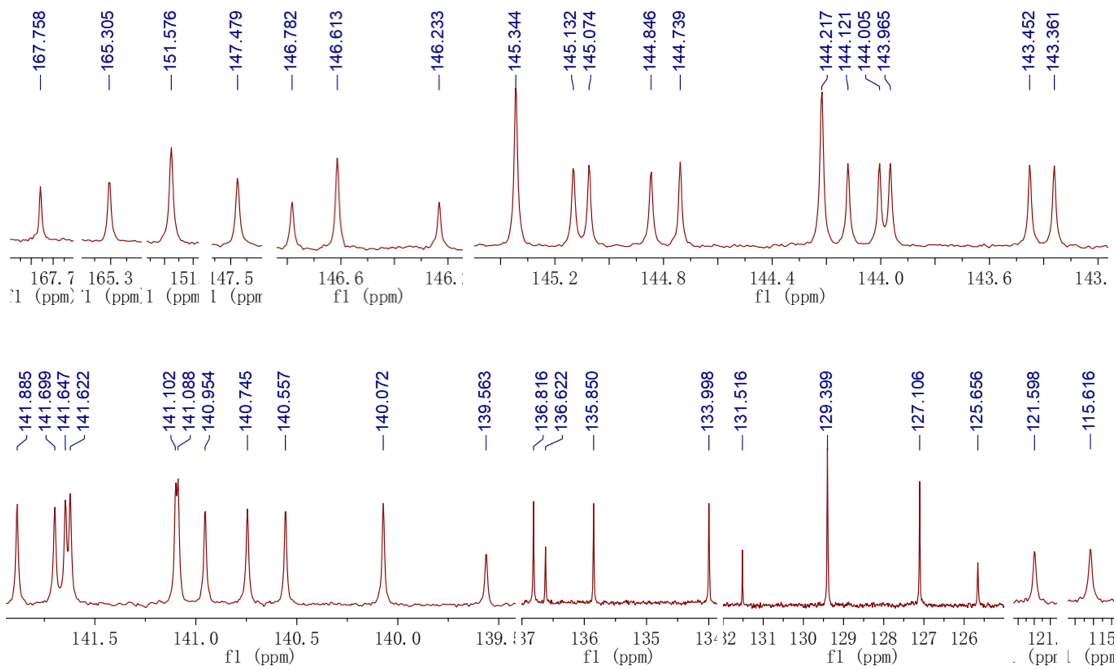

Figure S18 Expanded ^{13}C NMR (126 MHz, CDCl$_2$CDCl$_2$) of compound 2f

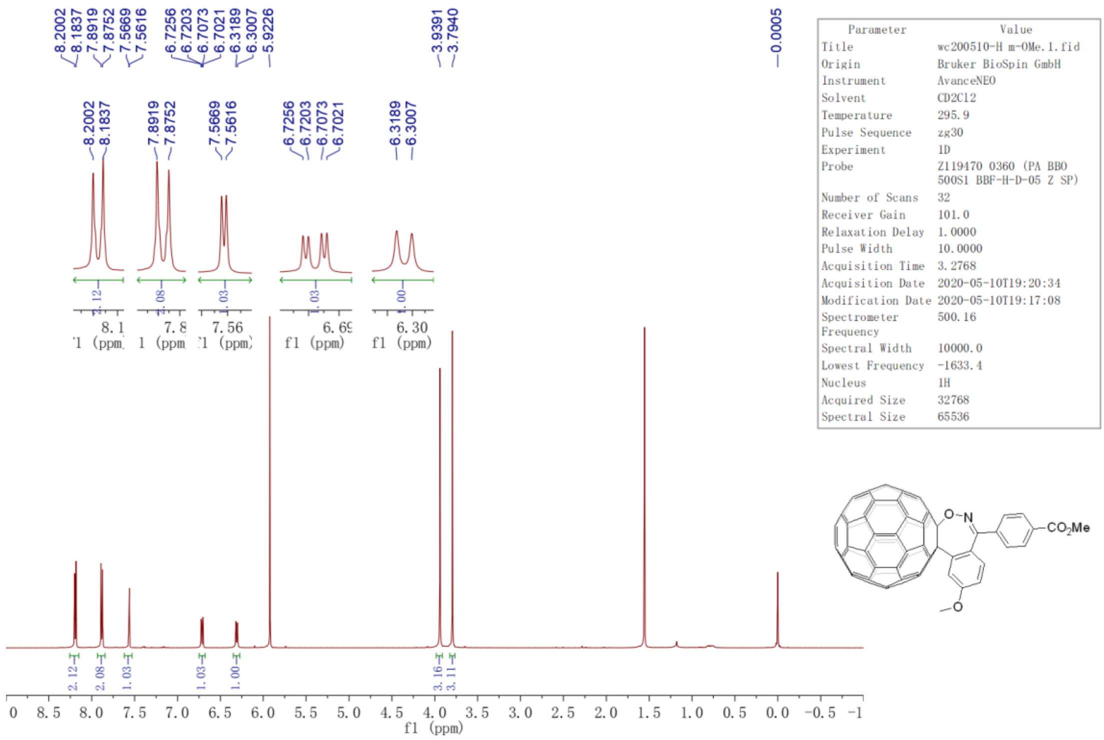

Figure S19 ^{1}H NMR (500 MHz, $CDCl_2CDCl_2$) of compound 2g

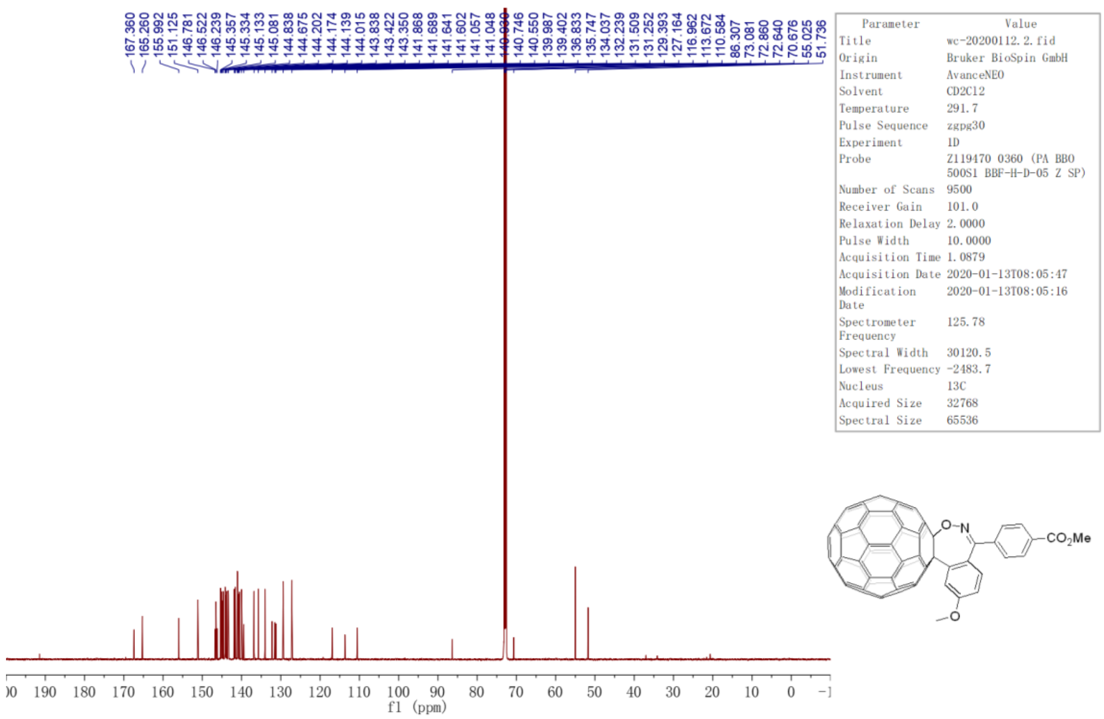

Figure S20 ^{13}C NMR (126 MHz, $CDCl_2CDCl_2$) of compound 2g

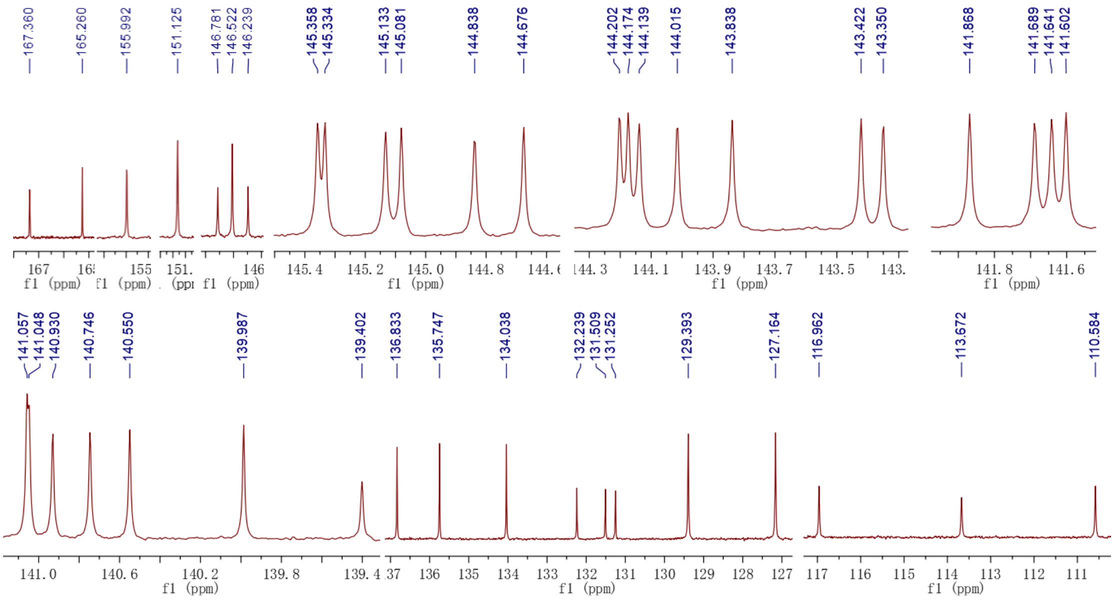

Figure S21 Expanded ^{13}C NMR (126 MHz, $CDCl_2CDCl_2$) of compound 2g

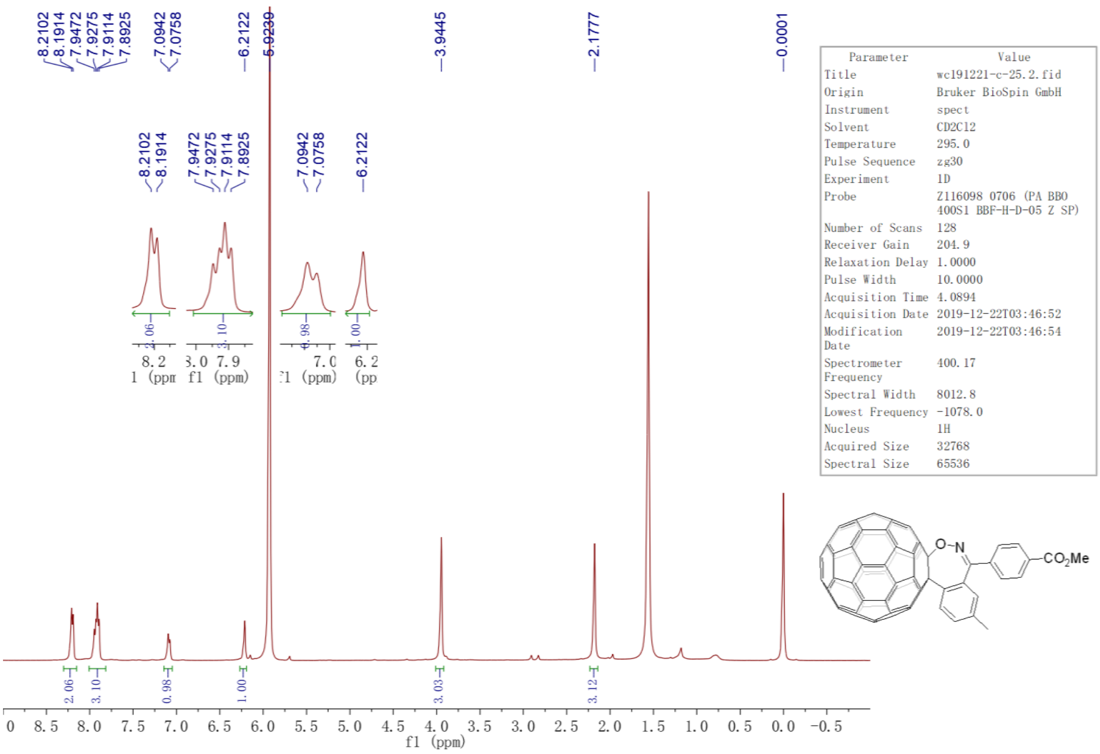

Figure S22 ^{1}H NMR (400 MHz, $CDCl_2CDCl_2$) of compound 2h

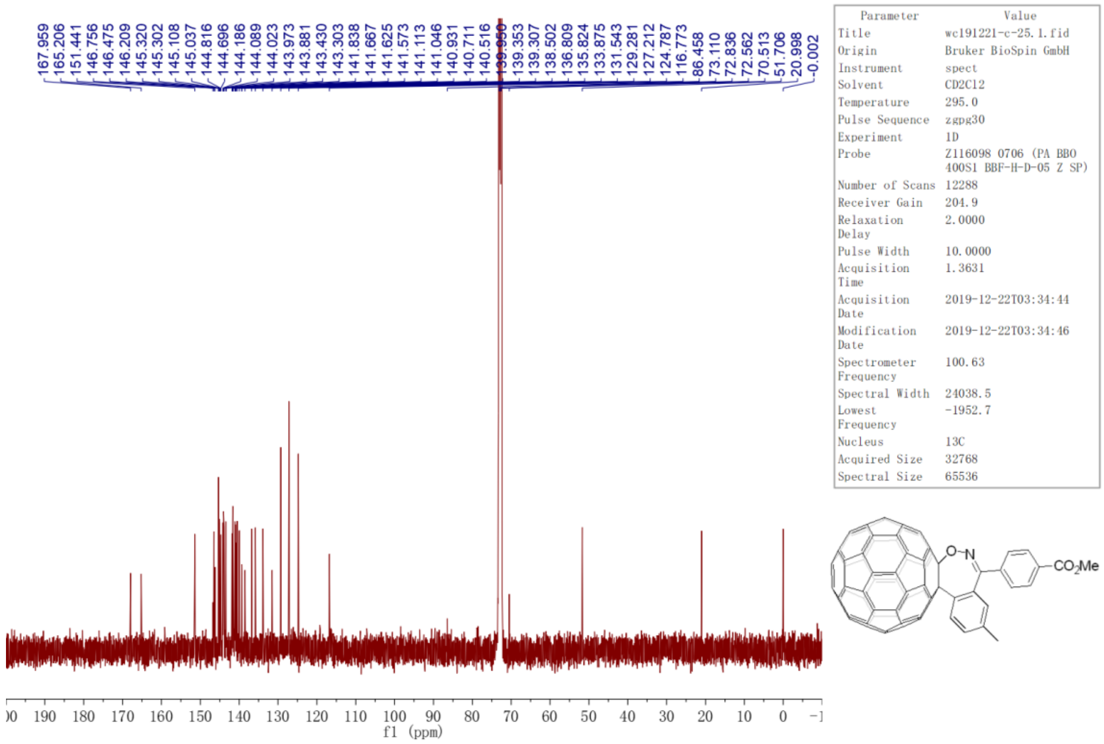

Figure S23 ^{13}C NMR (101 MHz, $CDCl_2CDCl_2$) of compound 2h

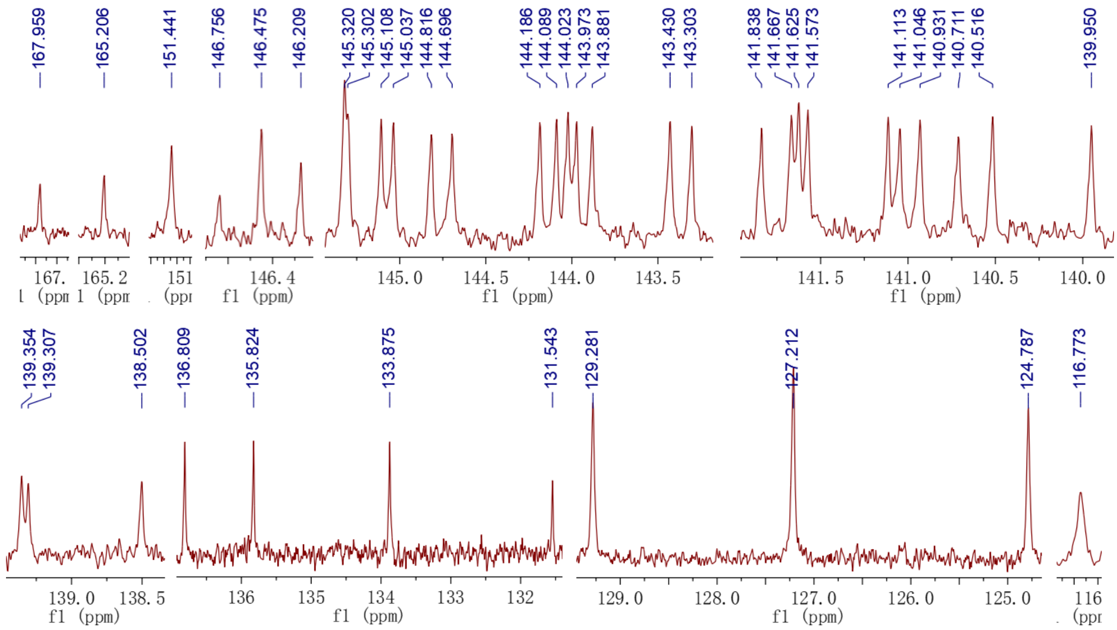

Figure S24 Expanded ^{13}C NMR (101 MHz, $CDCl_2CDCl_2$) of compound 2h

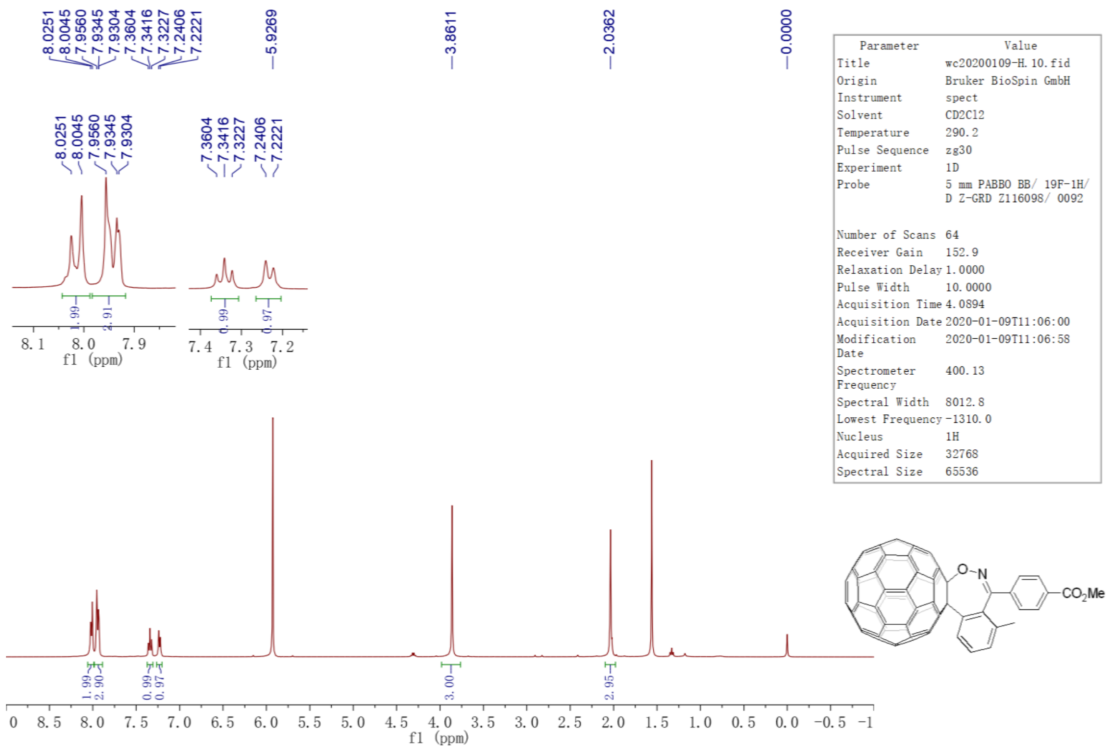

Figure S25 ^{1}H NMR (400 MHz, $CDCl_2CDCl_2$) of compound 2i

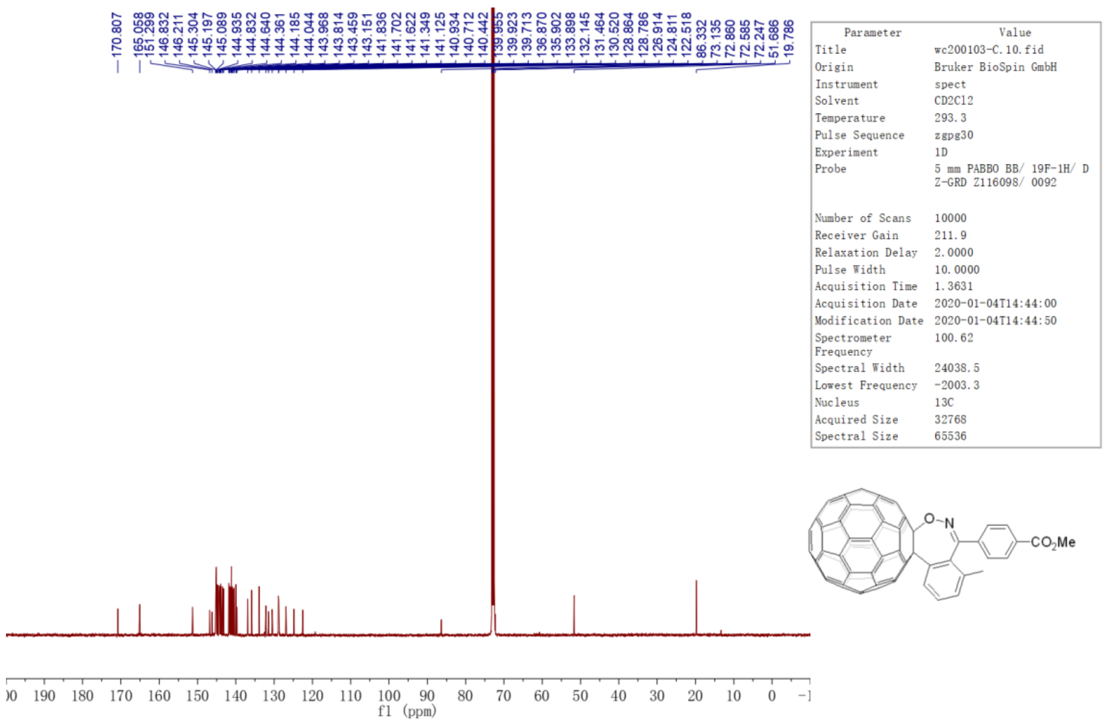

Figure S26 ^{13}C NMR (101 MHz, $CDCl_2CDCl_2$) of compound 2i

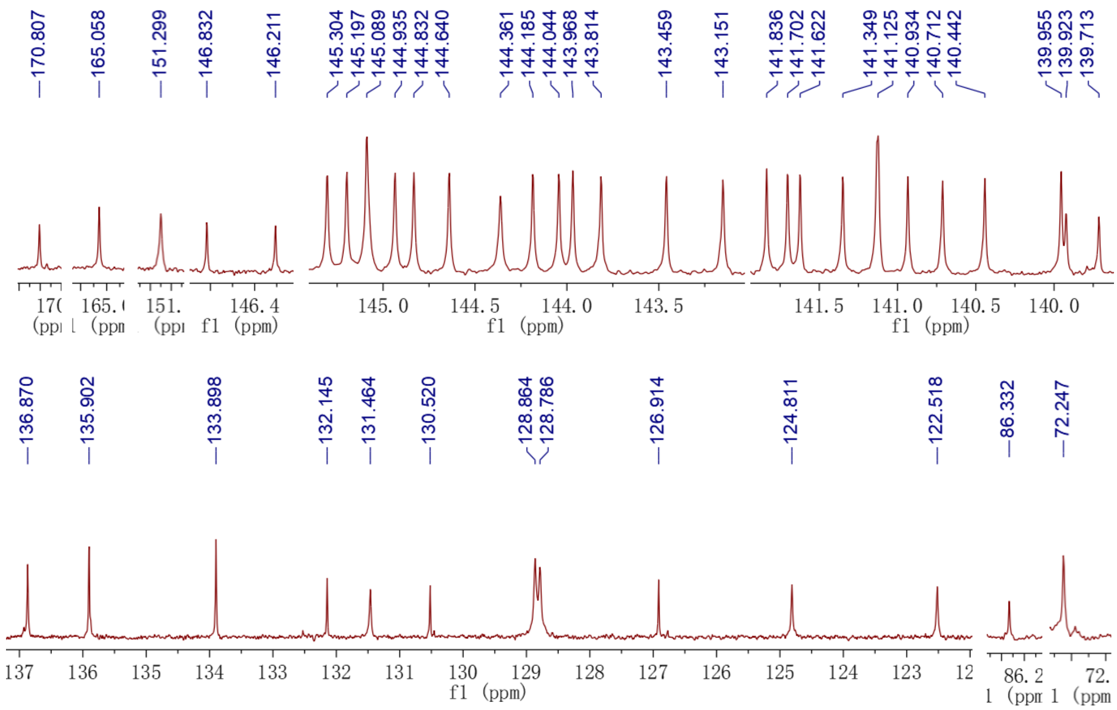

Figure S27 Expanded ^{13}C NMR (101 MHz, $CDCl_2CDCl_2$) of compound 2i

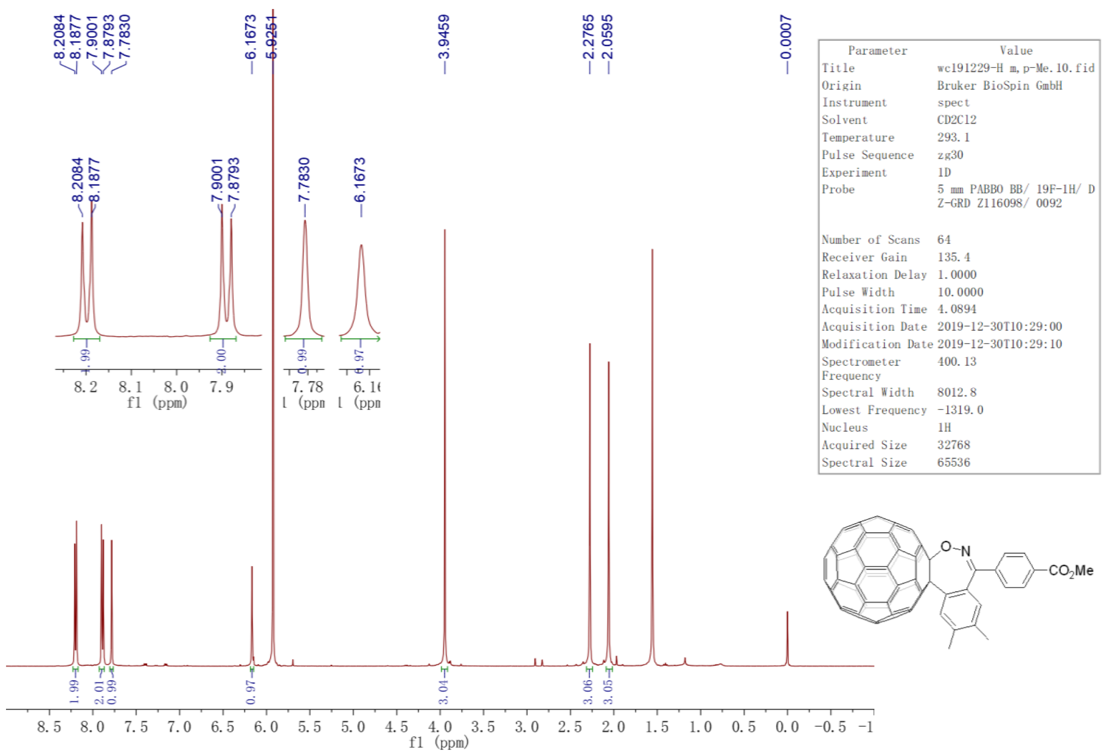

Figure S28 ^{1}H NMR (400 MHz, $CDCl_2CDCl_2$) of compound 2j

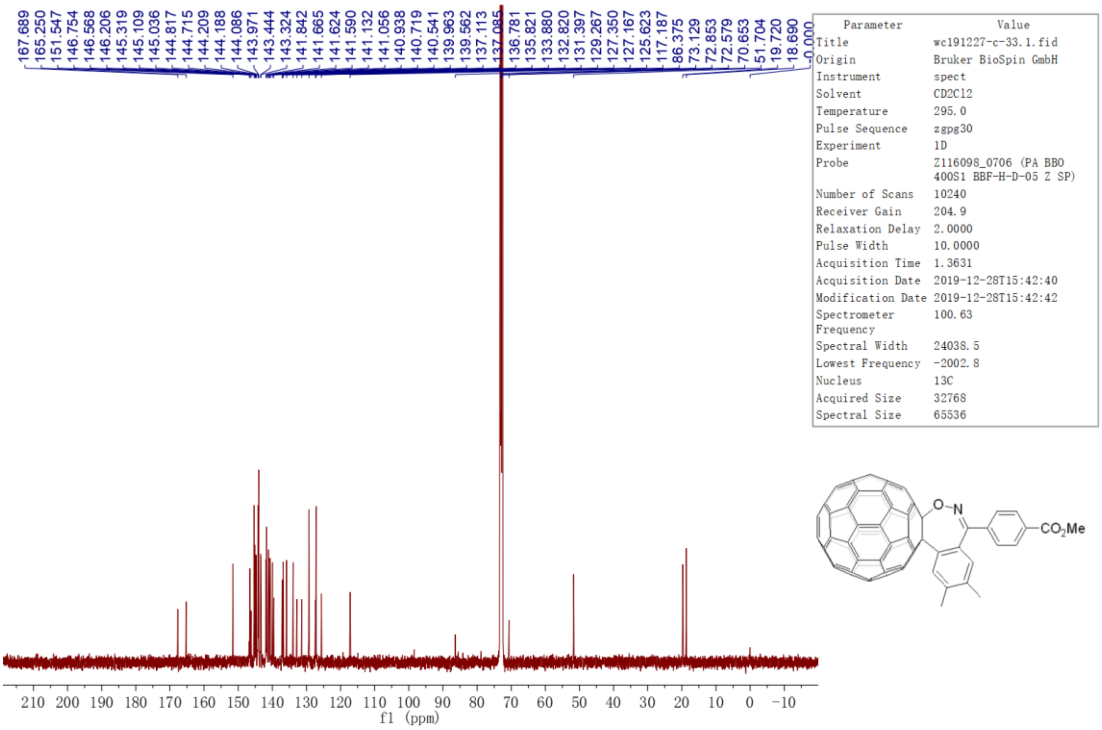

Figure S29 ^{13}C NMR (101 MHz, CDCl₂CDCl₂) of compound 2j

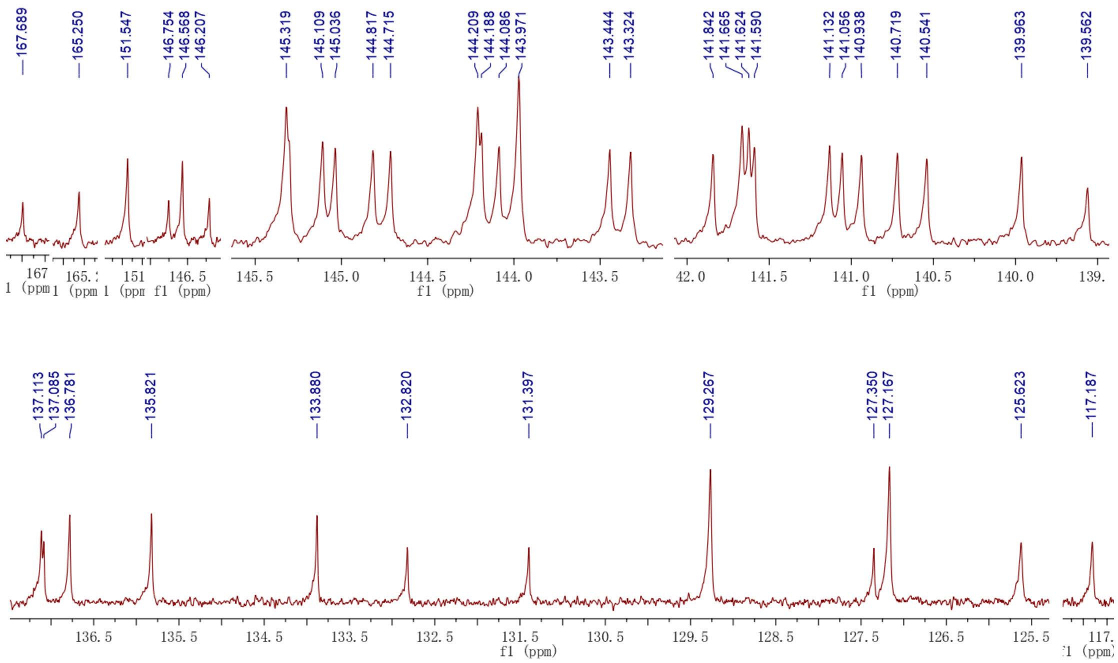

Figure S30 Expanded ^{13}C NMR (101 MHz, CDCl₂CDCl₂) of compound 2j

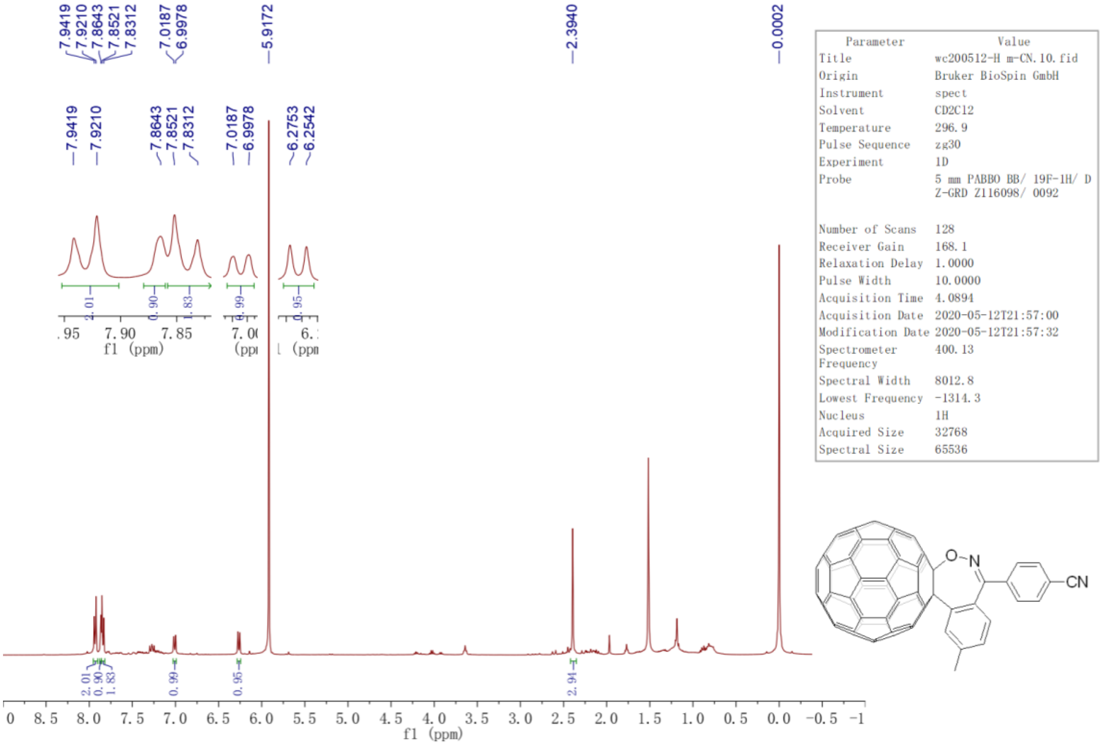

Figure S31 ¹H NMR (400 MHz, CDCl₂CDCl₂) of compound 2j

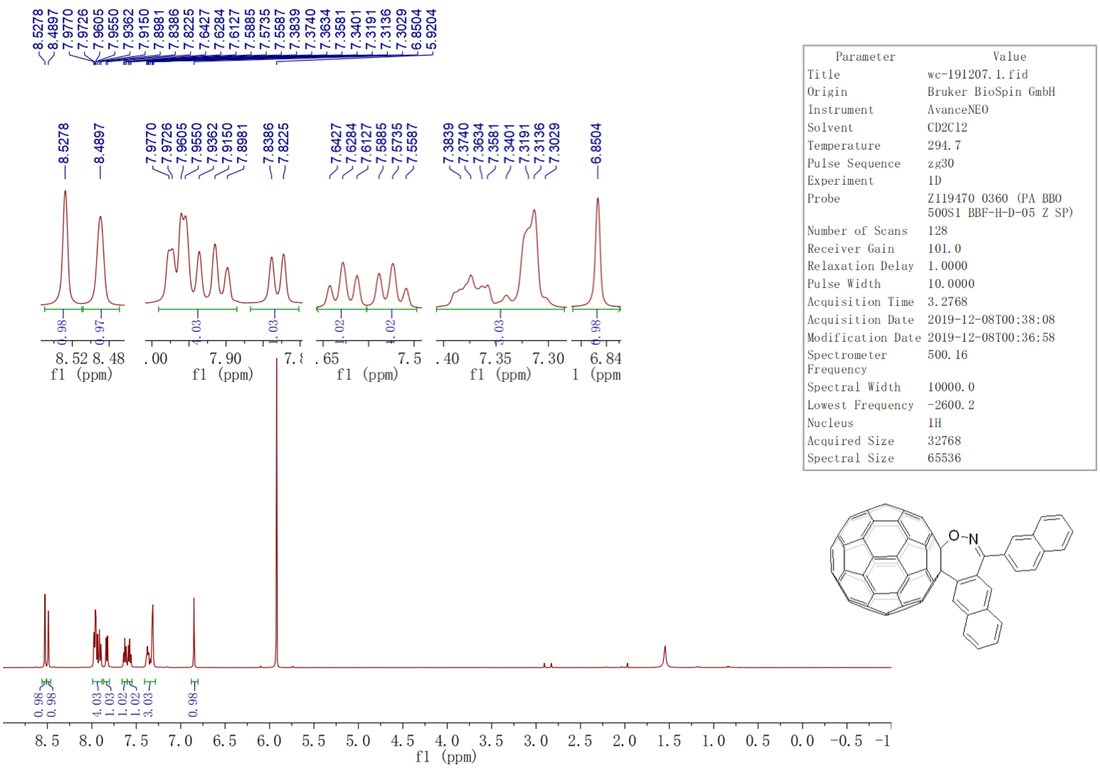

Figure S32 ¹H NMR (500 MHz, CDCl₂CDCl₂) of compound 2l

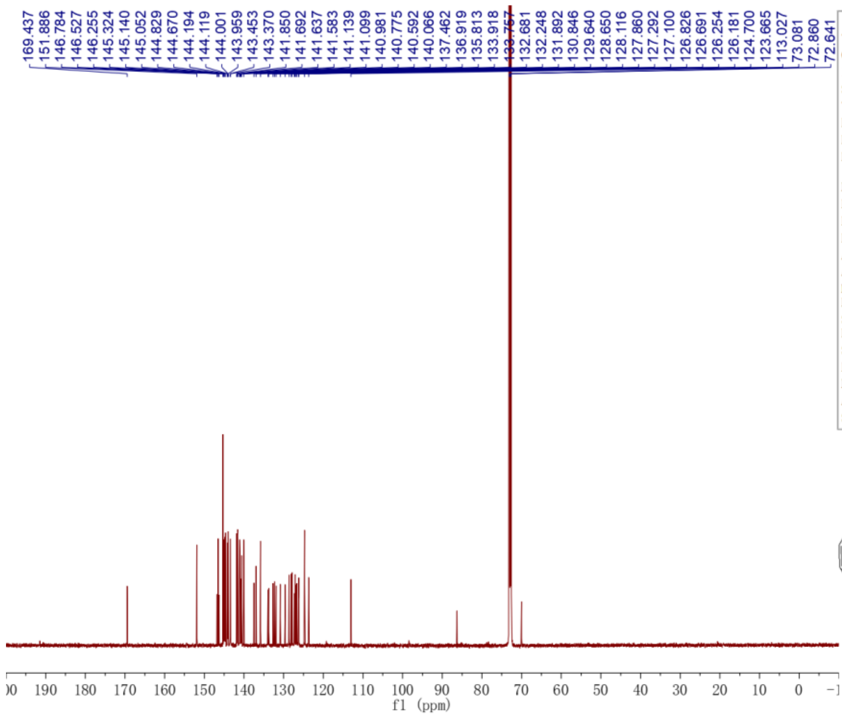

Parameter	Value
Title	wc-191207.2.fid
Origin	Bruker BioSpin GmbH
Instrument	AvanceNEO
Solvent	CD2Cl2
Temperature	295.3
Pulse Sequence	zgpg30
Experiment	1D
Probe	Z119470_0360 (PA BBO 500S1 BBF-H-D-05 Z SP)
Number of Scans	9000
Receiver Gain	101.0
Relaxation Delay	2.0000
Pulse Width	10.0000
Acquisition Time	1.0879
Acquisition Date	2019-12-08T08:31:15
Modification Date	2019-12-08T08:30:02
Spectrometer Frequency	125.78
Spectral Width	30120.5
Lowest Frequency	-2798.9
Nucleus	13C
Acquired Size	32768
Spectral Size	65536

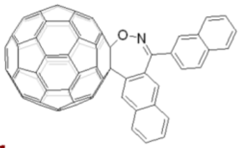

Figure S33 ^{13}C NMR (126 MHz, $CDCl_2CDCl_2$) of compound 2l

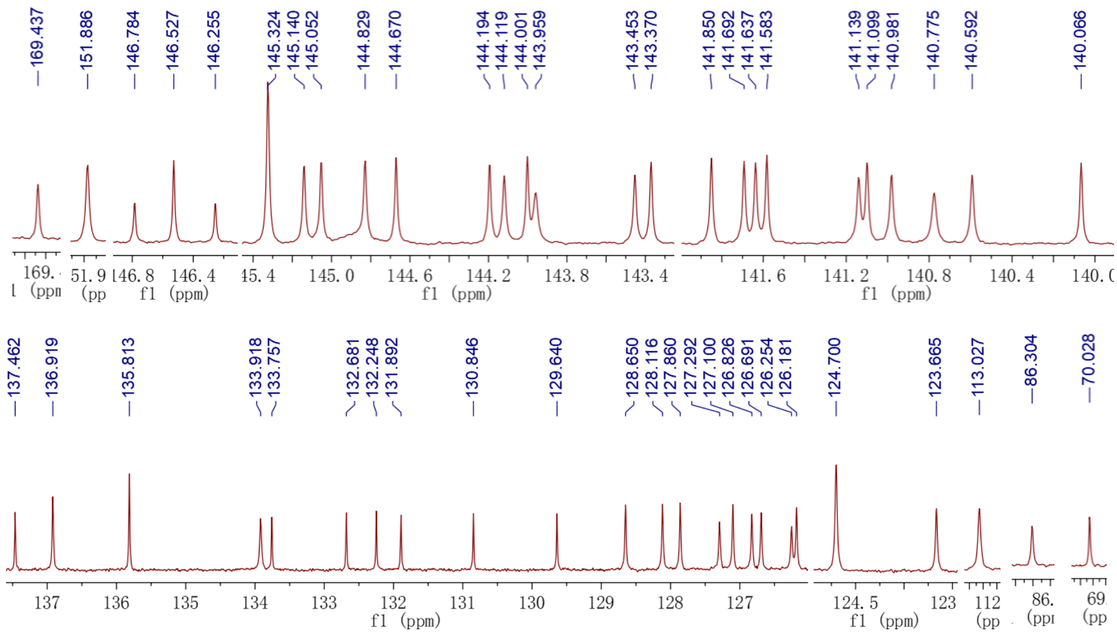

Figure S34 Expanded ^{13}C NMR (126 MHz, $CDCl_2CDCl_2$) of compound 2l

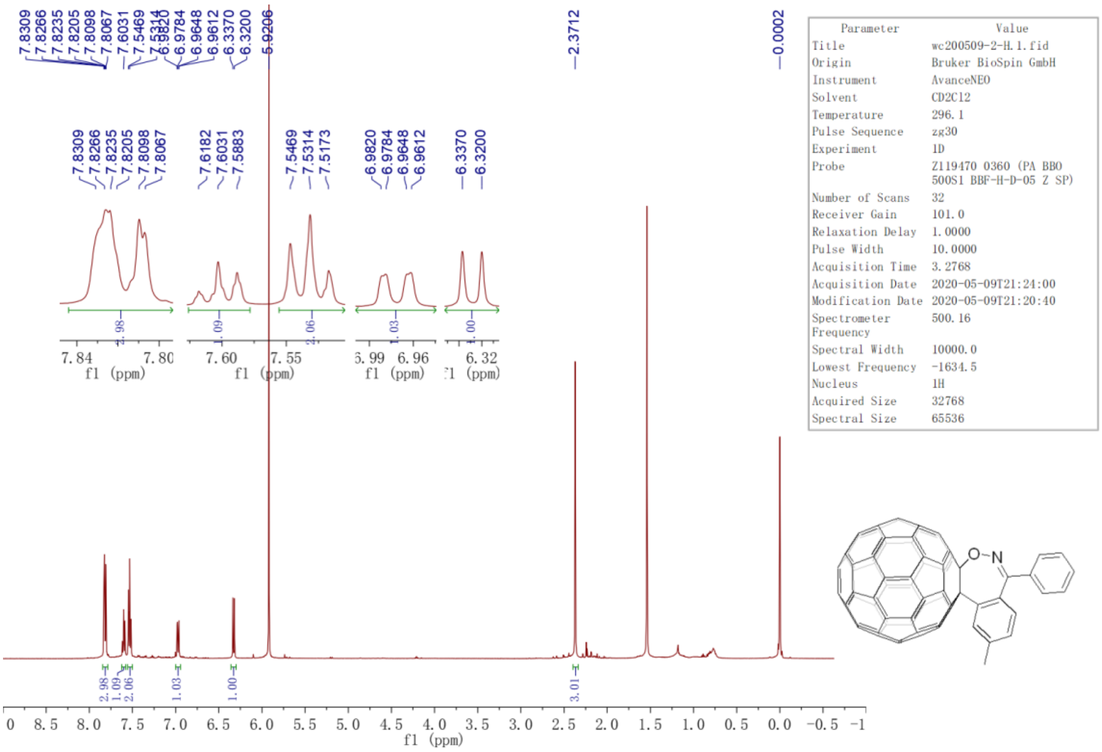

Figure S35 ^{1}H NMR (500 MHz, $CDCl_2CDCl_2$) of compound 2m

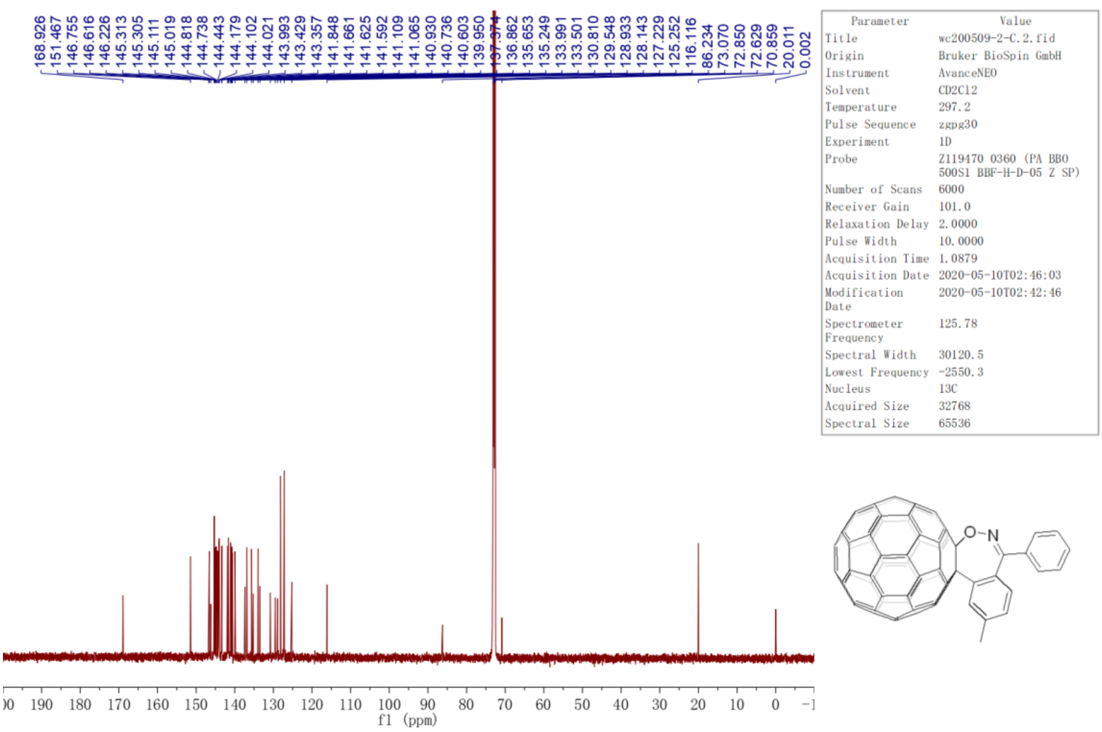

Figure S36 ^{13}C NMR (126 MHz, $CDCl_2CDCl_2$) of compound 2m

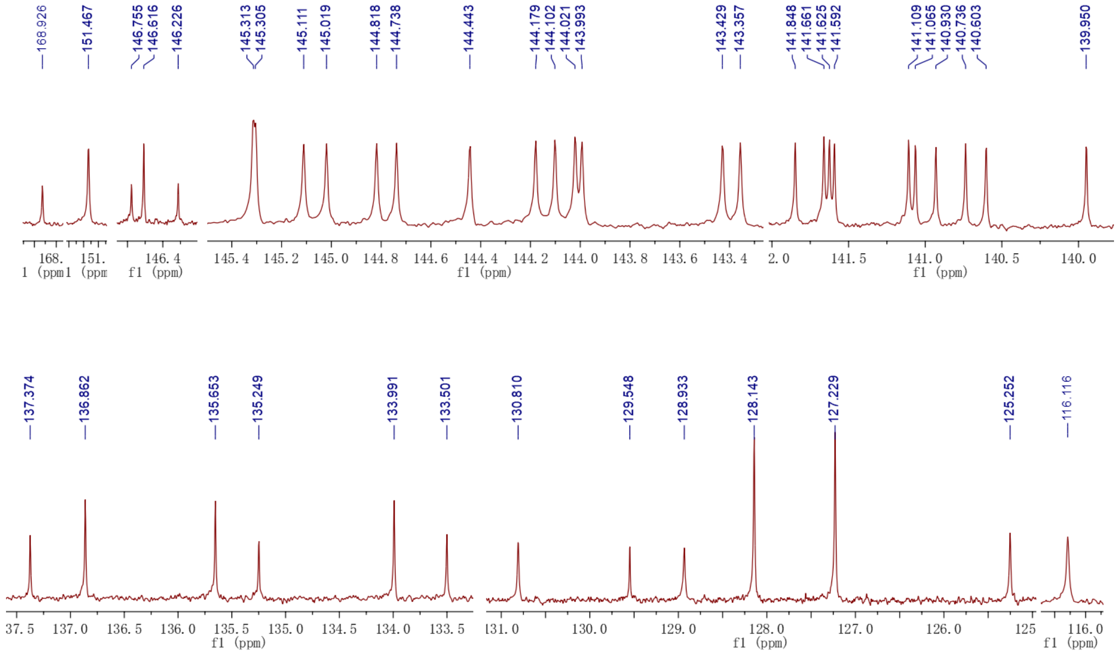

Figure S37 Expanded ^{13}C NMR (126 MHz, $CDCl_2CDCl_2$) of compound 2m

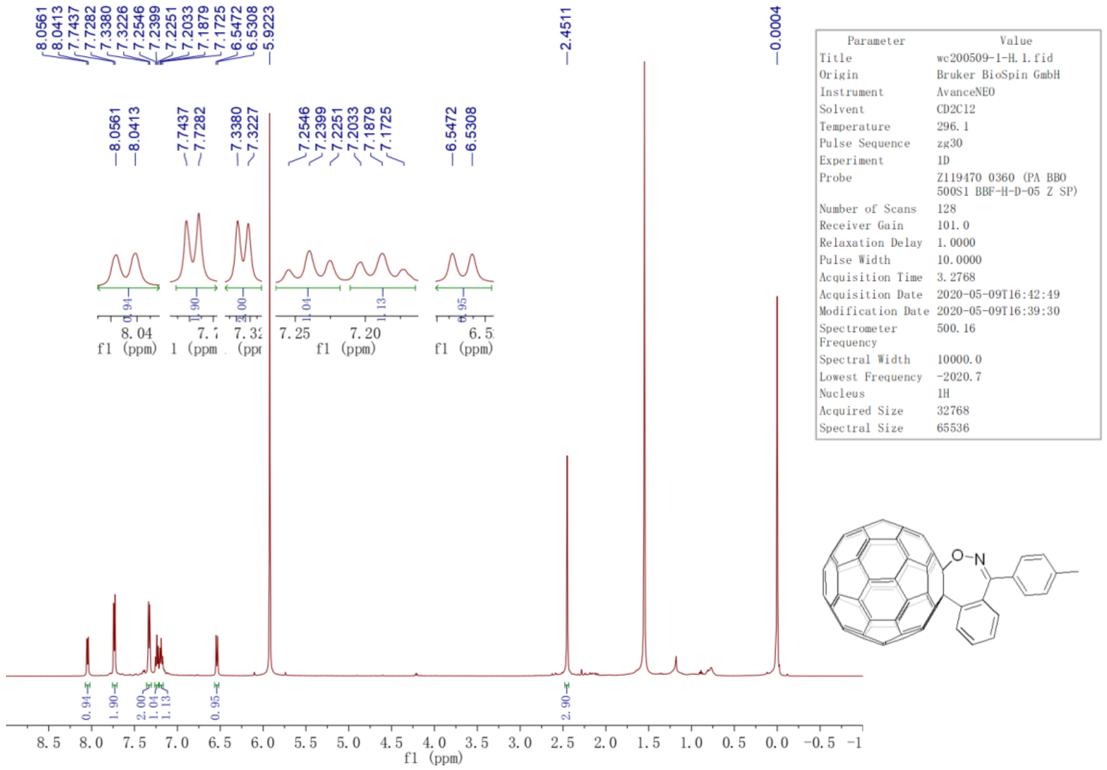

Figure S38 ^{1}H NMR (500 MHz, $CDCl_2CDCl_2/CS_2$) of compound 2m'

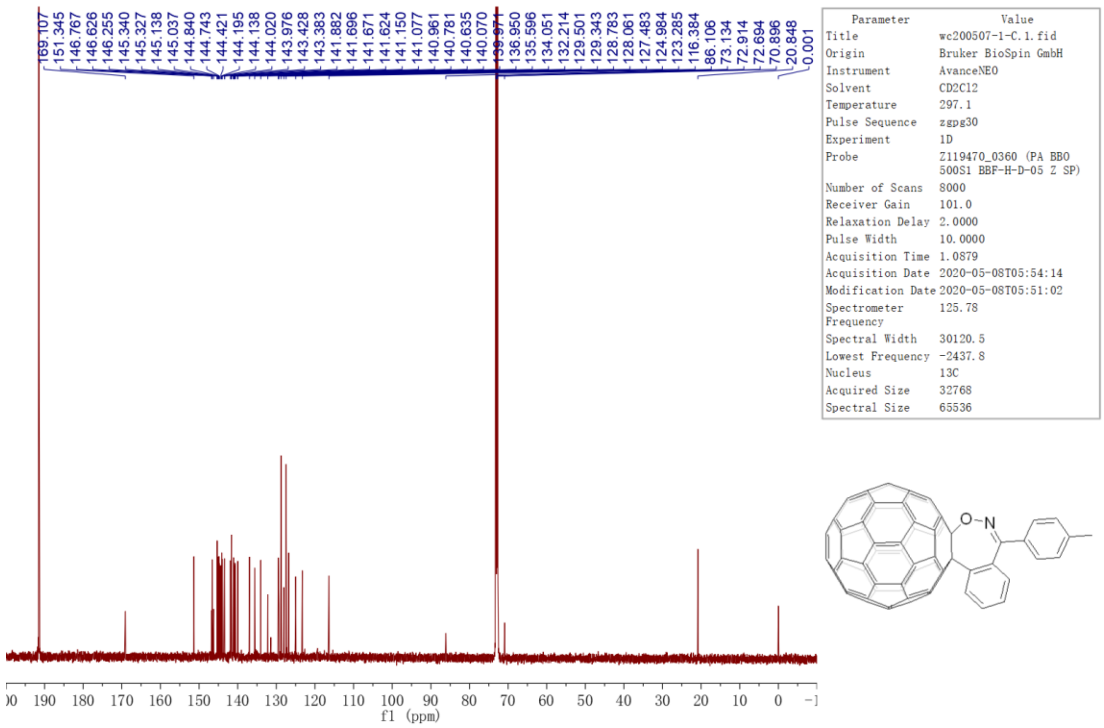

Figure S39 ^{13}C NMR (126 MHz, $CDCl_2CDCl_2/CS_2$) of compound 2m'

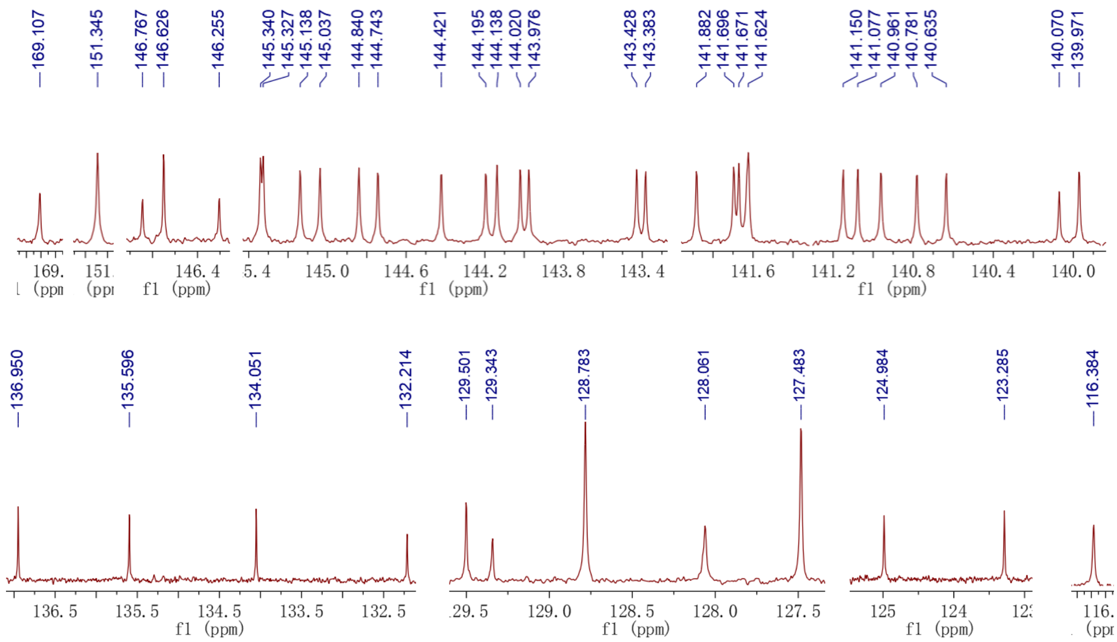

Figure S40 Expanded ^{13}C NMR (126 MHz, $CDCl_2CDCl_2/CS_2$) of compound 2m'

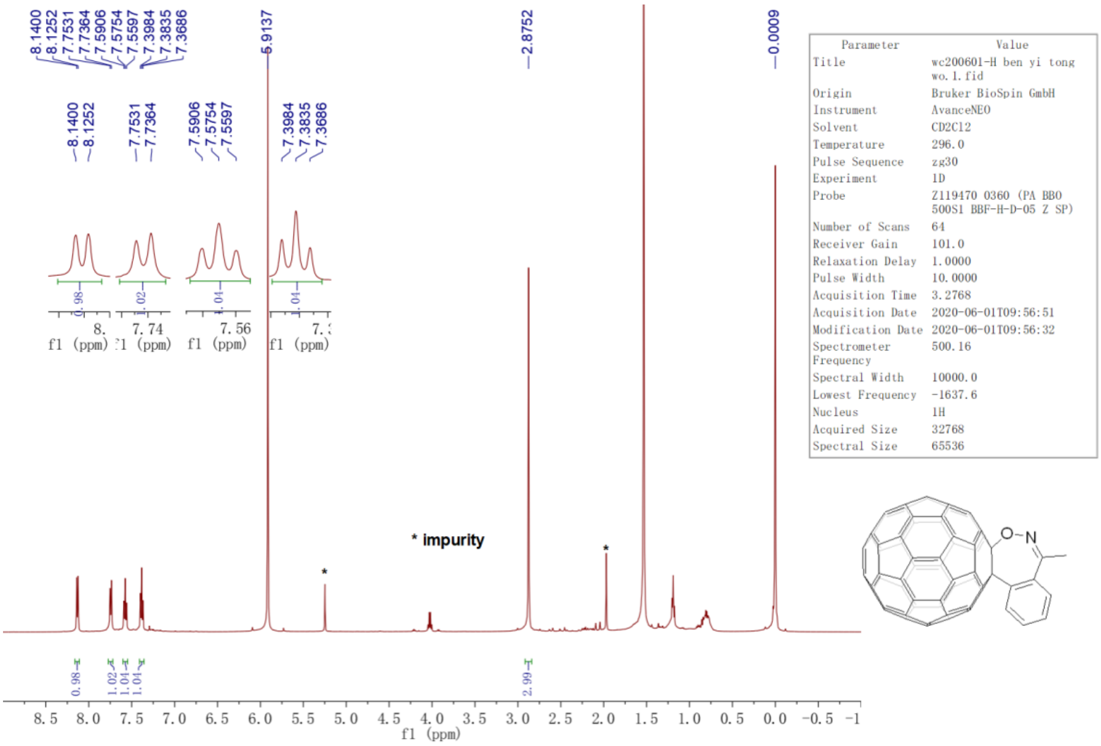

Figure S41 ^{1}H NMR (500 MHz, $CDCl_2CDCl_2/CS_2$) of compound 2n

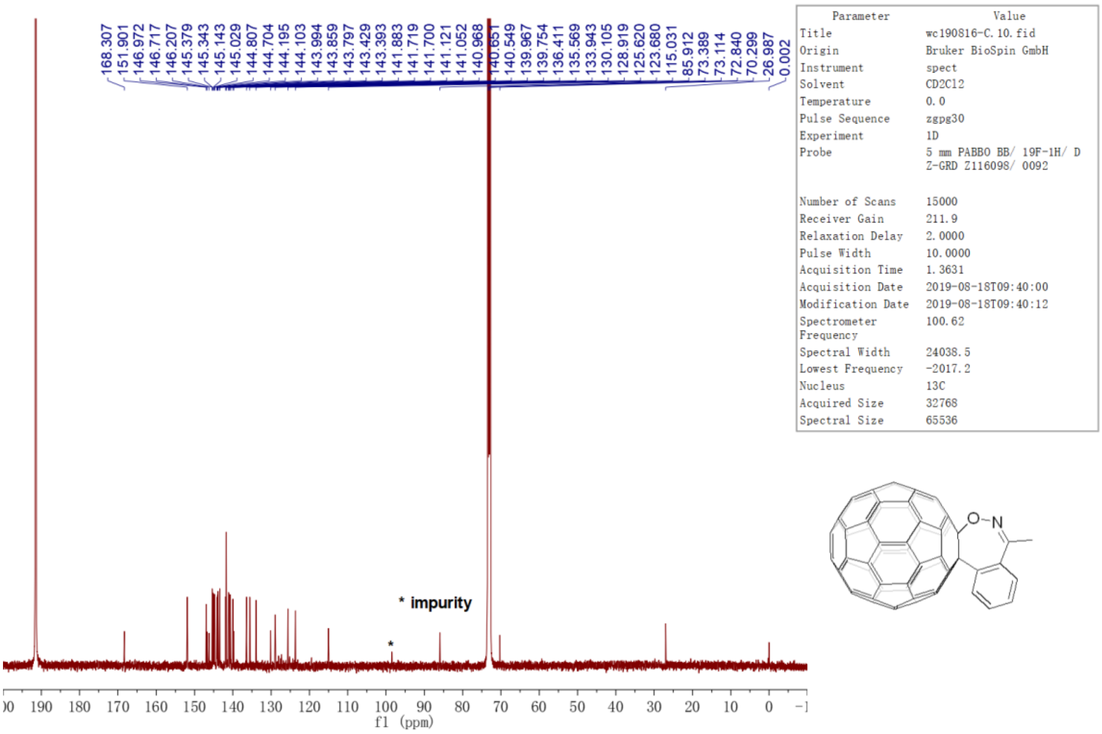

Figure S42 ^{13}C NMR (101 MHz, $CDCl_2CDCl_2/CS_2$) of compound 2n

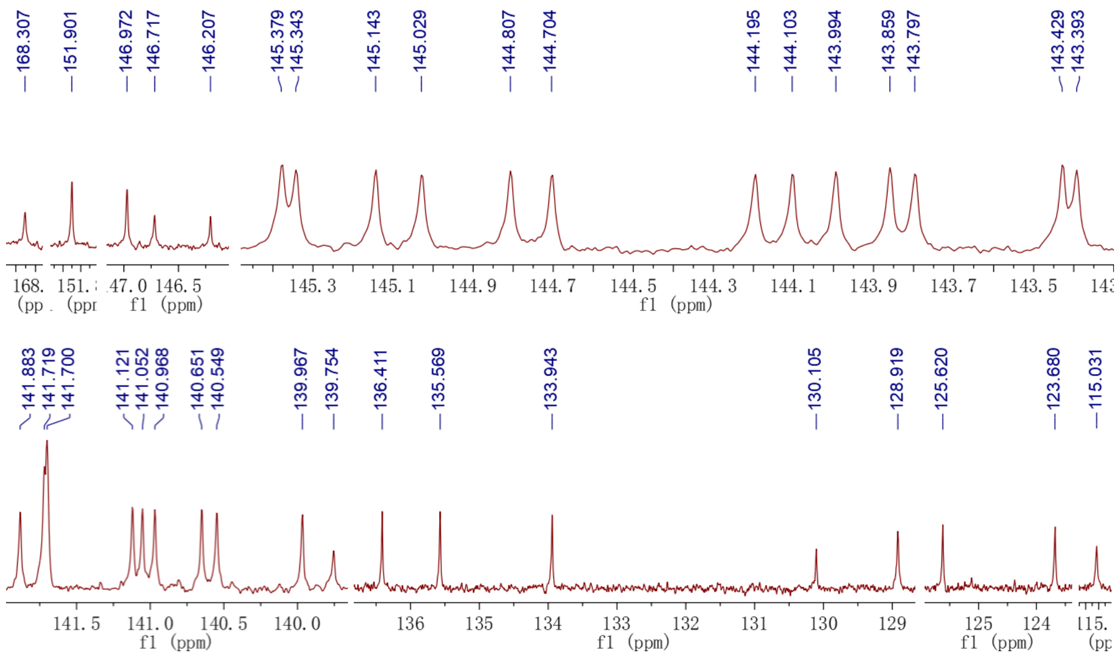

Figure S43 Expanded ^{13}C NMR (101 MHz, $CDCl_2CDCl_2/CS_2$) of compound 2n

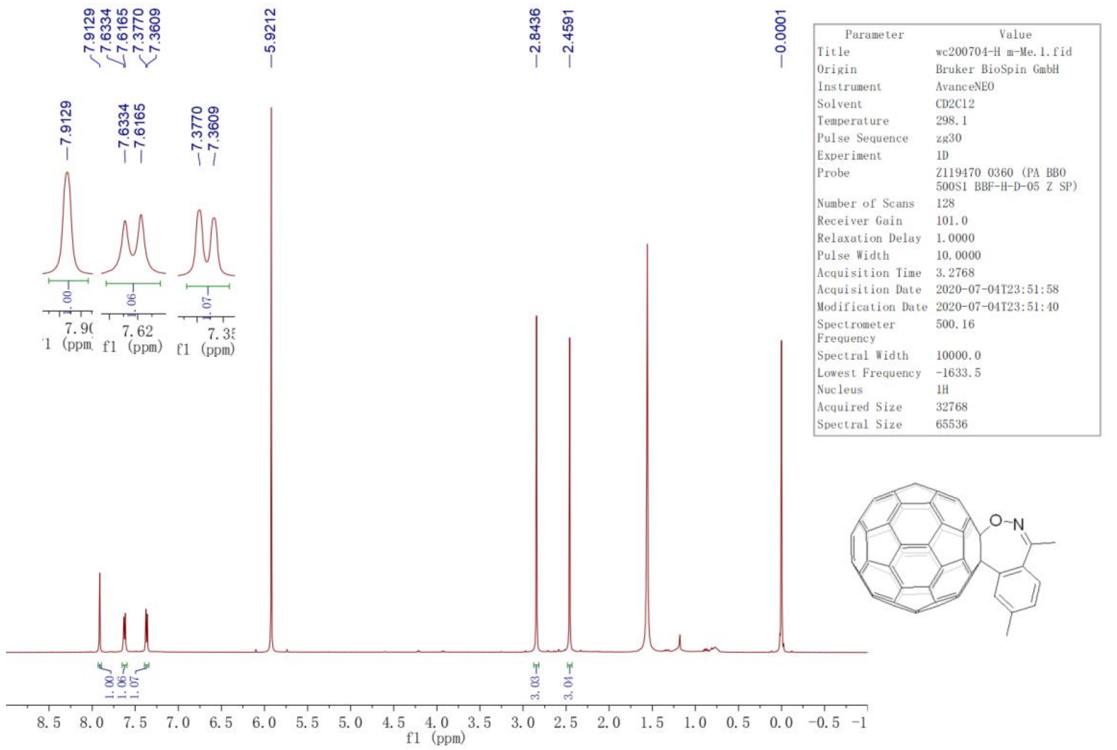

Figure S44 ^{1}H NMR (500 MHz, $CDCl_2CDCl_2$) of compound 2o

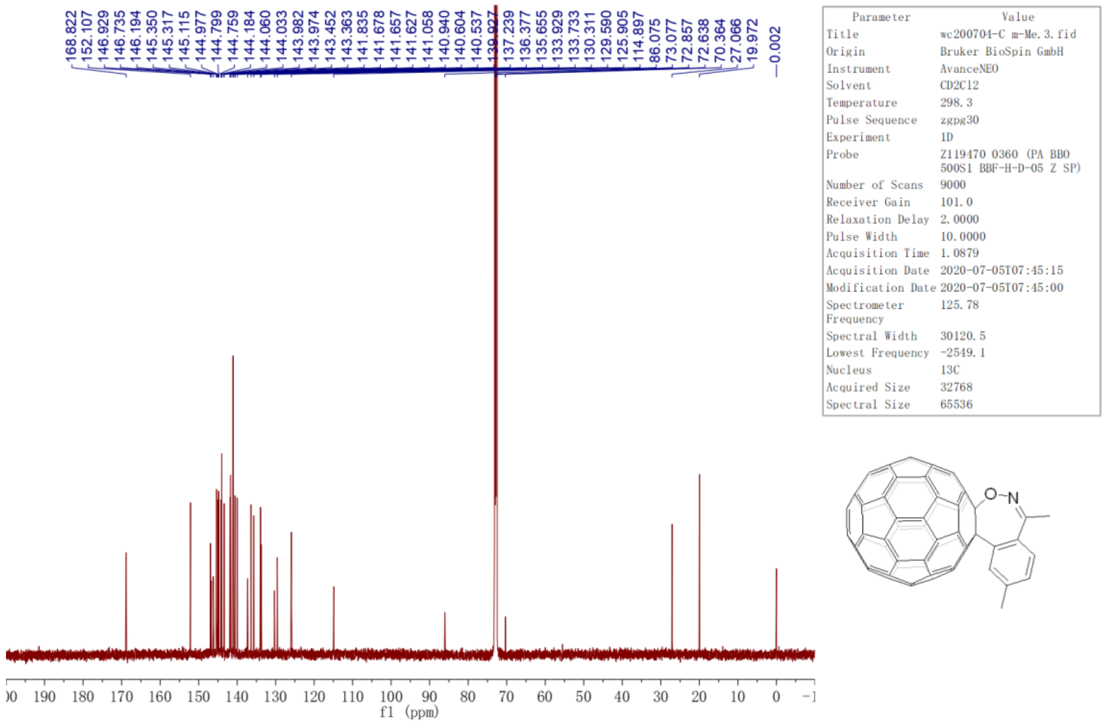

Figure S45 ^{13}C NMR (126 MHz, $CDCl_2CDCl_2$) of compound 2o

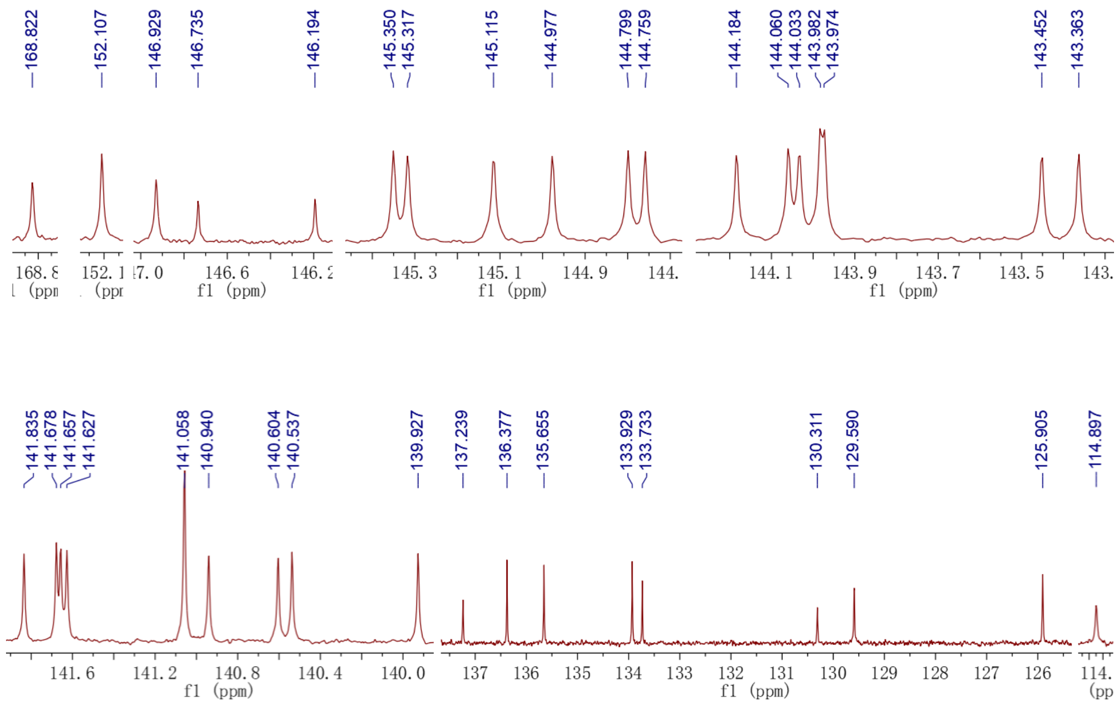

Figure S46 Expanded ^{13}C NMR (126 MHz, $CDCl_2CDCl_2$) of compound 2o

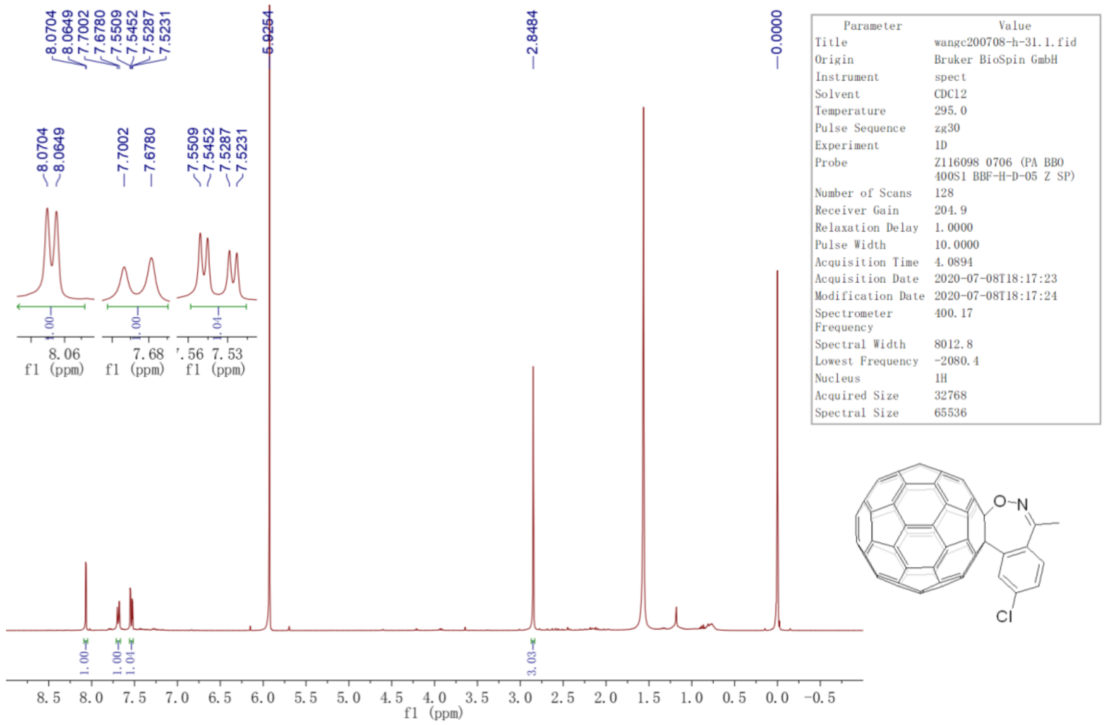

Figure S47 ^{1}H NMR (400 MHz, $CDCl_2CDCl_2$) of compound 2p

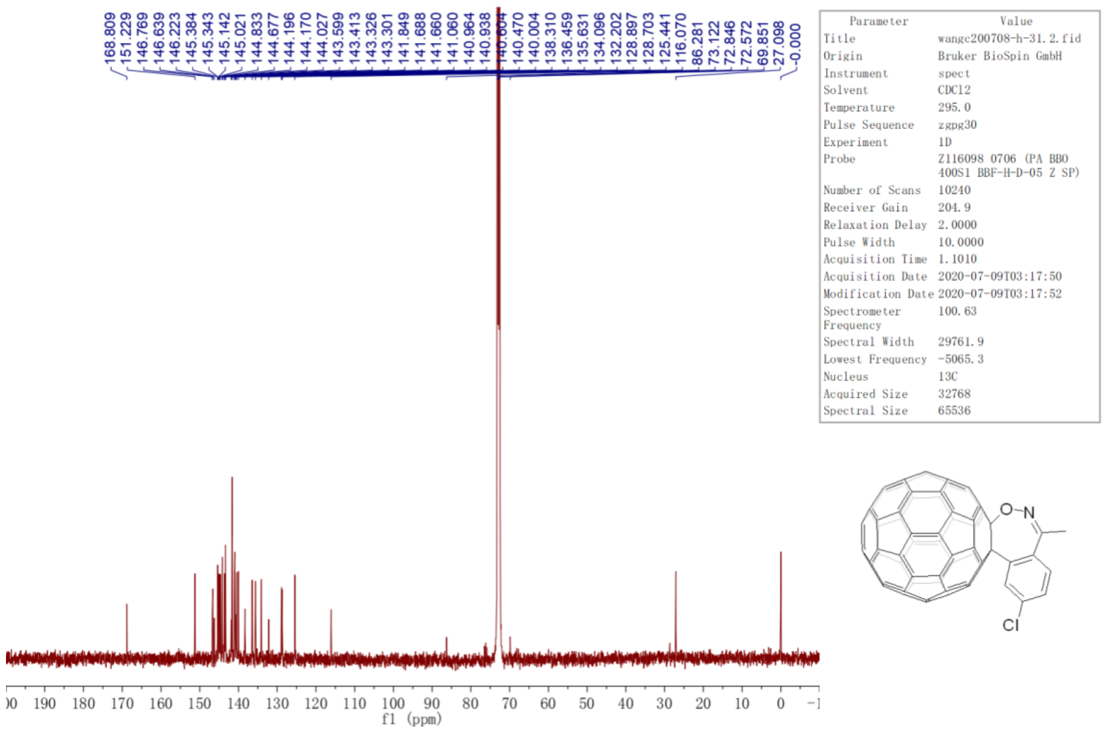

Figure S48 ^{13}C NMR (101 MHz, $CDCl_2CDCl_2$) of compound 2p

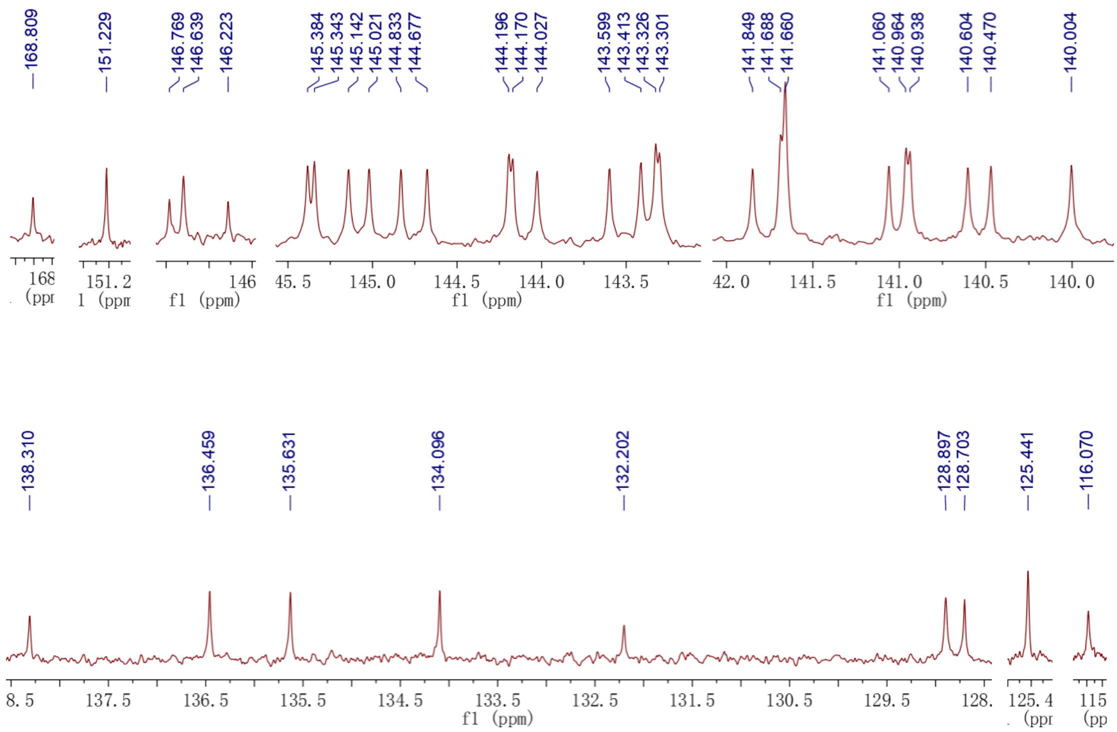

Figure S49 Expanded ^{13}C NMR (101 MHz, $CDCl_2CDCl_2$) of compound 2p

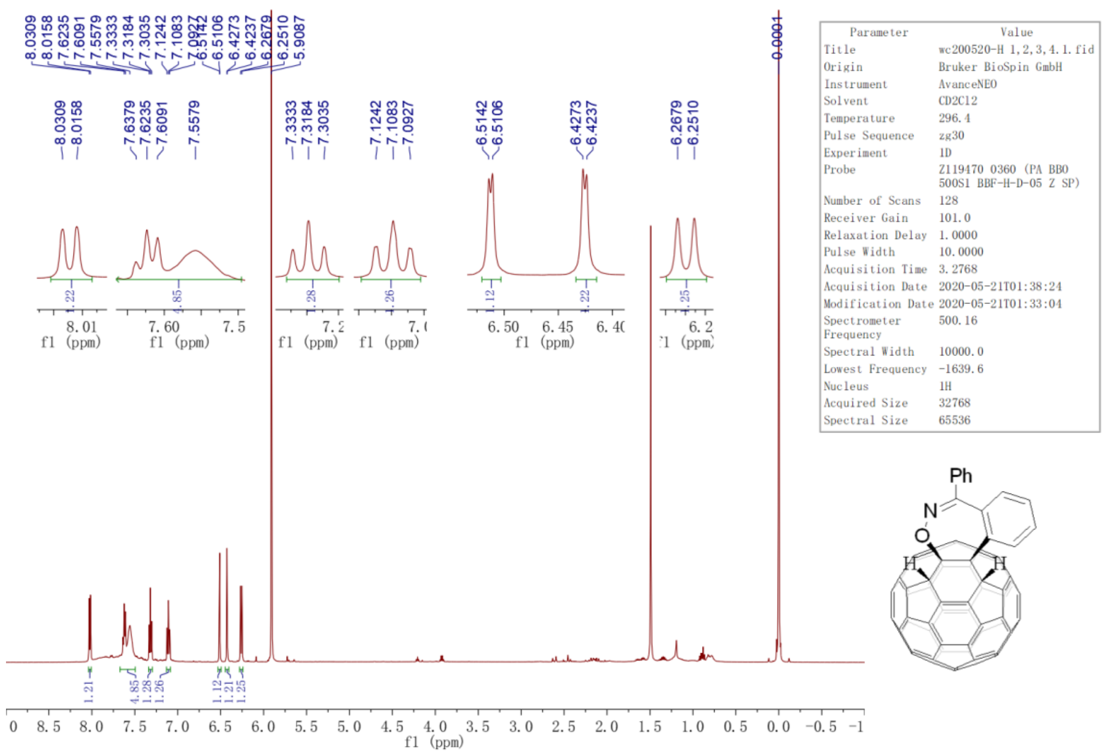

Figure S50 ^1H NMR (500 MHz, $CDCl_2CDCl_2/CS_2$) of compound 3a

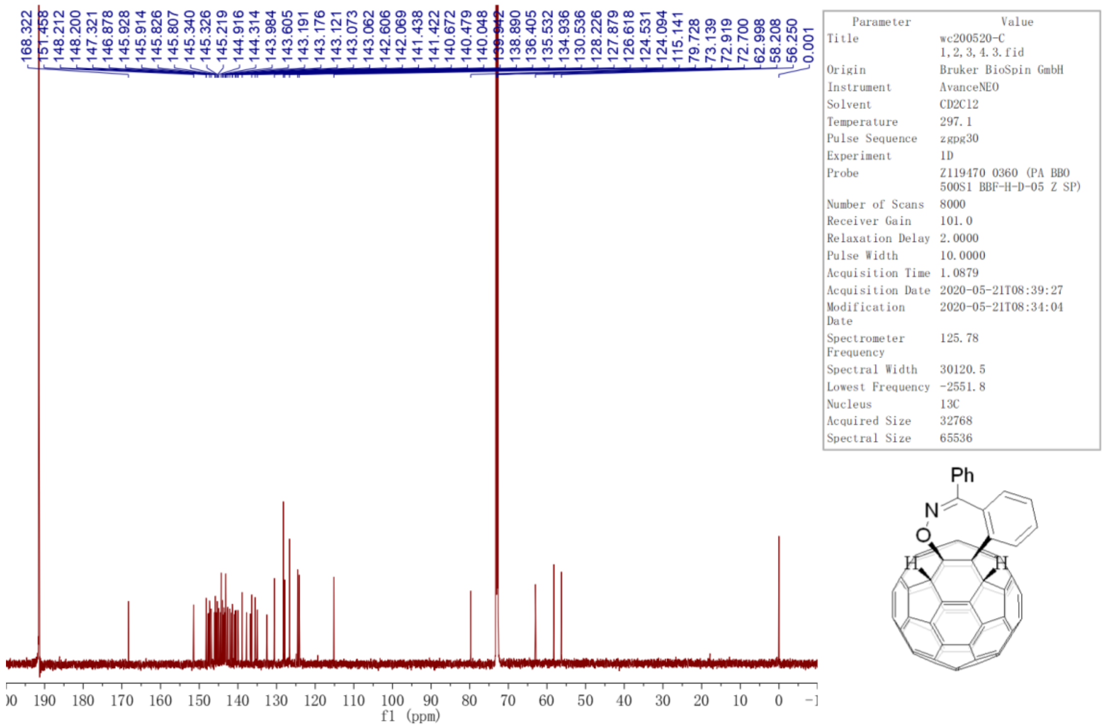

Figure S51 ^{13}C NMR (126 MHz, $CDCl_2CDCl_2/CS_2$) of compound 3a

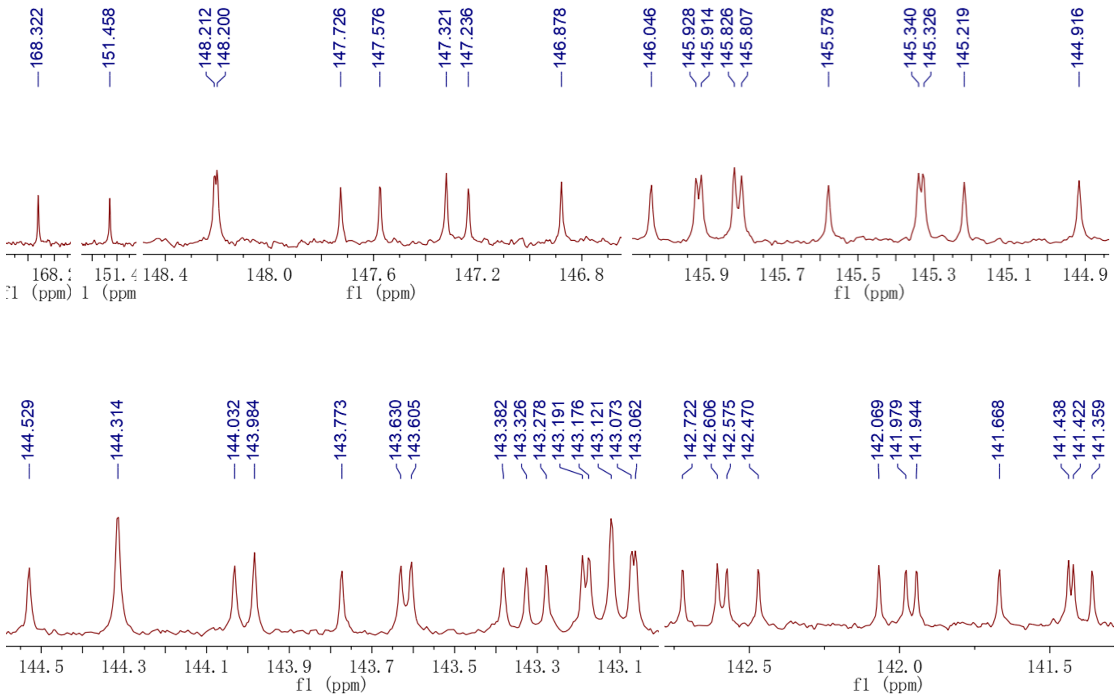

Figure S52 Expanded ^{13}C NMR (126 MHz, $CDCl_2CDCl_2/CS_2$) of compound 3a

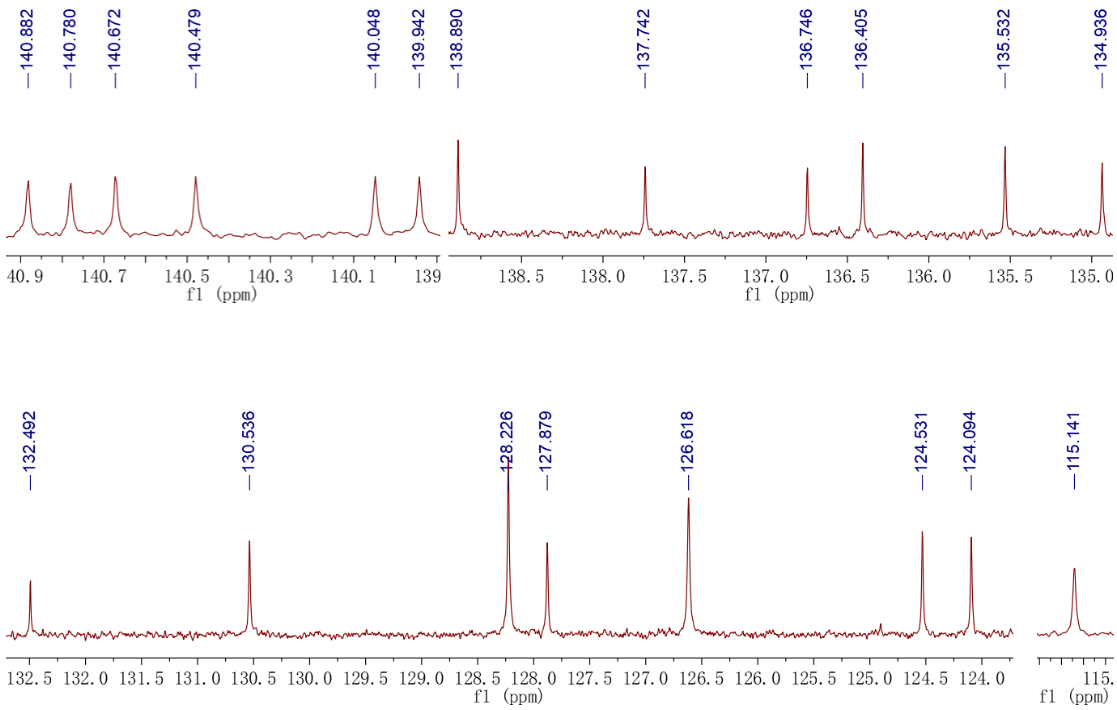

Figure S53 Expanded ^{13}C NMR (126 MHz, $CDCl_2CDCl_2/CS_2$) of compound 3a

Figure S54 ^{1}H NMR (400 MHz, CS_2/DMSO-d_6) of compound 3b

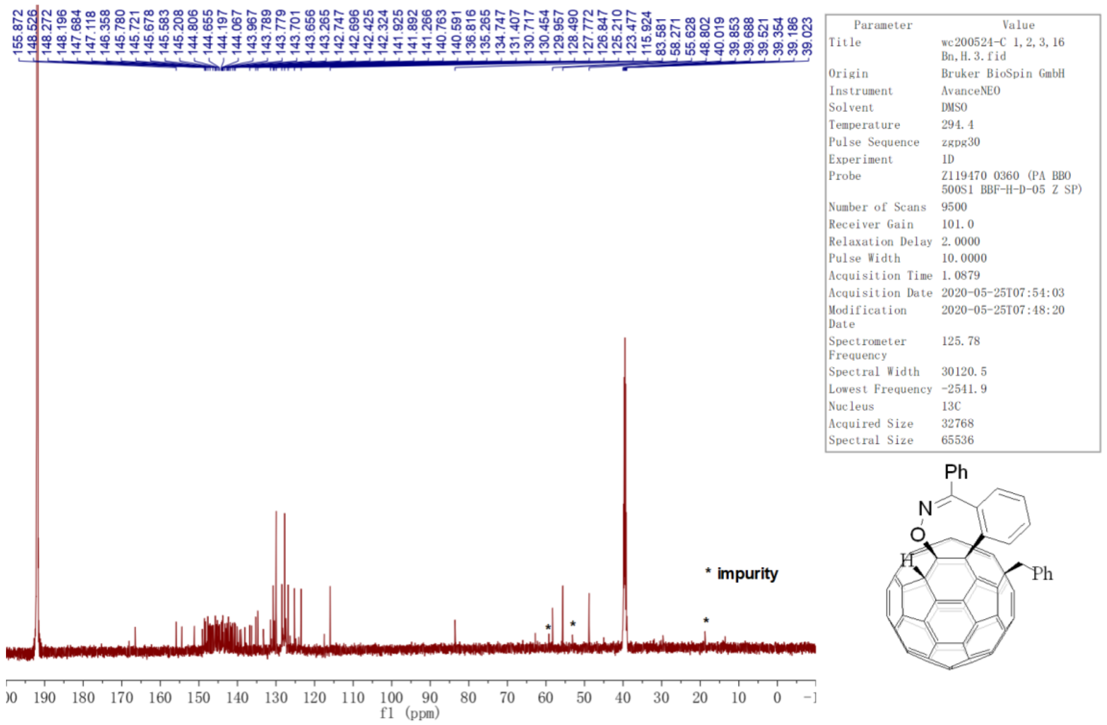

Figure S55 ^{13}C **NMR (126 MHz, CS_2/DMSO-*d_6*) of compound 3b**

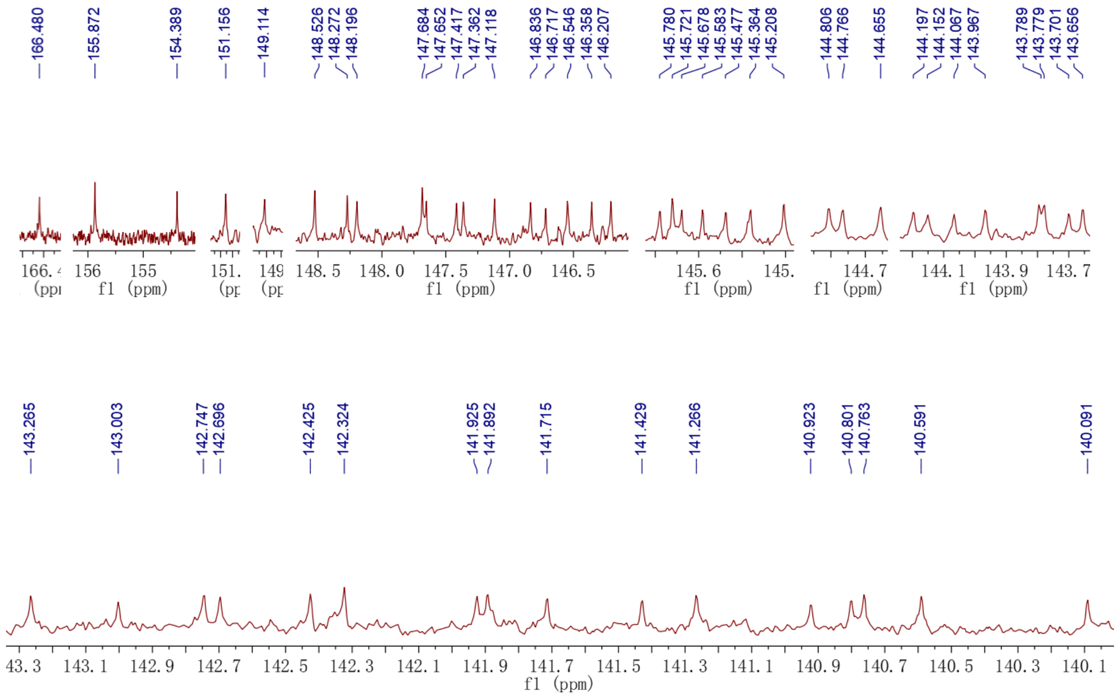

Figure S56 Expanded ^{13}C **NMR (126 MHz, CS_2/DMSO-*d_6*) of compound 3b**

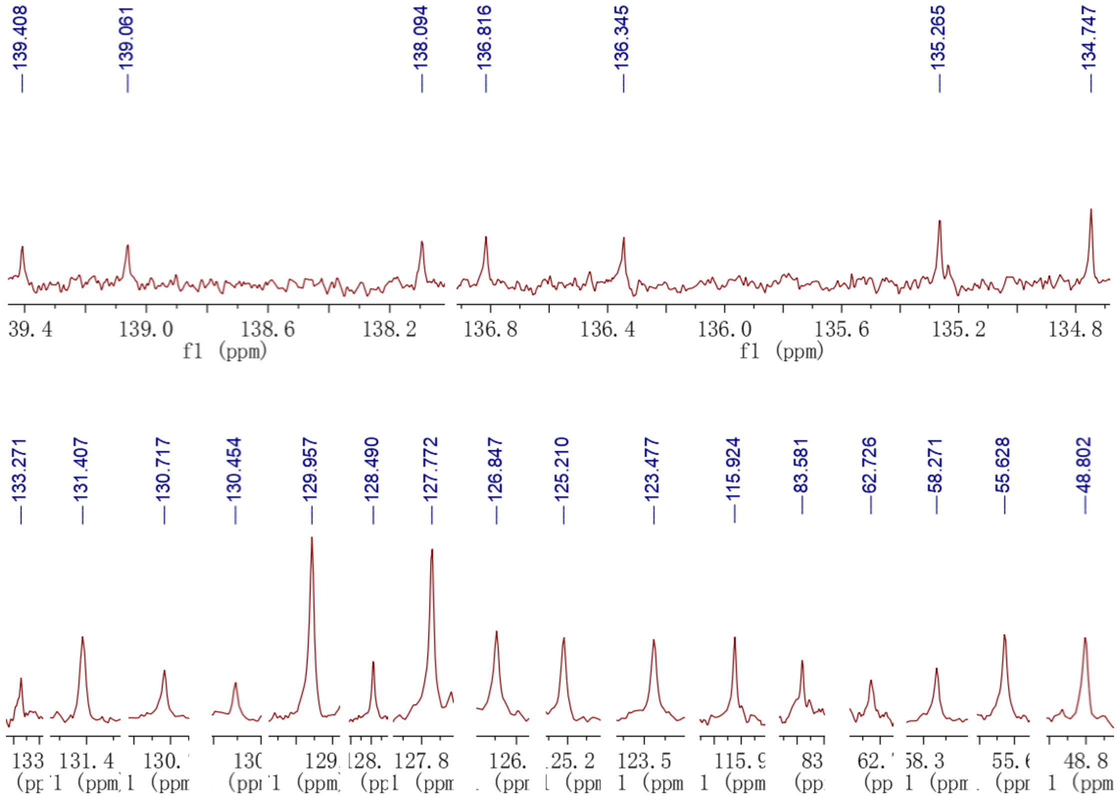

Figure S57 Expanded ^{13}C NMR (126 MHz, CS_2/DMSO-d_6) of compound 3b

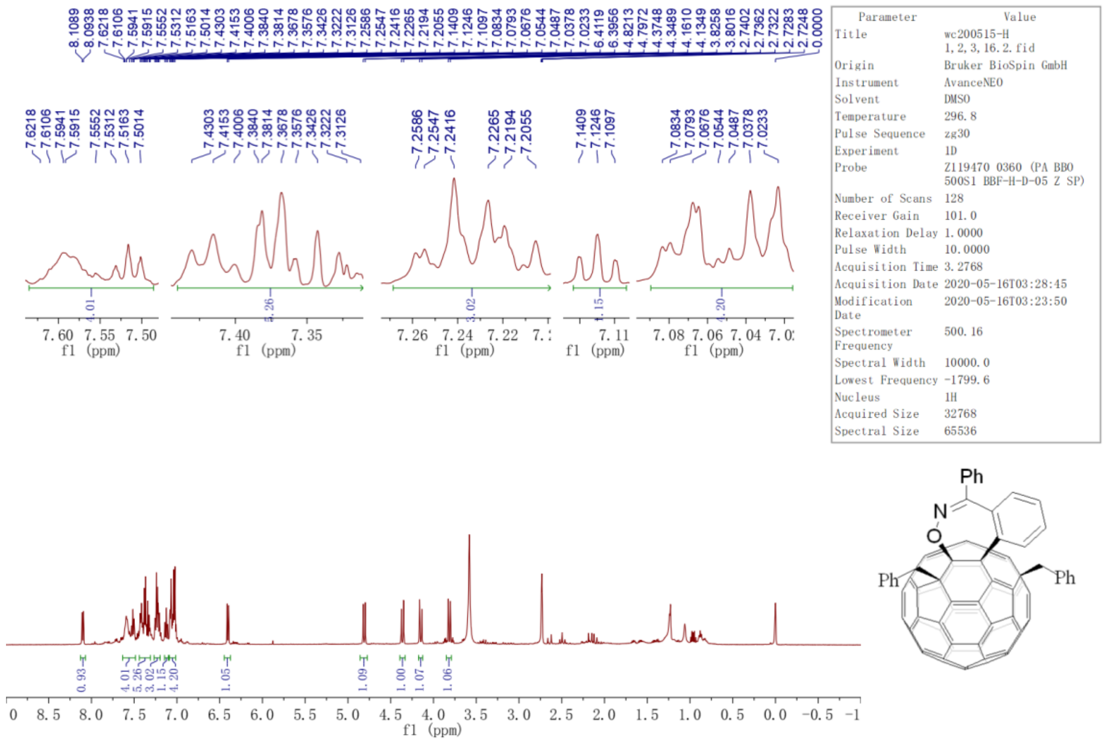

Figure S58 ^1H NMR (500 MHz, CS_2/DMSO-d_6) of compound 3c

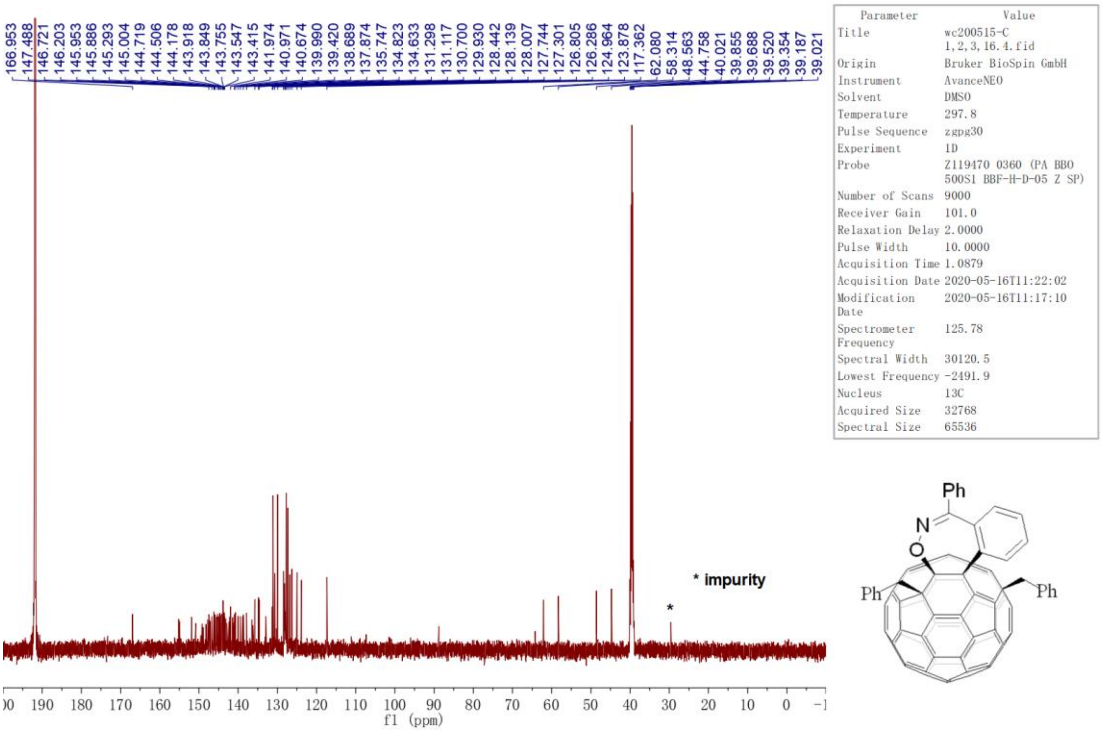

Figure S59 ^{13}C NMR (126 MHz, CS_2/DMSO-d_6) of compound 3c

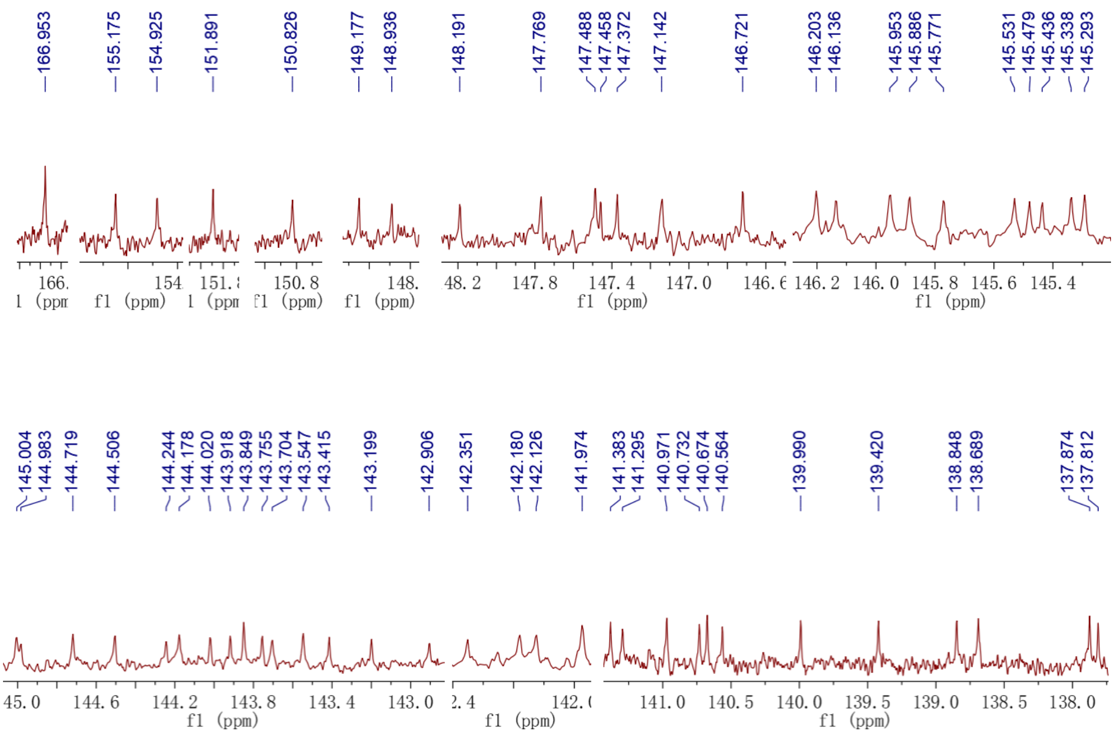

Figure S60 Expanded ^{13}C NMR (126 MHz, CS_2/DMSO-d_6) of compound 3c

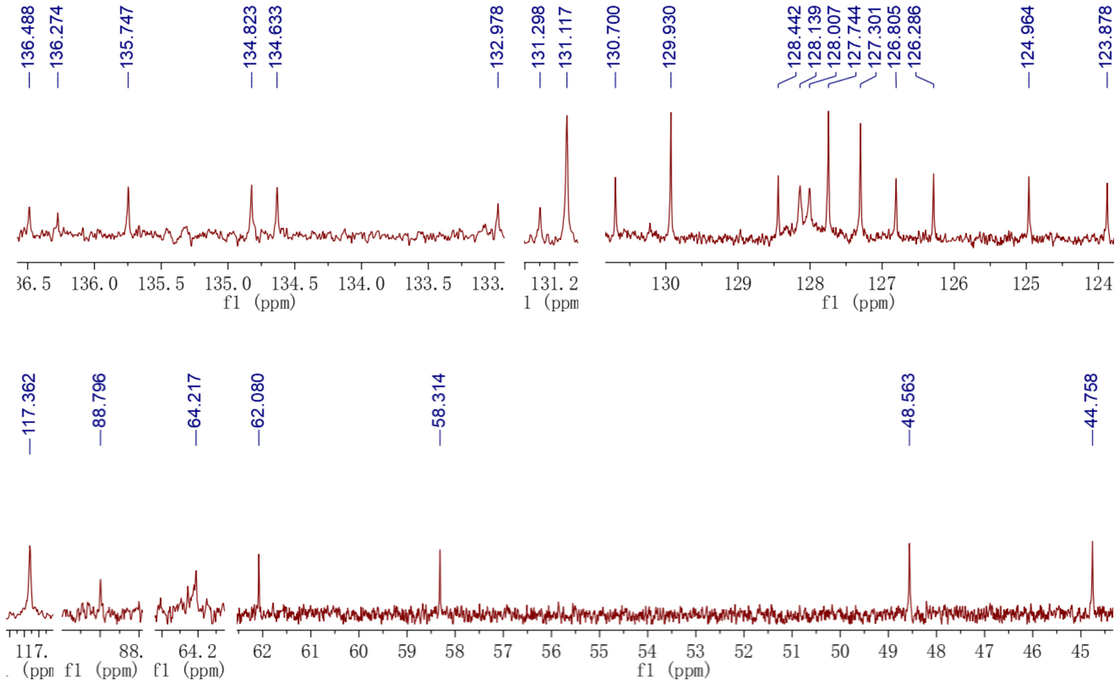

Figure S61 Expanded ^{13}C NMR (126 MHz, CS_2/DMSO-d_6) of compound 3c

6. ^{1}H NMR spectrum of compounds 2d and 2d-d_4

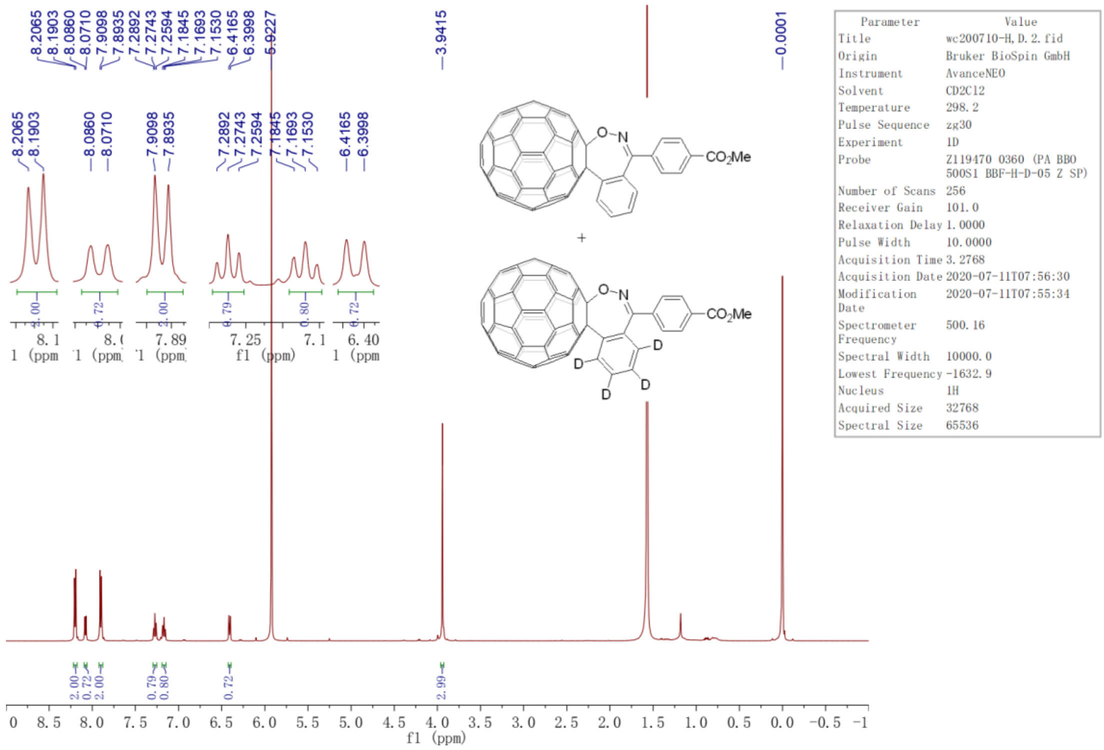

Figure S62 ^{1}H NMR (500 MHz, $CDCl_2CDCl_2$) of compounds 2d and 2d-d_4

7. UV-Vis spectra of compounds 2a–p and 3a–c

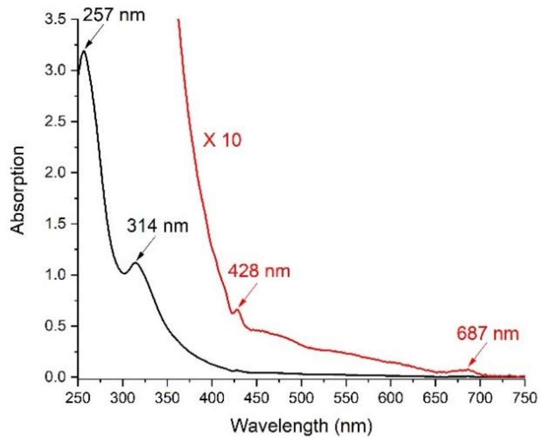

Figure S63 UV-Vis absorption of compound 2a

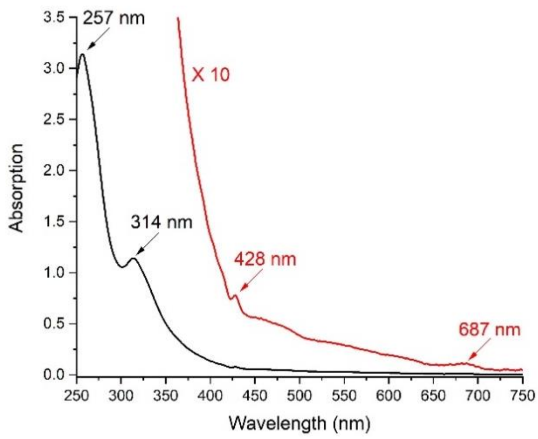

Figure S64 UV-Vis absorption of compound 2b

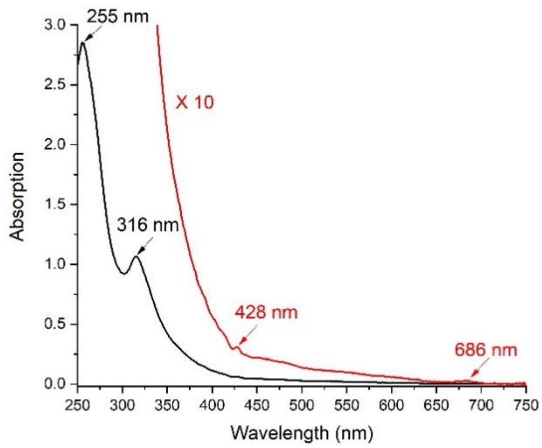

Figure S65 UV-Vis absorption of compound 2c

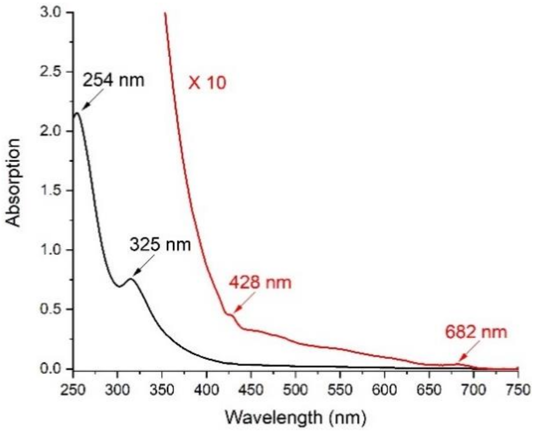

Figure S66 UV-Vis absorption of compound 2d

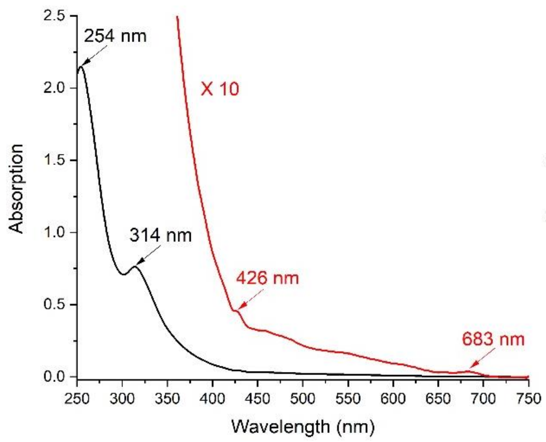

Figure S67 UV-Vis absorption of compound 2e

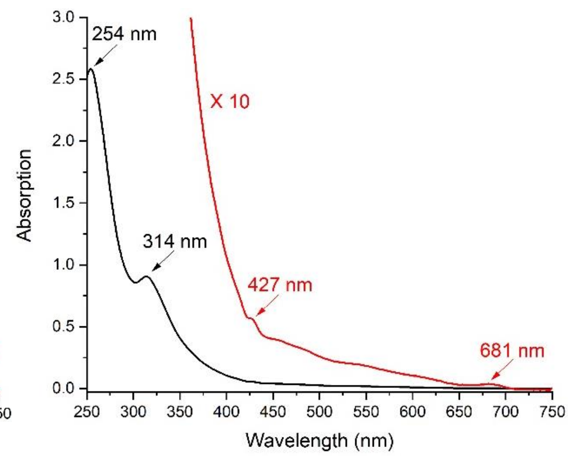

Figure S68 UV-Vis absorption of compound 2f

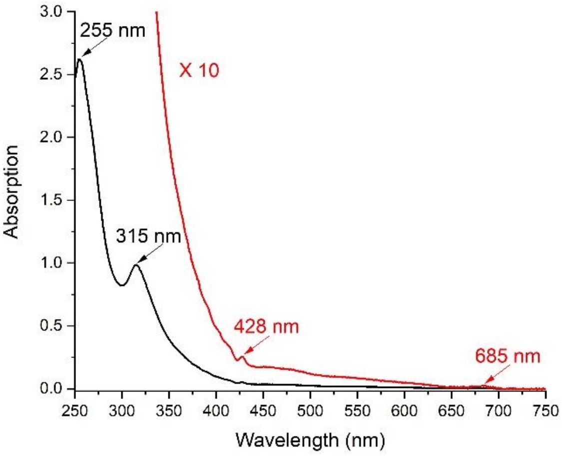

Figure S69 UV-Vis absorption of compound 2g

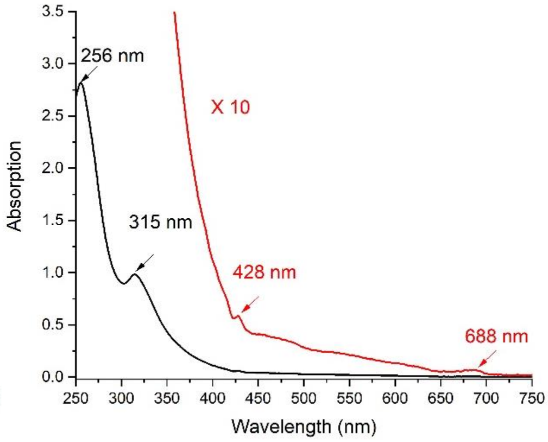

Figure S70 UV-Vis absorption of compound 2h

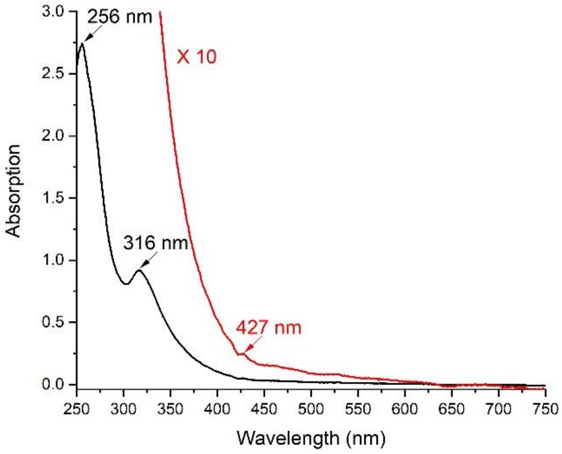

Figure S71 UV-Vis absorption of compound 2i

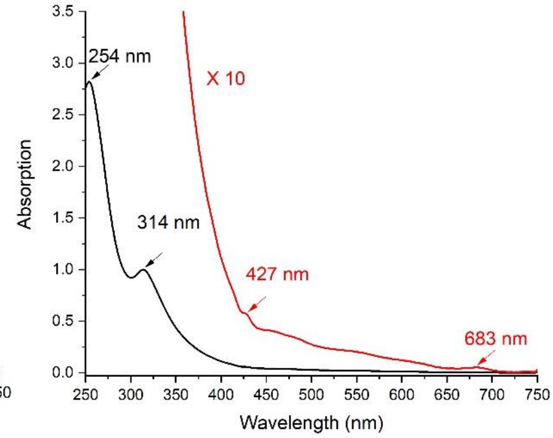

Figure S72 UV-Vis absorption of compound 2j

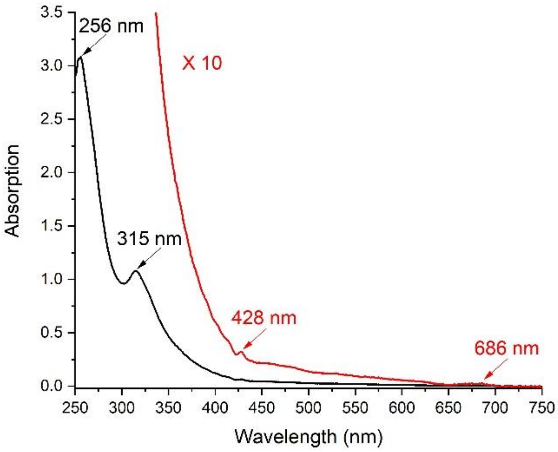

Figure S73 UV-Vis absorption of compound 2k

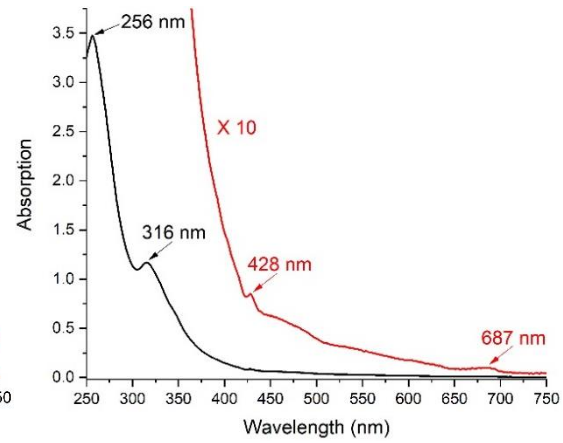

Figure S74 UV-Vis absorption of compound 2l

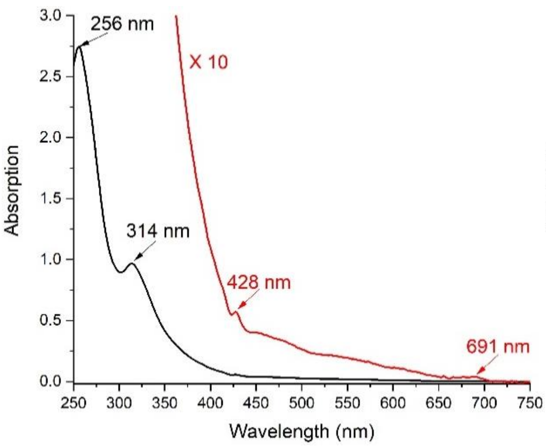

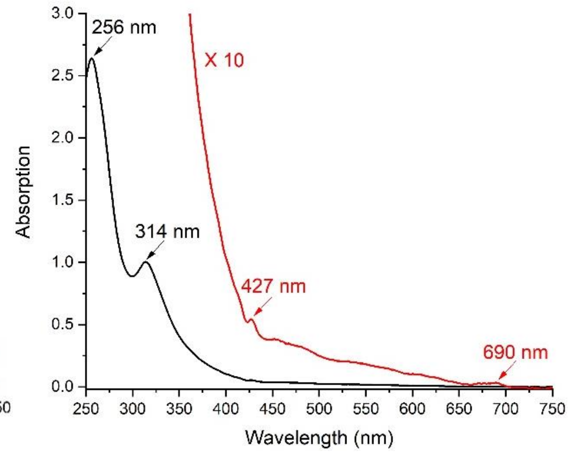

Figure S75 UV-Vis absorption of compound 2m

Figure S76 UV-Vis absorption of compound 2m'

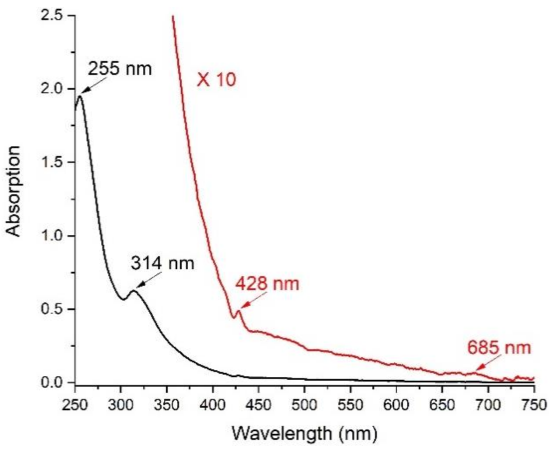

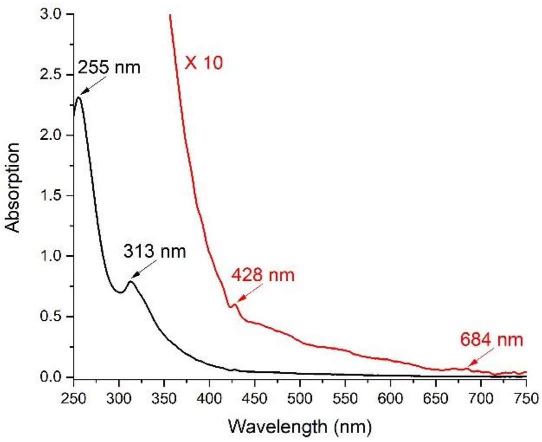

Figure S77 UV-Vis absorption of compound 2n

Figure S78 UV-Vis absorption of compound 2o

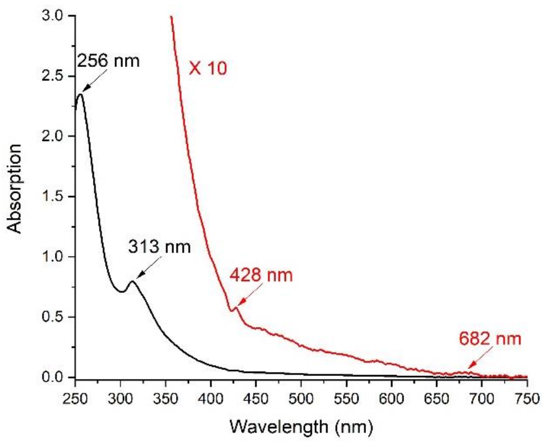

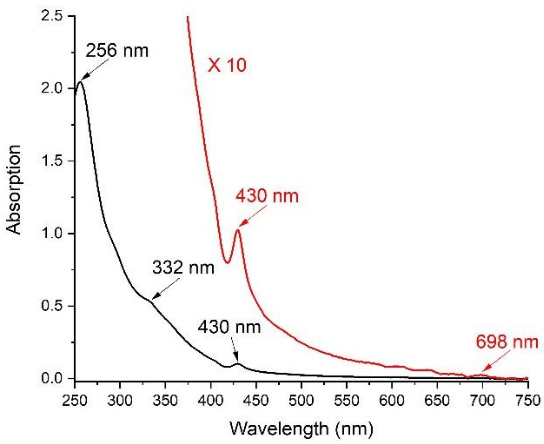

Figure S79 UV-Vis absorption of compound 2p

Figure S80 UV-Vis absorption of compound 3a

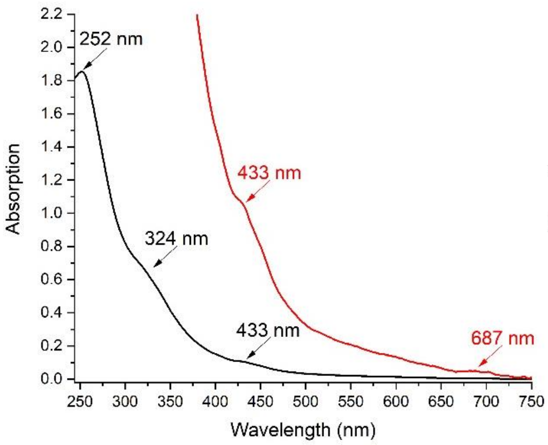

Figure S81 UV-Vis absorption of compound 3b

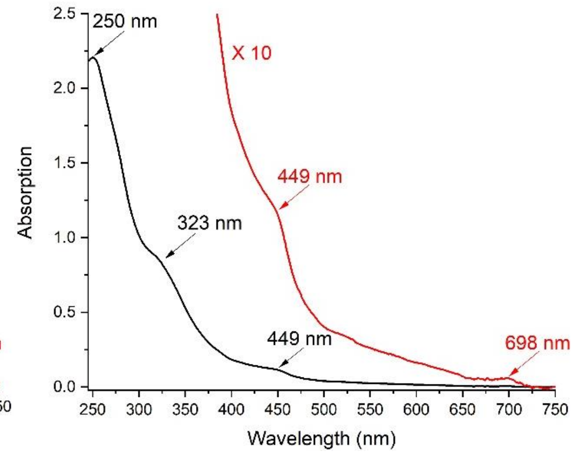

Figure S82 UV-Vis absorption of compound 3c

8. CV and DPV of compounds 2a–p and 3a–c

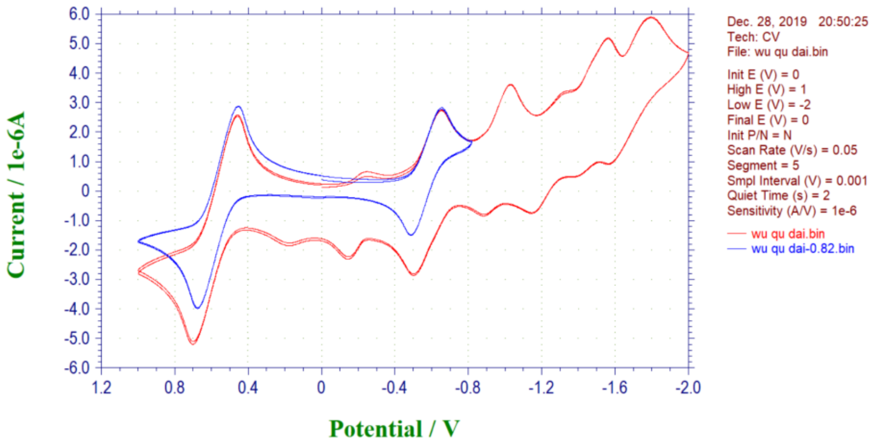

Figure S83 Cyclic voltammogram of compound 2a (scanning rate: 50 mV s^{-1})

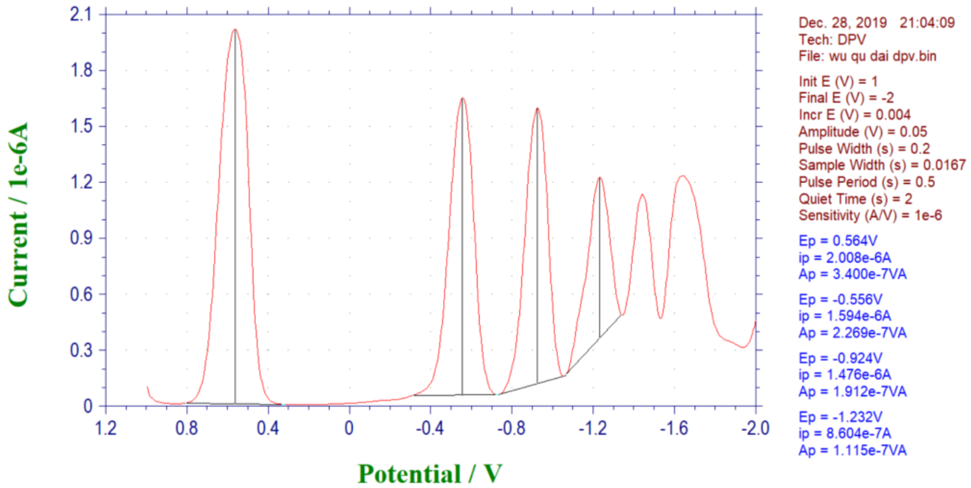

Figure S84 Differential pulse voltammogram of compound 2a

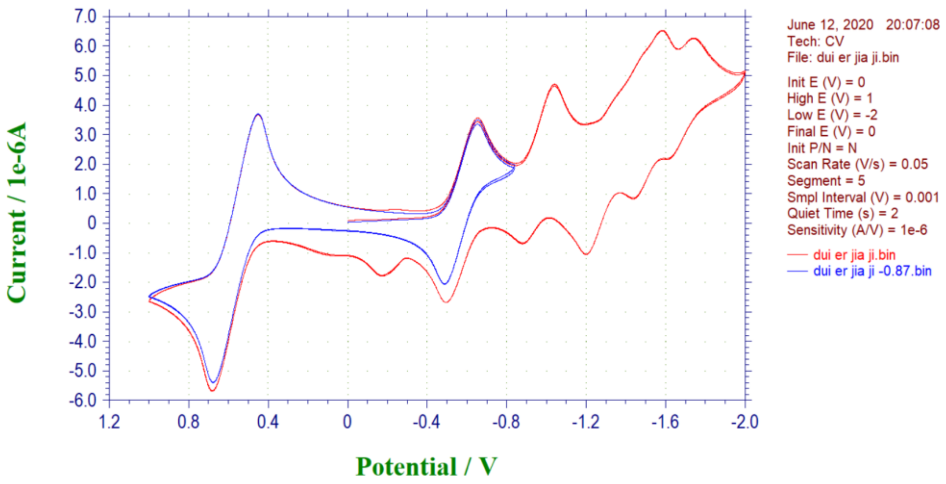

Figure S85 Cyclic voltammogram of compound 2b (scanning rate: 50 mV s^{-1})

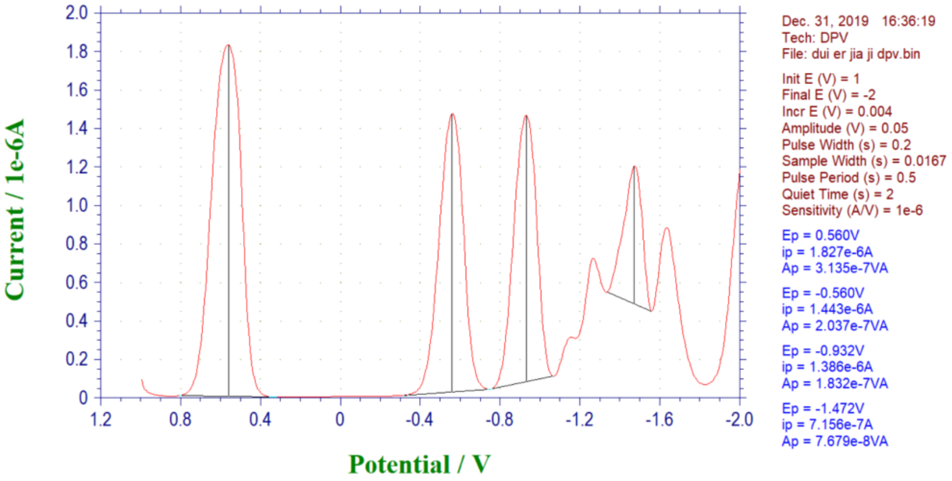

Figure S86 Differential pulse voltammogram of compound 2b

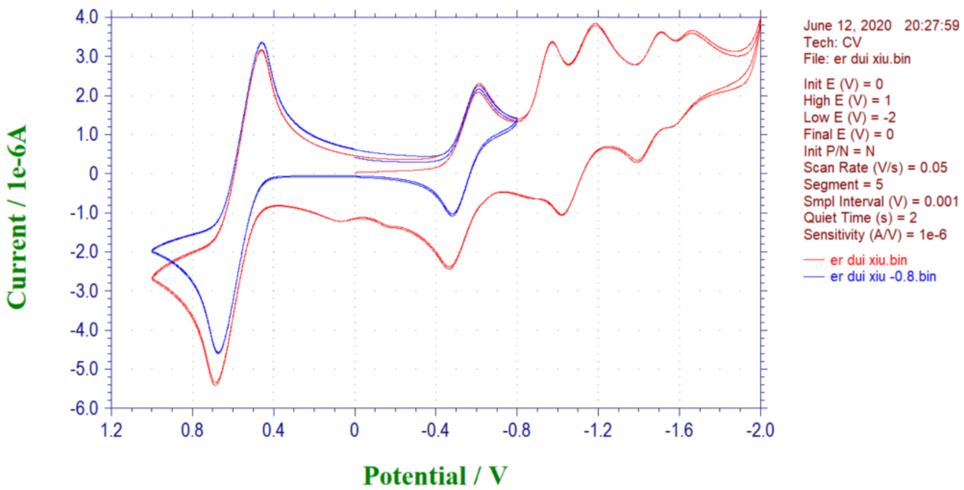

Figure S87 Cyclic voltammogram of compound 2c (scanning rate: 50 mV s^{-1})

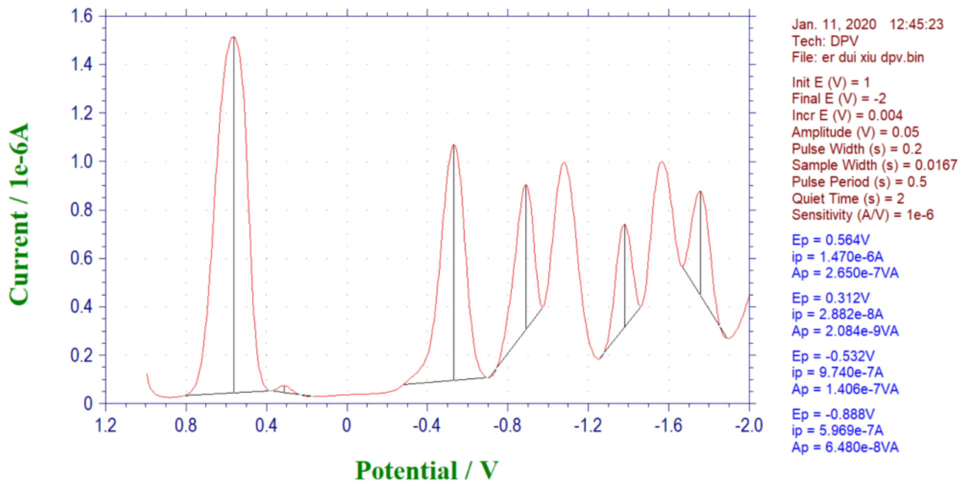

Figure S88 Differential pulse voltammogram of compound 2c

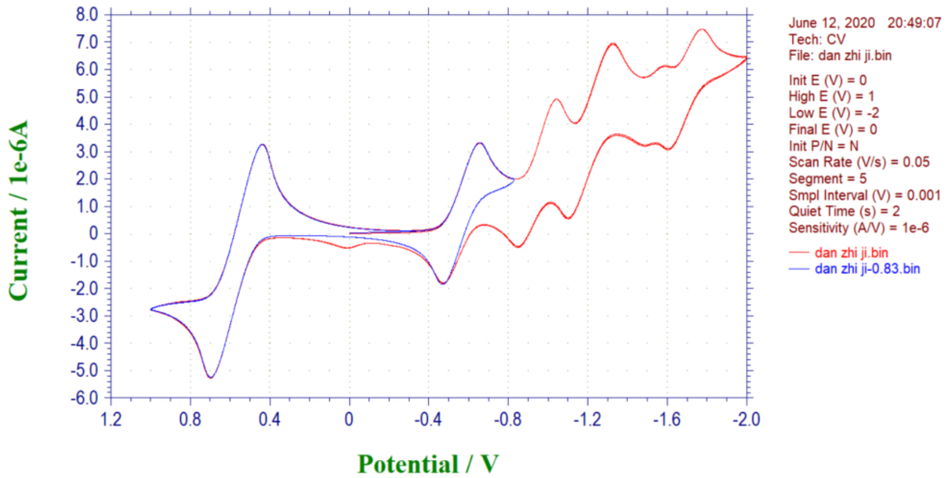

Figure S89 Cyclic voltammogram of compound 2d (scanning rate: 50 mV s^{-1})

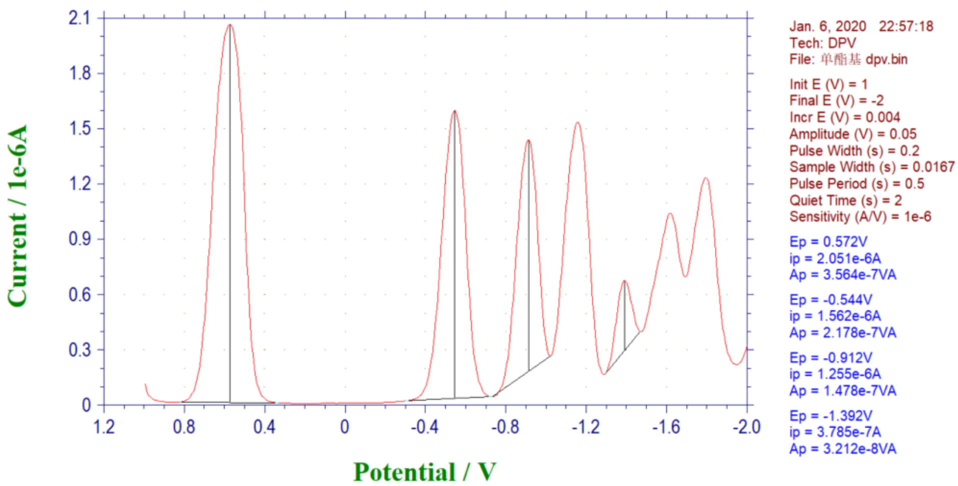

Figure S90 Differential pulse voltammogram of compound 2d

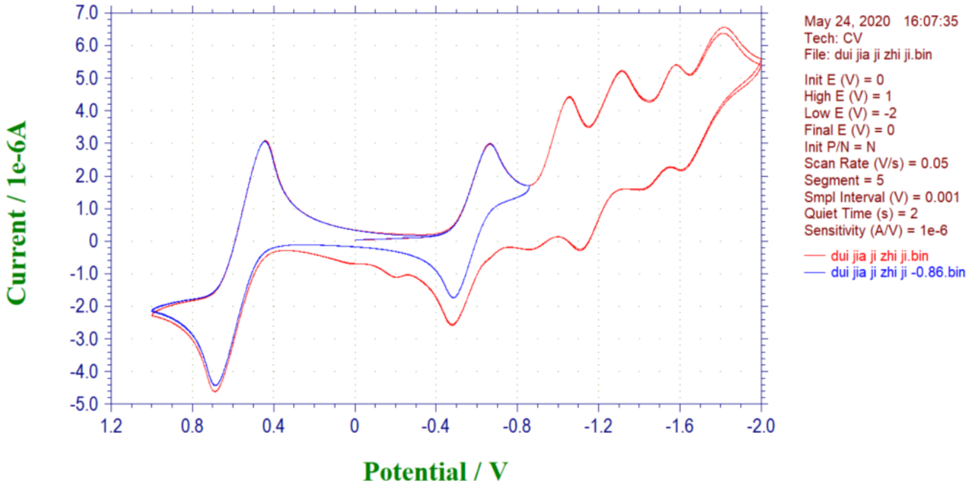

Figure S91 Cyclic voltammogram of compound 2e (scanning rate: 50 mV s^{-1})

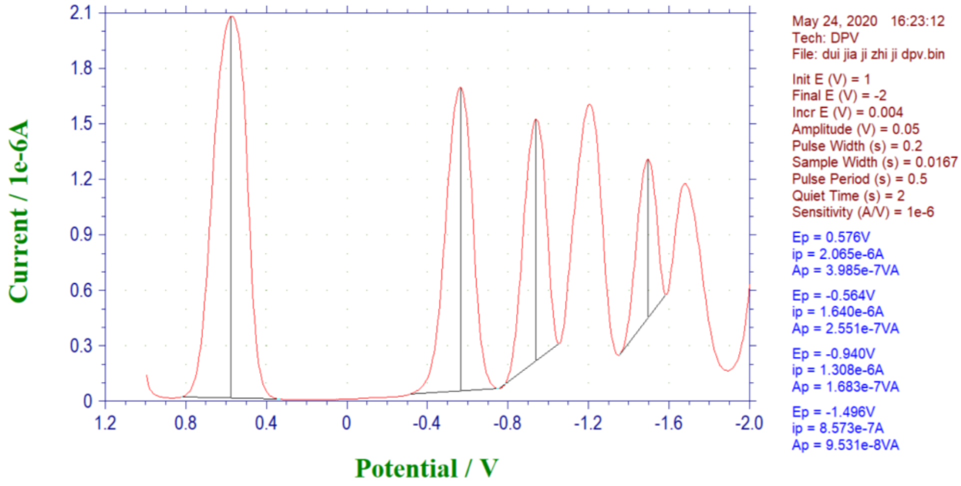

Figure S92 Differential pulse voltammogram of compound 2e

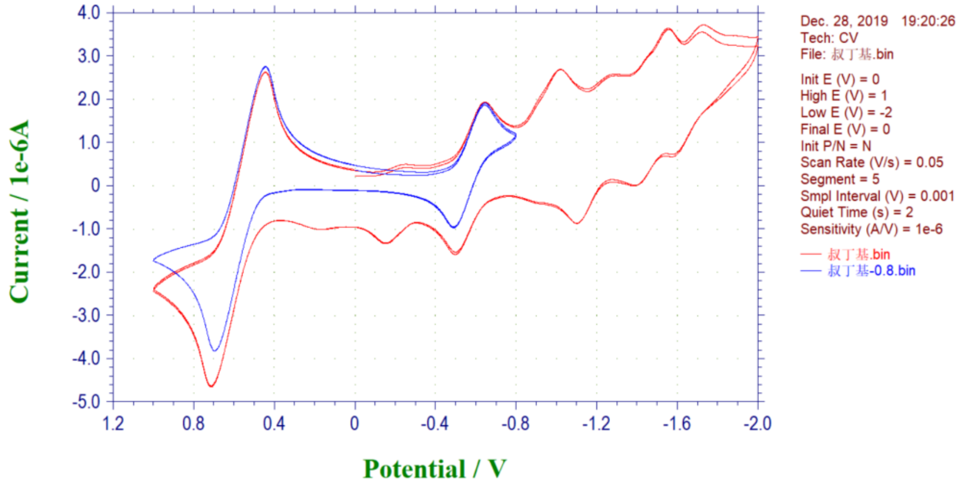

Figure S93 Cyclic voltammogram of compound 2f (scanning rate: 50 mV s^{-1})

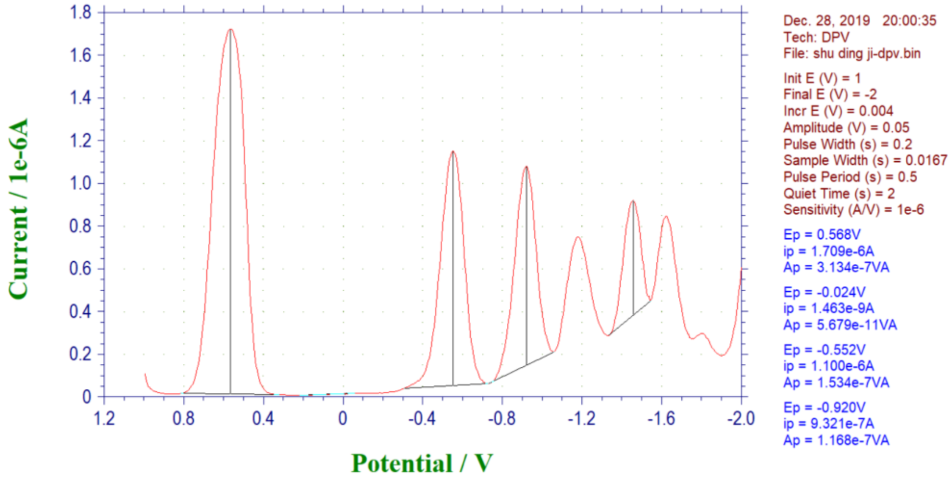

Figure S94 Differential pulse voltammogram of compound 2f

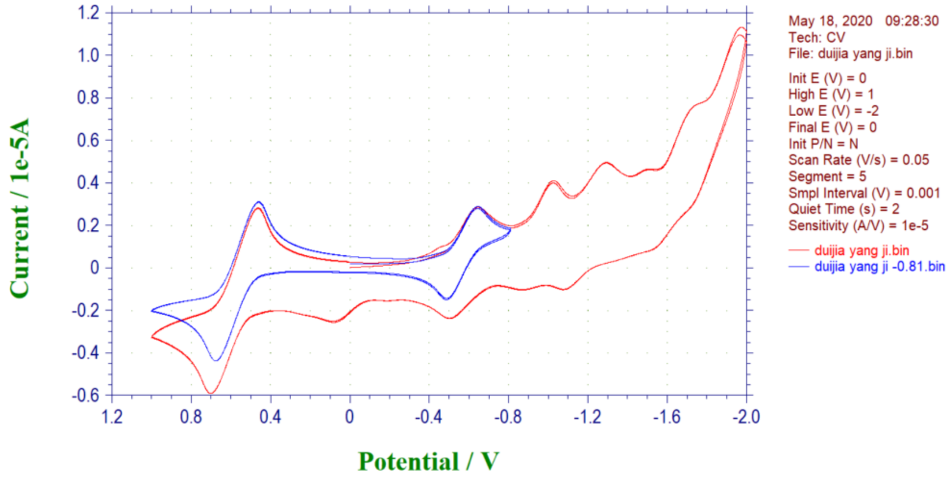

Figure S95 Cyclic voltammogram of compound 2g (scanning rate: 50 mV s^{-1})

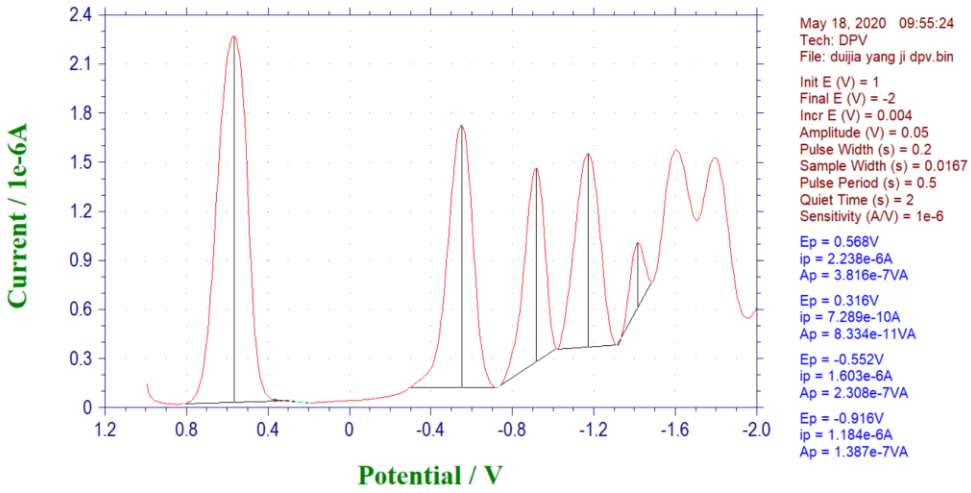

Figure S96 Differential pulse voltammogram of compound 2g

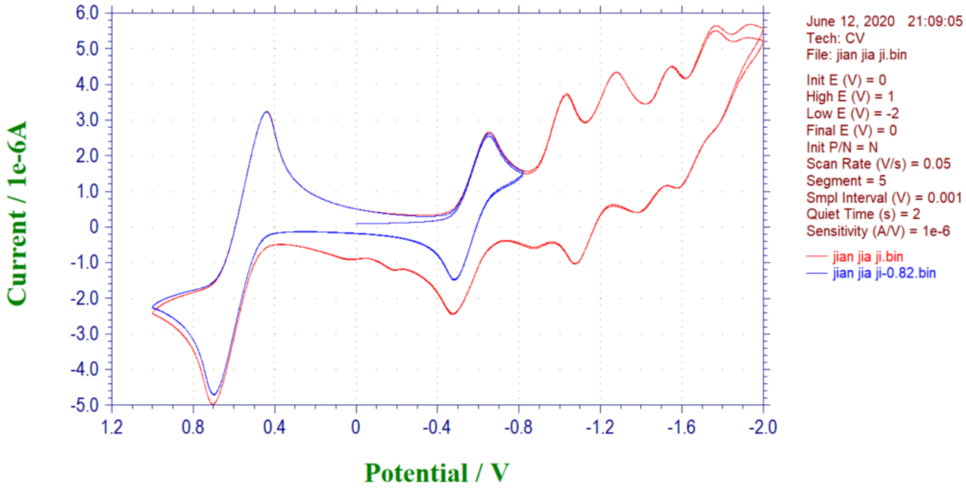

Figure S97 Cyclic voltammogram of compound 2h (scanning rate: 50 mV s^{-1})

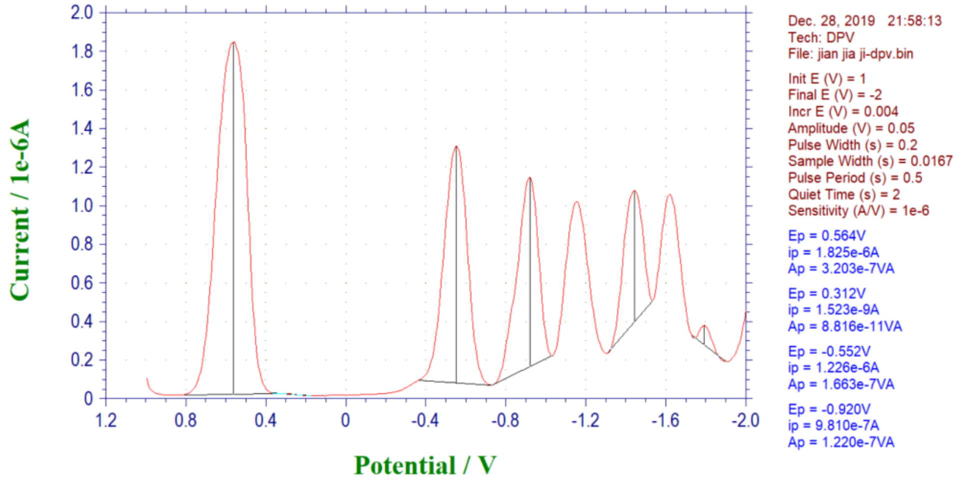

Figure S98 Differential pulse voltammogram of compound 2h

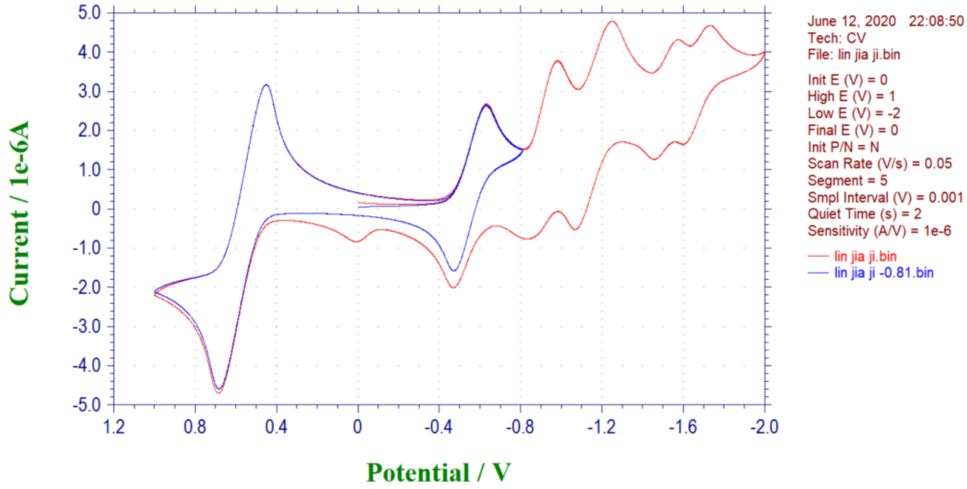

Figure S99 Cyclic voltammogram of compound 2i (scanning rate: 50 mV s^{-1})

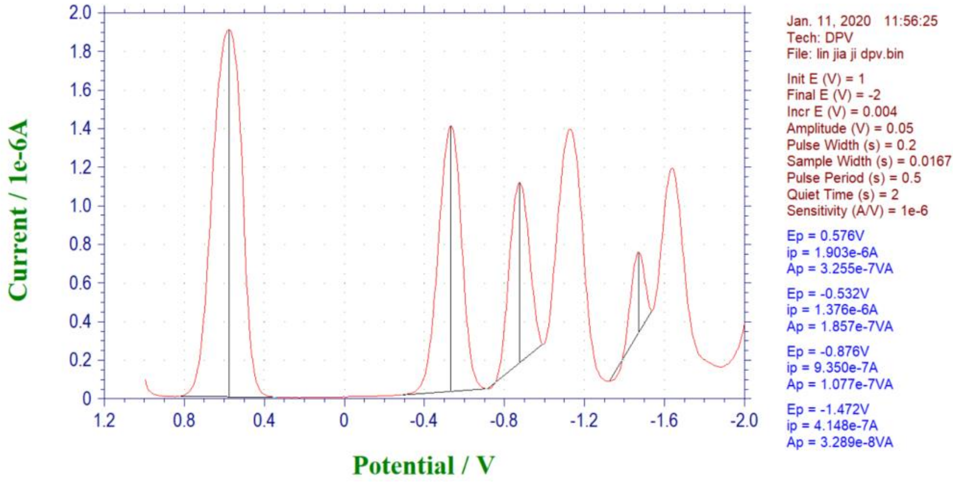

Figure S100 Differential pulse voltammogram of compound 2i

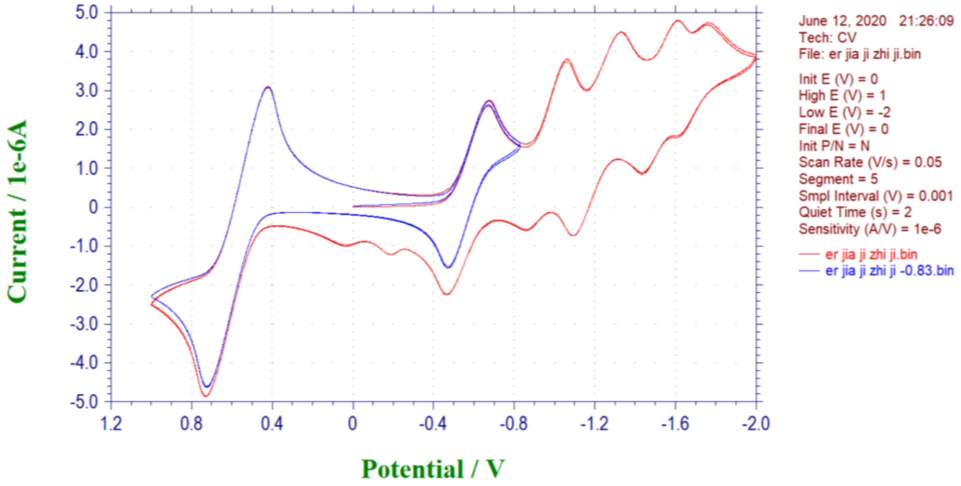

Figure S101 Cyclic voltammogram of compound 2j (scanning rate: 50 mV s^{-1})

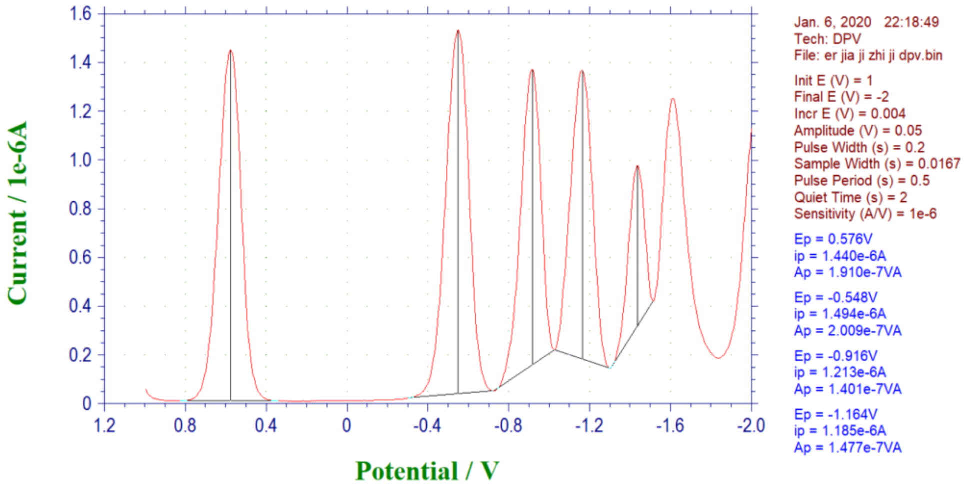

Figure S102 Differential pulse voltammogram of compound 2j

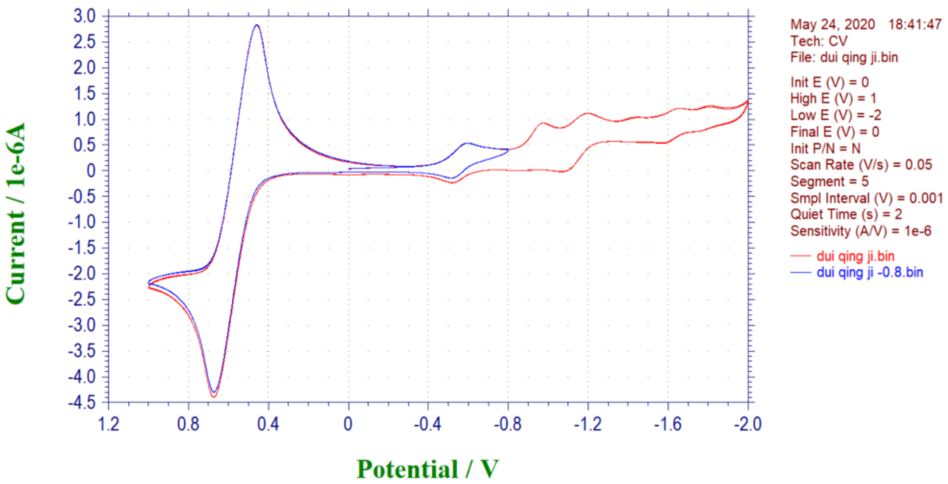

Figure S103 Cyclic voltammogram of compound 2k (scanning rate: 50 mV s^{-1})

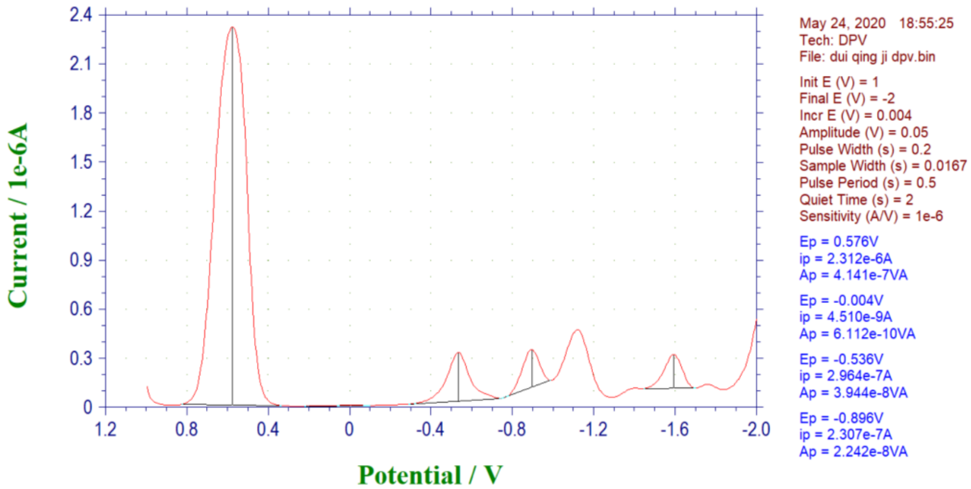

Figure S104 Differential pulse voltammogram of compound 2k

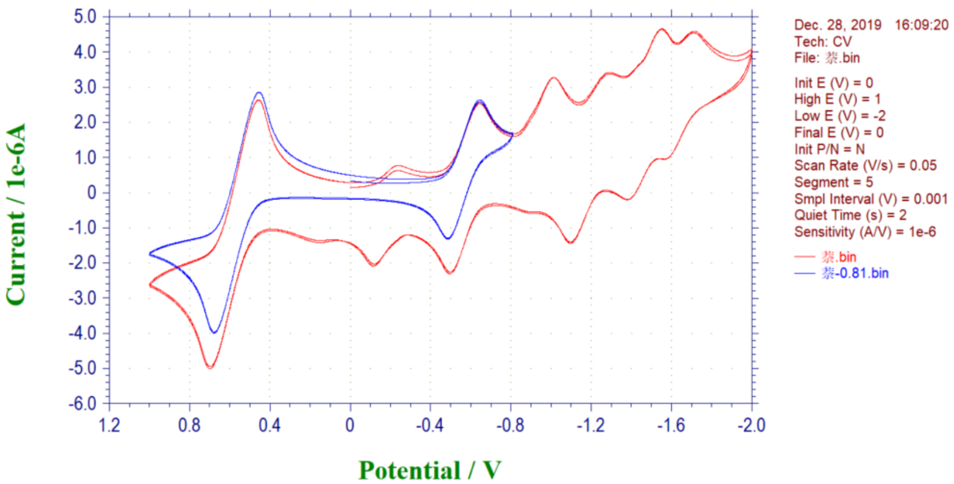

Figure S105 Cyclic voltammogram of compound 2l (scanning rate: 50 mV s^{-1})

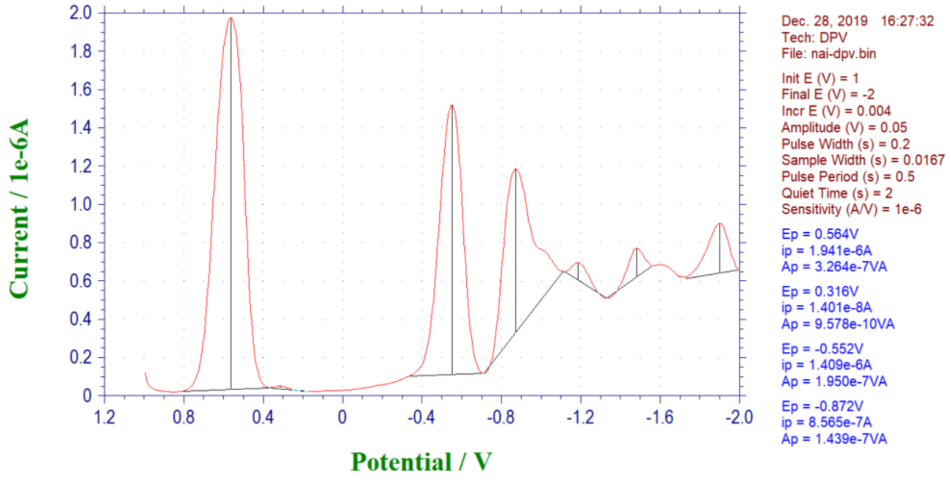

Figure S106 Differential pulse voltammogram of compound 2l

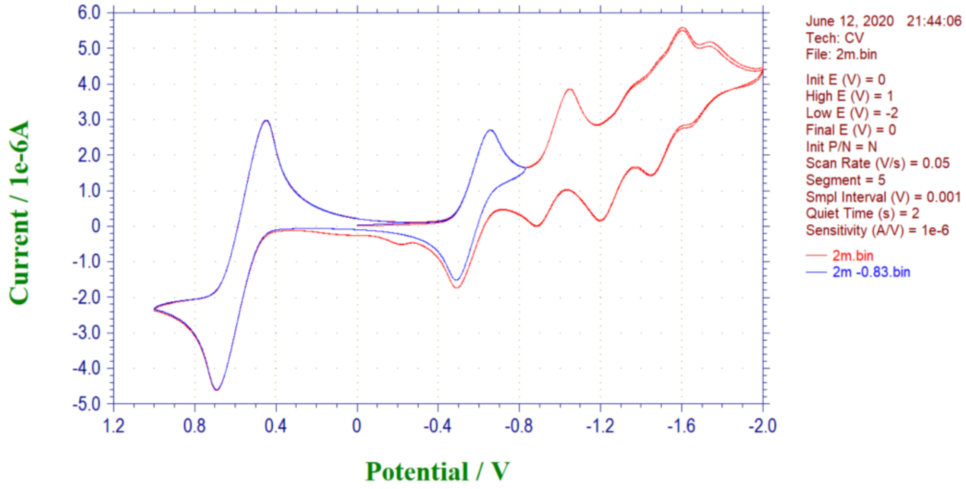

Figure S107 Cyclic voltammogram of compound 2m (scanning rate: 50 mV s^{-1})

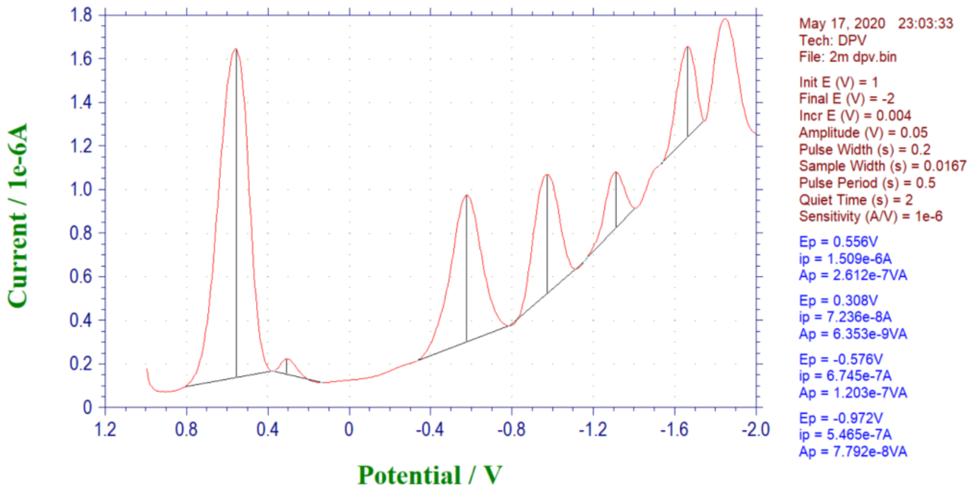

Figure S108 Differential pulse voltammogram of compound 2m

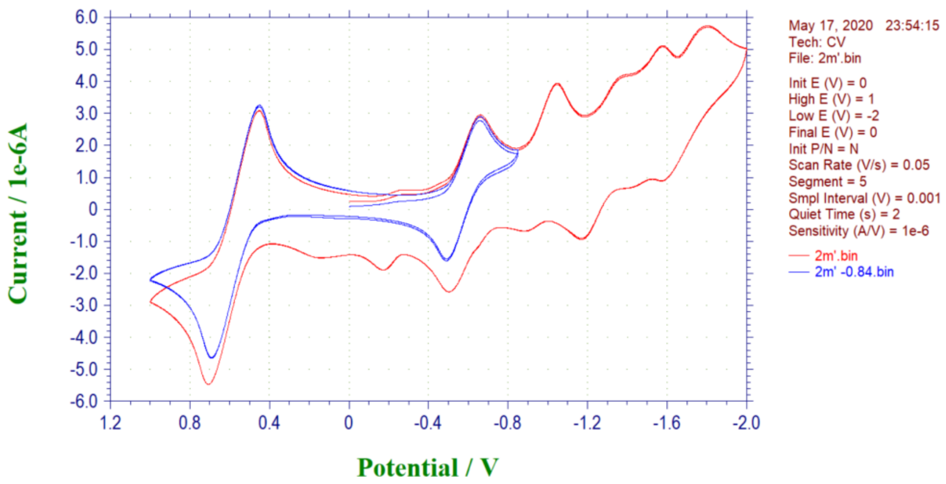

Figure S109 Cyclic voltammogram of compound 2m' (scanning rate: 50 mV s^{-1})

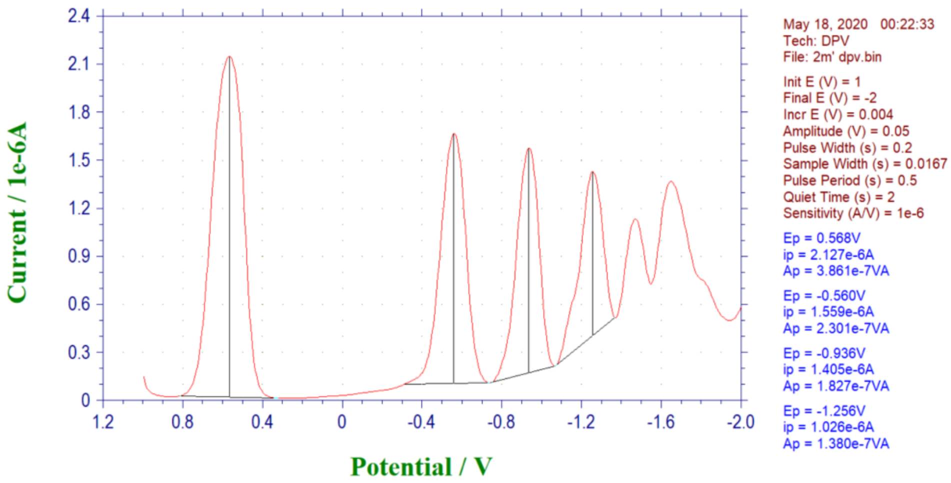

Figure S110 Differential pulse voltammogram of compound 2m'

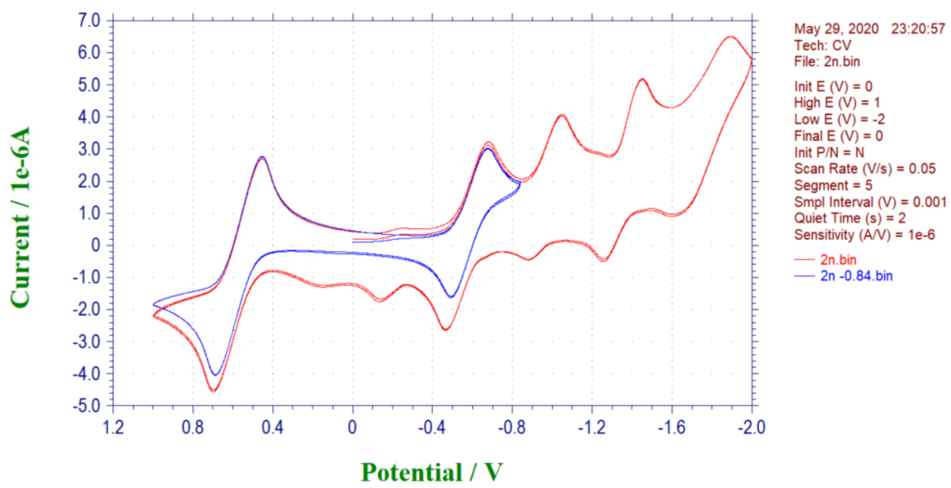

Figure S111 Cyclic voltammogram of compound 2n (scanning rate: 50 mV s^{-1})

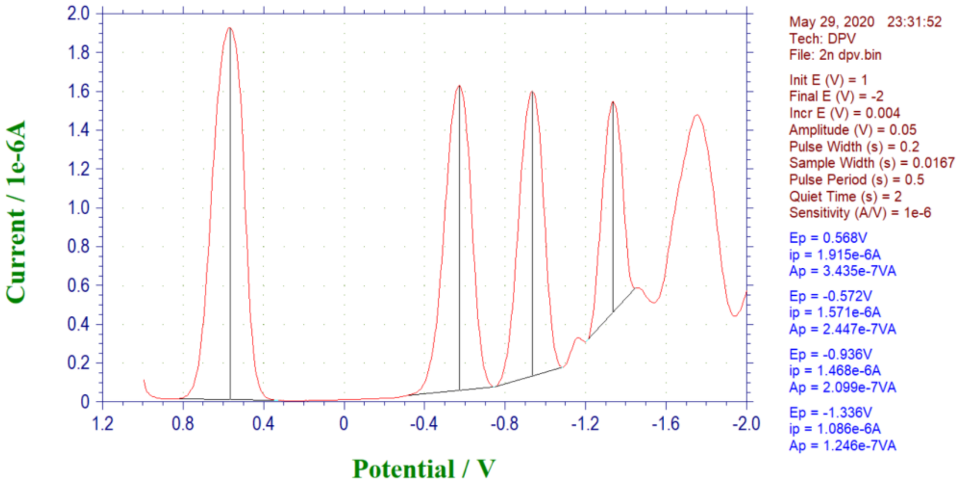

Figure S112 Differential pulse voltammogram of compound 2n

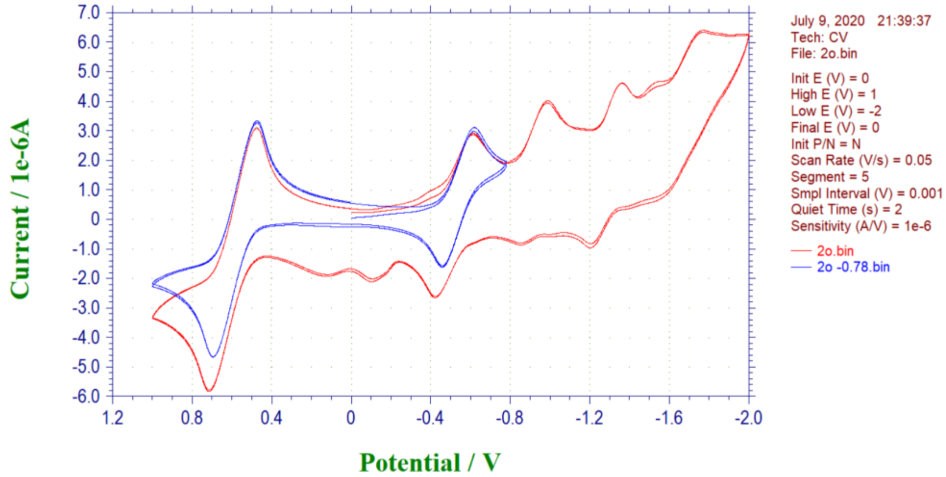

Figure S113 Cyclic voltammogram of compound 2o (scanning rate: 50 mV s^{-1})

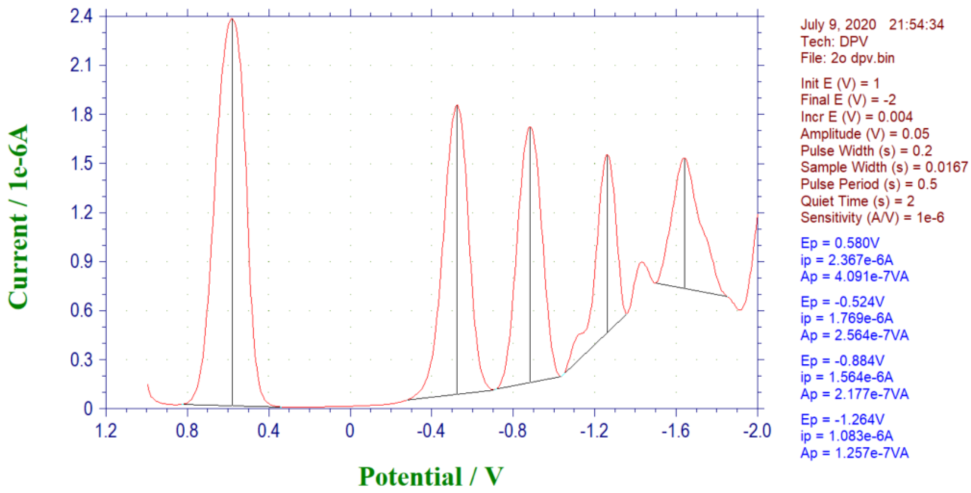

Figure S114 Differential pulse voltammogram of compound 2o

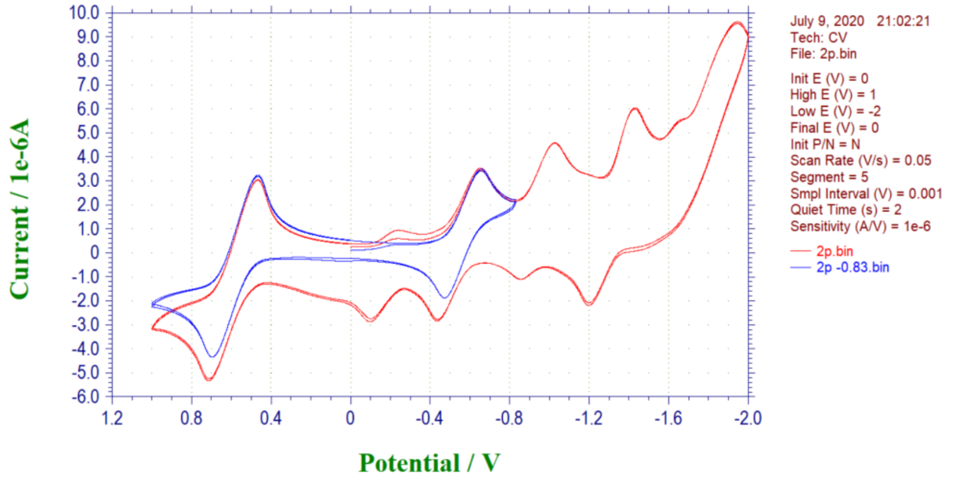

Figure S115 Cyclic voltammogram of compound 2p (scanning rate: 50 mV s^{-1})

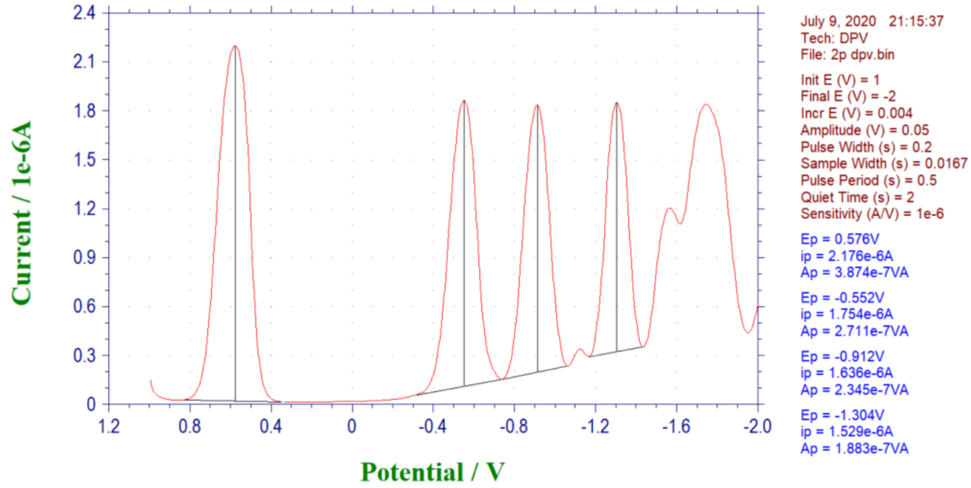

Figure S116 Differential pulse voltammogram of compound 2p

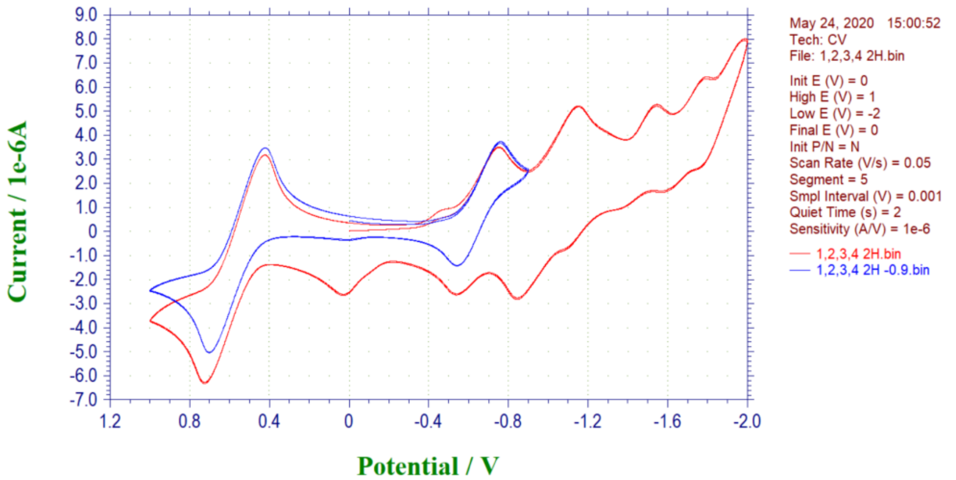

Figure S117 Cyclic voltammogram of compound 3a (scanning rate: 50 mV s^{-1})

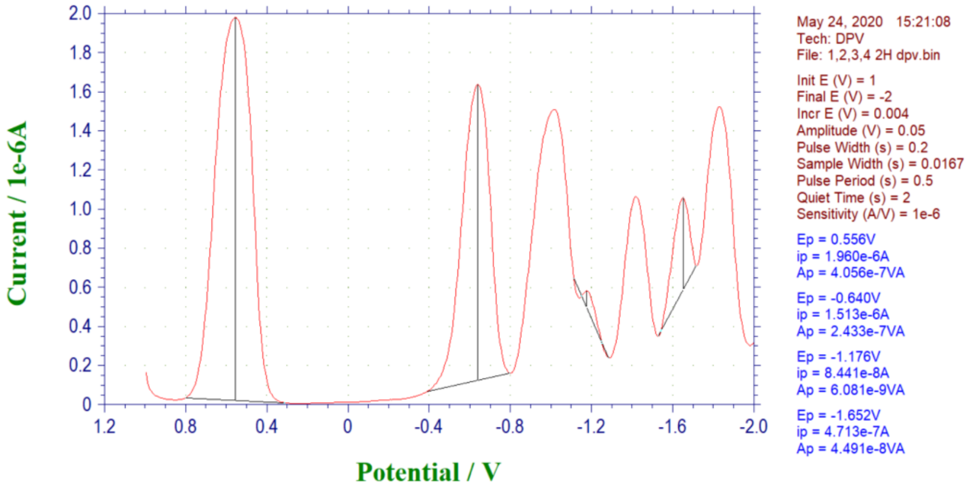

Figure S118 Differential pulse voltammogram of compound 3a

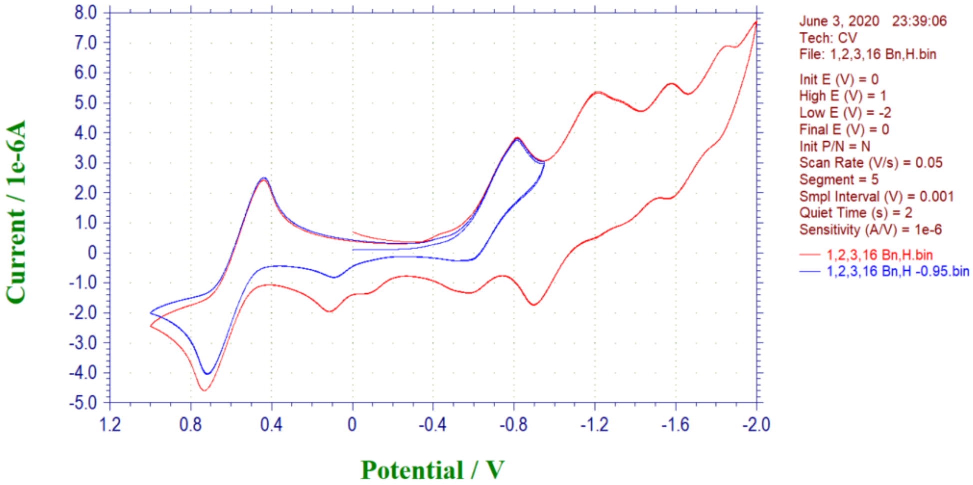

Figure S119 Cyclic voltammogram of compound 3b (scanning rate: 50 mV s^{-1})

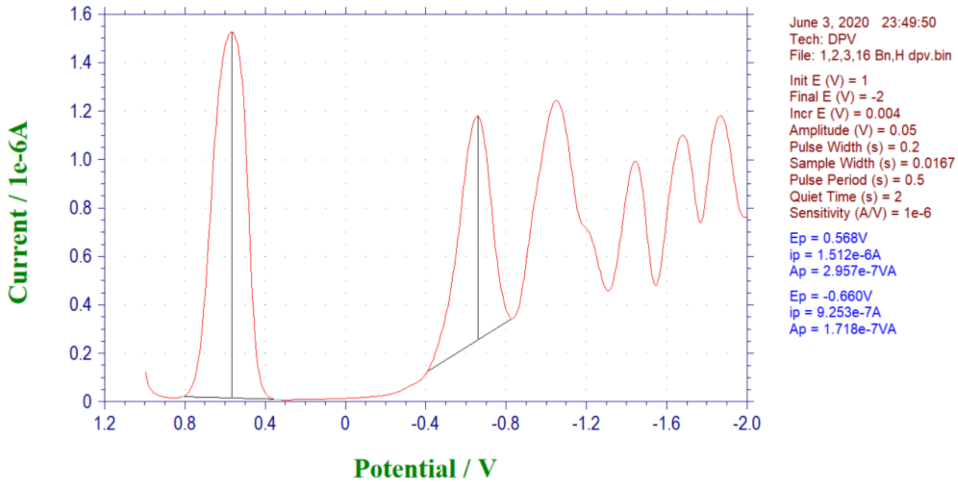

Figure S120 Differential pulse voltammogram of compound 3b

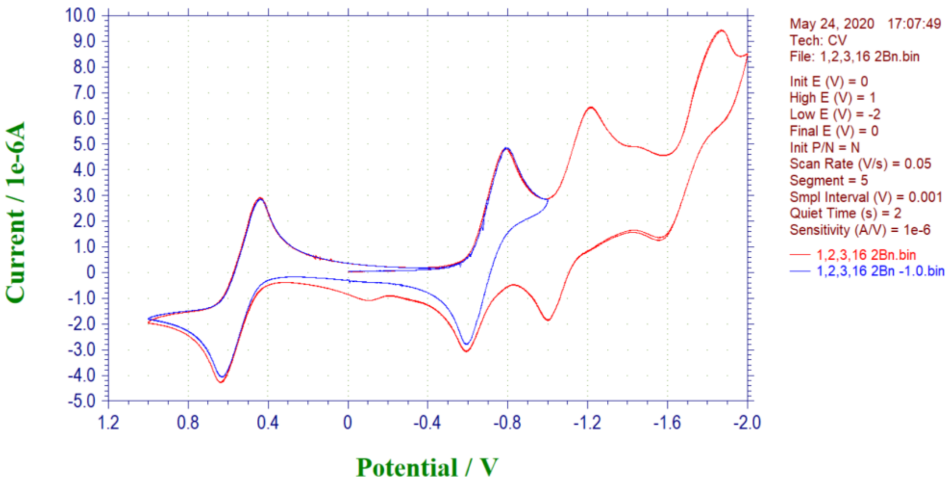

Figure S121 Cyclic voltammogram of compound 3c (scanning rate: 50 mV s^{-1})

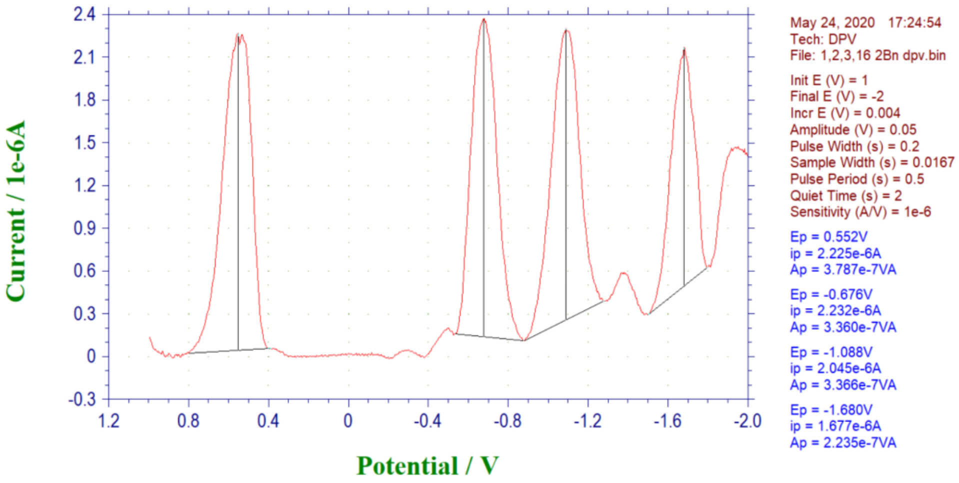

Figure S122 Differential pulse voltammogram of compound 3c